

Republic of Iraq
Ministry of Higher Education & Scientific Research
University of Kerbala
College of Engineering
Department of Civil Engineering



CLIMATE CHANGE EFFECT ON OPERATION OF STORM WATER NETWORKS: A CASE STUDY IN KARBALA CITY

A Thesis Submitted to the Department of Civil Engineering, University of Kerbala in
Partial Fulfillment of the Requirements for the Degree of Master of Science in Civil
Engineering (Infrastructure Engineering)

By

Ghofran Abdul-Alhussien Mohamed

BSc. in Civil Eng. / University of Kerbala (2015)

Supervised by

Prof. Dr. Basim Khilail Nile

Prof Dr. Waqed Hamed Hassan

بِسْمِ اللَّهِ الرَّحْمَنِ الرَّحِيمِ

نَرَفَعُ دَرَجَاتٍ مِّنْ نَّشَأٍ
وَفَوْقَ كُلِّ ذِي عِلْمٍ

عَلِيمٍ

صدق الله العلي العظيم

سورة يوسف - الآية (76) ﴿

ABSTRACT

The flooding of a storm water network may be caused by climate change, land-use change, increase in urbanization, and the wider population. Therefore, this study deals with the development of a computer model to extrapolate future change in rainfall events in order to protect the infrastructure of the storm water network from flooding. For the current study, the Al-Abbas quarter in Karbala city, Iraq was chosen as a case study. The historical data for the period of 1980-2016 was utilized to predict rainfall intensity for the future period 2017-2070 and study the effect of climate change on such prediction. The artificial neural network ANN model was used to analyze the data. The input layers that enter to ANN model include climate change parameters such as monthly rainfall, minimum and maximum temperature, wind speed, humidity, and sunshine. These data were divided into two groups: the first group 95% of the data and represent the training data, while the second represent the test data 5% of the data and used for calibration. Output parameter includes rainfall intensity. Following this, a Storm Water Management Model (SWMM) model is constructed in order to assess the flood conditions of the study area for expected rainfall intensities. The results indicate that the maximum rainfall intensity will reach 46.48 mm/h. in 2067. This value represents three times of the design intensity. The percent of the flooding manhole increases with the progress of time. Five design stages were selected for each specific time period during the design period of the study which was 53 years to show the variance in the flooding of manholes. It's an example, the flooding rate during the first stage decreases by 39.2% in 2070 while in the second stage the rate increases by 14.2%, the third stage increases 6 times, the fourth stage has no change, and fifth stage increases with a rate about 6% compared to the beginning period (2017).

SUPERVISOR CERTIFICATE

We certify that this thesis entitled "CLIMATE CHANGE EFFECT IN STORM WATER NETWORK SYSTEM:CASE STUDY IN KERBALA", which is prepared by " Ghofran Abdul-Alhussien Mohamed ", is under our supervision at University of Kerbala in partial fulfillment of the requirements for the degree of Master of Science in Civil Engineering (Infrastructure Engineering).

Signature:



Name: Prof. Dr. Basim Khalil Nile

(Supervisor)

Date: / / 2019

Signature:



Name: Prof Dr. Waqed H. Hassan

(Supervisor)

Date: / / 2019

EXAMINATION COMMITTEE CERTIFICATION

We certify that we have read the thesis entitled "CLIMATE CHANGE EFFECT ON OPERATION OF STORM WATER NETWORKS: A CASE STUDY IN KARBALA CITY" and as an examining committee, we examined the student "Ghofran Abdul-Alhussien Mohamed" in its content and in what is connected with it, and that in our opinion it is adequate as a thesis for degree of Master of Science in Civil Engineering (Infrastructure Engineering).

Signature:

Name: Prof. Dr. Basim Khilail Nile

Date: / / 2019

(Supervisor)

Signature:

Name: Prof. Dr. Waqed H. Hassan

Date: / / 2019

(Supervisor)

Signature: *Musa Halshammari*

Name: Asst. Prof. Dr. Musa Habib Jasim Al-Shammari

Date: / / 2019

(Member)

Signature:

Name: Prof. Dr. Isam Issa Omran

Date: / / 2019

(Member)

Signature:

Name: Prof. Dr. Jabbar H. Al-Baidhani

Date: / / 2019

(Chairman)

Approval of Civil Engineering
Department

Signature:

Name: Prof. Dr. Waqed H. Hassan

(Head of civil Engineering Dept.)

Date: 2/6 / 2019

Approval of Deanery of the College of Engineering -
University of Kerbala

Signature:

Name: Prof. Dr. Basim Khilail Nile

(Dean of the College of Engineering)

Date: 2/6 / 2019

This thesis is dedicated to:

***My parents and my family, brothers, sisters, uncle and cousin for
their love and continuous prayers***

ACKNOWLEDGMENTS

Praise and Glory be to **Almighty ALLAH** for bestowing me with health and power to complete this work and to achieve something that might serve humanity. I would like to thank my parents for their continuous support to complete my research work.

The author would also like to thank, in particular, his director of the study and main academic supervisor, **Dr. Basim Khalil Nile, Dr. Waqed Hamed Hassan** for their valuable assistance, suggestions, advice, continuous guidance and encouragement throughout the research.

Special thanks are also to those who provided help and support for completing the research work, especially my husband, Eng. Mostafa Amari for always hortative to completing the research work.

Ghofran Abdul-Alhussien Mohamed

CONTENTS

ABSTRACT.....	I
SUPERVISOR CERTIFICATE	II
LINGUISTIC CERTIFICATE.....	III
EXAMINATION COMMITTEE CERTIFICATION	IV
ACKNOWLEDGMENTS	VI
CONTENTS.....	VII
LIST OF FIGURES	I
LIST of TABLES.....	II
ABBREVIATIONS	II
Chapter One.....	1
INTRODUCTION	1
1.1 Introduction.....	1
1.2 Statement of the problem.....	2
1.3 Objective of the study	3
1.4 The Methodology of the study.....	3
1.5 Thesis Structure	4
Chapter Two.....	5
LITERATURE REVIEW.....	5
2.1 Climate change.....	5
2.3 Flooding model	7
2.3.1 SWMM definition	7
2.3.2 SWMM Modeling Capabilities	7
2.3.3 Typical Applications of SWMM.....	9
2.4 Artificial neural network (ANN).....	11
2.4.1 ANN components.....	15

2.4.2 ANN and Civil engineering applications	15
----------------------------------------------------	----

Chapter Three..... 17

MODELING AND CASE STUDY	17
3.1 Stages of the research	17
3.2.1 Artificial neural network (ANN).....	19
3.3 Storm water management model (SWMM).....	26
3.3.2 System flow routing	27
3.3.3 Infiltration model	29
3.3.4 Building SWMM model.....	30
3.4 Study area and data	31
3.4.1 Description of the study area	31
3.4.2 Land use	33
3.4.3 The topography	34
3.4.4 Sub catchment.....	35
3.4.5 Field data.....	36
3.4.6 Metrological data	39
3.5 Suggestion scenario	43

Chapter Four..... 45

RESULTS AND DISCUSSION	45
4.1 Topics of search results.....	45
4.2 ANN Rainfall intensity model	45
4.2.1 Learning process of ANN models functions.....	45
4.2.2 Weights distributions of models	50
4.2.3 Calibration of the ANN model.....	54
4.2.4 Effect of climate change on the ANN model.....	58
4.3 Flooding model.....	60
4.3.1 Model calibration	60

4.3.2	Climate change simulation results by SWMM	62
4.4	Result of Suggested scenario	81
	Chapter Five.....	83
	CONCLSION AND FUTURE RECOMMENDATIONS	83
5.1	Introduction.....	83
5.2	Conclusion	83
5.3	Recommendations:.....	85
5.4	Recommendations for future studies:	85
	APPENDIX A – GIS STORM NETWORK DATA.....	91

LIST OF FIGURES

Figure 2-1 A schematic presentation for ANN methodology(Cybenko, 1989, Hornik, 1991).	13
Figure 2-2 examples of ANN working methodology(Yılmaz and Yuksek, 2008)	14
Figure 3-1 Flowchart of the research methodology.	18
Figure 3-2 Structure of the neural network system(Dawson and Wilby, 1998).	19
Figure 3-3 learning process of artificial neural network (Xn: input, Wn: weights, Yn: outputs)(Cho et al., 2014).....	23
Figure 3-4 an example for the effect of a number of neurons on ANN model accuracy (Murata et al., 1994).....	24
Figure 3-5 Geographical location of the study area according to Iraqi map (M.C.H.M.PW).	32
Figure 3-6 land use of Al-Abbas quarter (M.C.H.M.PW).	34
Figure 3-7 topography of the study area (USGS, 2018).	35
Figure 3-8 the distribution of sub catchment areas in the study area(M.C.H.M.PW).	36
Figure 3-9 the storm drainage network of Al-Abbas quarter(M.C.H.M.PW).....	38
Figure 3-10 the average of montly rainfall for period (1980-2016).....	40
Figure 3-11 the average of max temperture for period(1980-2016).	40
Figure 3-12 average of min temperture for period(1980-2016).....	41
Figure 3-13 average of relative humidity for period(1980-2016).....	41
Figure 3-14 average of wind speed for period(1980-2016).	42
Figure 3-15 average of sun shine for period(1980-2016).	42
Figure 3-16 average of rainfall intensity for period (1981-1990).....	43
Figure 4-2 Correlation strength of the fitting line between observed and learned data for 10 years.	48
Figure 4-1 ANN learning process of a ten years testing data.	48
Figure 4-3 RMSE function behavior during the function learning process.	49
Figure 4-4 ANN learning process for 36 years testing data.	49
Figure 4-5 Correlation strength of the fitting line between observed and learned data for 36 years.	50
Figure 4-6 RMSE function behavior during the function learning process.	50

Figure 4-7 weight distribution process, A- for 1 hidden layer contains 9 nodes, B- for 2 hidden layers contains 19 nodes.....	51
Figure 4-8 show the distribution of the weights of model 1.	52
Figure 4-9 show the distribution of the weights of model 2.	52
Figure 4-10 show distribution of the weights of model 3.	53
Figure 4-11 show the distribution of the weights of model 4.	53
Figure 4-12 show the distribution of the weights of model 5.	54
Figure 4-13 predict versus observation intensity values of model 3 (($R^2=0.640$, RMSE=3.460).	56
Figure 4-14 Predict versus observation intensity values of model 4 ($R^2=0.620$, RMSE=3.680).	56
Figure 4-15 predict versus observation intensity for model 5 ($R^2=0.410$, RMSE=5.25).	57
Figure 4-16 observation data of rainfall intensity.	58
Figure 4-17 Prediction of rainfall intensity by ANN model (model 3).	58
Figure 4-18 model importance distribution parameters of model 1.....	59
Figure 4-19 model importance distribution parameters of model 3.....	59
Figure 4-20 model calibration result under different rainfall intensity.....	61
Figure 4-21 The flooding manhole under rainfall intensity (27.5 mm/h) at peak time in winter 2017.	64
Figure 4-22 The flooding manhole under rainfall intensity (34.74 mm/h) at peak time in winter 2019.	65
Figure 4-23 The flooding manhole under rainfall intensity (28.82 mm/h) at peak time in winter 2024.	67
Figure 4-24 The flooding manhole under rainfall intensity (29.62 mm/h) at peak time in winter 2028.	68
Figure 4-25 The flooding manhole under rainfall intensity (25.28 mm/h) at peak time in winter 2037.	70
Figure 4-26 The flooding manhole under rainfall intensity (26.34 mm/h) at peak time in winter 2042.	72
Figure 4-27 The flooding manhole under rainfall intensity (45.98 mm/h) at peak time in winter 2055.	74
Figure 4-28 The flooding manhole under rainfall intensity (44.9 mm/h) at peak time. .	76

Figure 4-29 The flooding manhole under maximum rainfall intensity (46.48 mm/h) at peak time in winter206778

Figure 4-30 The flooding manhole under rainfall intensity (46.42 mm/h) at peak time in winter 2070.80

Figure 4-31 suggestion scenario for future flooding occurrence forecasting (2070).82

LIST of TABLES

Table 3-1 Determining the Number of Hidden Layers(Luk et al., 2001).	23
Table 3-2: formula of data using in ANN.	25
Table 3-3 Parameters of Green-Ampt for different soil type, Rawls et al. (1983)...	30
Table 3-4 clarify min and max value of climate of the case study(Meehl et al., 2007).	32
Table 3-5 Values of Manning roughness coefficients for different materials of pipes(Rothman et al., 1998).	37
Table 3-6 Rational Method Runoff Coefficients(Kadioglu and ŞEN, 2001).	44
Table 4-1 present effect different training function and the number of hidden layers on the strength of the correlated function.	46
Table 4-2 The model description, number of hidden layers, and its parameter.....	55
Table 4-3 the result of calibration of SWMM.....	62

ABBREVIATIONS

Abbreviation	Description
ANN	Artificial Neural Network
D.S.K	Directorate of the Stream of Karbala
DC	Determination Coefficient
DEM	Digital Elevation Model
G.A.M.S.O	General Authority for Meteorology and Seismic Observation
GIS	Geographic Information System
IPCC	Intergovernmental Panel on Climate Change
M.C.H.PM	Ministry of Construction and Housing and Public Municipalities
R	Correlation coefficient square
RMSE	Root Mean Square Error
SPSS	statistical package for the social sciences
SSA	Storm and Sanitary Analysis
SWMM	Storm Water Management Model
TIN	Triangular irregular network
USGS	U.S Geological Survey

Chapter One

INTRODUCTION

1.1 Introduction

The growth of cities worldwide is associated with an increase demand for sanitation and drainage infrastructure in the terms of the water cycle with the effect of climate change. The situation of this system in environmental urban is critical. The part of the existing sewer network required an imminent renovation ,other must be constructed in developing area, as where storm water runoff becomes a threat in terms of flooding because of soil impervious .In this part, should be determine the best practices aimed at reducing these issues from innovative environmental and economic view point and at the same time adapt cities to climate change([Boix, 2017](#)).

The Climate change significantly impact on precipitation, when the rainfall increase this led to urban flooding in storm network. Global warming cause all over the globe increase in temperature and sea level , this increase causing a rise in rainfall intensity and frequency, then this led to flooding.([Jung et al., 2015](#)).

Increase population and urbanization led to increase impervious area this decrease infiltration and increase runoff quantity, so this also led to flooding. To reduce the hazard of flooding would predict the rainfall intensity, artificial neural network (ANN) model used to predict rainfall intensity under the effect of climate change.

The origins of artificial neural networks (ANN) are in the field of biology. The biological brain consists of billions of highly interconnected neurons forming a neural network. Human information processing depends

on this connectionist system of neurons cells. Based on this advantage of information processing, neural networks can easily exploit the massively parallel local processing and distributed storage properties in the brain ([Jeng et al., 2003](#)).

Storm water management model (SWMM) has the ability to link many of parameter on the performance of storm network to get many of option such as water flooding and water depth.

The model is widely used for planning, analysis and design related to drainage systems in urban areas. The model provides an integrated Windows environment for editing input data, running simulations, and viewing the results in the form of thematic maps, graphs, tables, profile plots and statistical reports ([Gironás et al., 2010](#)).

The study area is Karbala, Iraq is faster urbanization city because it's characterize by religious nature and also the political conditions in the country caused immigration thousands of citizens from different cities to it. The urbanization in the study area [al-Abbas section, Karbala] converts the most of the lands from pervious into impervious area where that increase the urban flooding. Due to that the control of the urban flooding quantity become an important issue to reduce the cost of infrastructure damage..

1.2 Statement of the problem

Al-Abbas section located at the north-east of Karbala city center. The aim of this research is the study of urban flooding problem in the storm network. This problem developed with climate change and population and urbanization growth. The climate change led to an increase of the rainfall intensity higher than the design intensity of the storm network of the study area. This change cause flooding.

1.3 Objective of the study

The aim of this research is to study the impact of climate change on rain intensities. This study is used to expect the rainfall intensity of the study area. Also, this study is used to determine the expected flood ratios in rainwater drainage networks

1.4 The Methodology of the study

The Methodology of the study can be summarized as the following steps:

1. Using the metrological data from the General Authority for metrology and Seismic Observations (G.A.M.S.O) for period from 1980 to 2016. This data includes monthly rainfall (mm), mean maximum temperature(C °), mean minimum temperature(C °) mean relative humidity (%), mean wind speed (m/s), mean sun shine (hr./day). The data collected for period from 1981 to 1990 include rainfall intensity for Karbala station in (mm) for 1 hr.
2. Collect the field data of the Al-Abbas section from Directorate of the Sewage of Karbala (D.S.K) including pipe ,manhole ,and its properties for stormwater networks.
3. Built artificial neural network (ANN) model to predict rainfall intensity for the next 53 years next. And Made calibration for the ANN model to choose the best model by using many statistical indicators.
4. The expected rainfall intensity can be applied on the storm network for the study area by using SWMM model to estimating the flooding ratio.

1.5 Thesis Structure

This thesis consists of five chapters as follows:

- Chapter 1 illustrates introduction, statement of problems , objectives and methodology of the thesis.
- Chapter 2 shows the previous studies for the various parts, the first part deals with climate change. The second part deals with flooding and its reasons. The penultimate part reviews ANN model, and the final part deals with SWMM model.
- Chapter 3 descriptions ANN model, SWMM model and states the study area and the properties of all collected data.
- Chapter 4 displays the result of rainfall intensity model. The result of flooding model are discussed. Furthermore, a suggestion scenario are presented for the future work.
- Chapter 5 contains the conclusions of the present study and recommendations.

Chapter Two

LITERATURE REVIEW**2.1 Climate change**

Climate change is the changing of climate parameter such as rainfall, temperature, wind speed, humidity, sun shine. So, and the rainfall and temperature parameters significant impact on flooding

The Middle East is largely arid to semi-arid and fresh water is often a scarce and precious resource. The combination between a stressed fresh water resource and rapid population growth. Substantially increases the vulnerability of the region to future climate change. Simulating the climate of the region is a challenge for climate models ([Evans, 2009](#)).

The Intergovernmental Panel on Climate Change (IPCC) state that an increase in temperature of between 1°C and 3.5°C due to rising in greenhouse gases by the end of this century ([Houghton, 1996](#)) and ([Bijlsma et al., 1996](#)) state that is rising in sea level between 13 and 94 cm.

[Denault et al. \(2006\)](#) Studied the effects of increased rainfall intensity and evaluated infrastructure future drainage capacity in Mission/Wagg Creek watershed in British Columbia, Canada by utilizing the SWMM technique. The result concluded that, in future, rainfall intensity with short duration may be slightly increased. However, this phenomena does not happen as sharply in the Mission/Wagg Creek system.

[Sansom and Renwick \(2007\)](#) evaluated the impact of future climate change, this effect can cause both floods and droughts. Using general circulation models (GCMs) to estimate climate change in New Zealand, the

result that found an increase in rainfall intensity due to increases in rainfall with climate change.

[Evans \(2009\)](#) studied the prediction of future climate change in the Middle East. 18 global climate models was using in the Intergovernmental Panel on Climate Change. The study conclude the temperature rising (1.4 °C at mid century_4 °C at the end century) and lower in precipitation epically in, Turkey Syria, Northern Iraq, Northeastern Iran and the Caucasus.

[Nie et al. \(2009\)](#) Studied the effect of climate change on urban drainage systems at Veumdalen catchment in Fredrikstad, Norway as a case study. By using predicted and artificial climate scenarios to evaluate climate change. The result concludes the number of flooding manholes and number of surcharging sewers may change hugely and irregularly with a small change of precipitation, and change with events and periods.

[Hassan et al. \(2017\)](#) Evaluated the behavior of storm networks of the Middle East region (Karbala city, Iraq) to predict future flooding hazards caused by climate change, specifically in case of inadequate sewer connections. The study utilized the SWMM model for Karbala's storm drainage network simulation. Continuous hourly rainfall intensity data was using from 2008 to 2016. It was concluded that, without consideration of additional sewage due to an illegal sewer connection, the system was sufficient as designed. The results indicated that the SWMM was efficient for modelling urban flood forecasting, and without surface runoff routing, the urban flooding might not perfectly forecast.

[Osman \(2017\)](#) Studied climate change effect on precipitation in the dry medium of Iraq by using Seven Global Climate Models (GCMs) for three

period selected 2011-2030, 2046-2065 and 2080-2099. The study reported that annual mean precipitation decrease for the most region of Iraq at end of the 21st century.

2.3 Flooding model

2.3.1 SWMM definition

Flooding can be defined as incapability of storm water network to accommodating of incoming of water. So, there is many reasons cause the flooding such as climate change, change of land use, and an increase of urbanization, population, CO₂ concentration.

The EPA Storm Water Management Model (SWMM) utilized to the simulation of runoff quantity and quality from primarily urban. SWMM was first developed in 1971 ([Rossman, 2010](#)). The simulated network in SWMM contained of pipe, manhole, and subcatchment connected to the nearest manhole.

2.3.2 SWMM Modeling Capabilities

SWMM calculations for various hydrological processes that produce runoff from urban areas. These include as reported:

- Precipitation of varying time.
- Evaporation of permanent surface water.
- Snow melt and accumulation
- Intercept the rain from storing depression
- Rainfall leakage phenomenon in unstable soil layers
- percolation the water that infiltrated into groundwater layers.
- Mixing happened between the drainage system and groundwater.
- Directed the nonlinear reservoir to the wild flow. ([Rossman, 2010](#))

The study area was subdivided into a group of smaller and homogeneous sub-regions to achieve spatial change in all of these processes.

SWMM also includes an elastic group of hydraulic modelling abilities used to guide external inflows and runoff through the drainage system network of pipes, channels, storage/treatment units and conversion structures. These contain the ability to:

- Dealing with networks of unbounded size.
- A various collection of open conduit and standard closed forms, as well as natural channels are used.
- Special modular items like pumps, openings, dams, flow separators, and storage/processing units.
- apply groundwater, water quality inputs from surface runoff, and external flows.
- Dry weather sanitary flow, interflow, rainfall-dependent infiltration/inflow, and user defined inflows.
- Using either full dynamic wave flow routing or kinematic wave methods.
- model different flow regimes, like surcharging, backwater, surface ponding, and reverse flow.
- apply user-defined dynamic control basics to simulate the working of pumps, weir crest levels, and orifice openings. ([Rossman, 2010](#))

SWMM can also evaluate the production of pollutant loads associated with this runoff, In addition to modelling the generation and transport of runoff flows. The following operations can be designed for any number of user-defined water quality components:

- Accumulation of pollutants in dry weather on different land uses.
- Pollution gases from land use during storm events – a direct contribution to rainfall precipitation.

- Reduction buildup in dry-weather due to street cleaning.
- Due to BMPs, the wash offload is a reduction.
- To any point in the drainage system can entry of user-specified external inflows and dry weather sanitary flows.
- Directed of water quality components out of the drainage system.
- Decrease the component focus out of natural processes in pipes and channels or by treatment in storage units. ([Rossman, 2010](#))

2.3.3 Typical Applications of SWMM

SWMM has been utilized in thousands of sewage and rainwater surveys worldwide. Typical applications include:

- Flooding control by design and sizing of drainage system components
- Determine the size of retention facilities and their appendixes for water quality protection and flood control.
- Normal flood mapping of the natural channel system.
- Reducing the combined sewer overflows by designing control strategies.
- Assess the effect of infiltration and inflow on sewage nozzles.
- Production of non-point-of-point contaminated loads for trash distribution studies.
- minimizing wet weather pollutant loadings by assessing evaluating the effectiveness of BMPs . ([Rossman, 2010](#)).

[Schreider et al. \(2000\)](#) reported how a significant amount of CO₂ concentration in the atmosphere could contribute to the extent of flooding. The study features two main sections. Firstly, the modelling of frequency and magnitude of the flood in the context of global warming is assessed. This phenomenon is associated with rainfall intensities. The second section involves the estimation of changes in the susceptibility of flooding. This appears in urban areas with the use of greenhouse effect-related flood data.

The results of modelling for all cases indicated that when CO₂ conditions were dual this led to a rise in the magnitude and frequency of the flooding events and these vary from one place to another.

[Reynard et al. \(2001\)](#) discussed the effect of climate and land use changes on the flood regimes of large U.K. catchments by using continuous flow simulation model (CLASSIC). They concluded that in the 2050s, climate change would increase the frequency and magnitude of flooding events in these catchments. However, land use changes show a marginal impact on the flooding.

[Denault et al. \(2006\)](#) studied the effects of increased rainfall intensity and evaluated infrastructure future drainage capacity in Mission/Wagg Creek watershed in British Columbia, Canada by utilizing the SWMM technique. The result concluded that, in future, rainfall intensity with short duration may be slightly increased. However, this does not happen as sharply in the Mission/Wagg Creek system.

[Nirupama and Simonovic \(2007\)](#) studied hazard of flooding due to rising urbanization in the City of London in the province of Ontario in Canada. Quantitative assessment for the hazard of river flooding to London by analysis meteorological and hydrological data in addition to analysis land use classification. The study found that between 1974 and 2000 there has densely urbanization in the watershed of the top Thames River, the City of London is the section of it so this led to increasing the hazard of floods.

[Semadeni-Davies et al. \(2008\)](#) estimated for storm water flow the climate change effect and urbanization in Helsingborg, south Sweden. using special drainage simulations for present situation. Moreover, two climates.

(Medium and high) are run, the period of simulations were 15 months. The result found raise in heavy rainfalls this led to increase volumes of peak flow peak flow volumes and raise the risk of flooding.

[Saghafian et al. \(2008\)](#) studied flooding cause by climate change, land use change due to roof roughness and infiltration in the Golestan watershed located northeast of Iran. using trend analysis for three stations inside the watershed showed that two stations were subject to human change on the yearly maximum flood record. To build a model for rainfall-runoff Using a calibrated event-based, the study found land use changes more effectively on the flood peak discharge from that some sub watersheds.

[Huong and Pathirana \(2013\)](#) assessed effect of climate change and urbanization on future urban flooding in Can Tho city, Vietnam. Built future scenario by using a group of simulation model include: using a land use simulation model (Dinamica EGO), atmospheric model (WRF). The study concluded that the worst situation happened when a sea level reaches 100 cm and the flow from upstream and Variation in river level.

[Jiang et al. \(2015\)](#) Utilized planning and management models for urban flooding, in the Dongguan City in southern China, an area which rapidly became urbanized. (SWMM) is a tool used for this application. The results indicate that the area studied will not experience flooding when the return period precipitation is one year. However, the area studied will be submerged when the return period precipitation is 2, 5, 10 and 20 years.

[Jung et al. \(2015\)](#) studied climate change effects on urban flooding in the drainage basin of Gunja, utilizing the SWMM model to make a single event simulation of runoff quantity. The results conclude that when there were increases in the short duration rainfall intensity, this led to the rising of the simulated peak discharge from SWMM.

2.4 Artificial neural network (ANN)

An artificial neuron network (ANN) is a computer model based on the functions and structure of biological neural networks.

ANNs are modelling tools for nonlinear statistical data where complex relationships between inputs and outputs are formed or patterns are found. ANN is also famous as a neural network.

ANN is used as a random function approximation tool because it has one of the most recognized features that it can actually learn from controlling data sets in addition to having many other features. . ANN takes data samples instead of full datasets to access solutions, saving money and time.

ANNs have three interconnected layers. The first layer consists of entered neurons. These neurons send data to the second layer, which in turn sends neurons to the third layer, as can be seen in Figure (2.1). And to clarify the idea better, Figure (2.2) describe how ANN internally working and gives the best results.

The training of the artificial neural network includes a selection of permitted models with several associated algorithms. ([Cybenko, 1989](#), [Hornik, 1991](#))

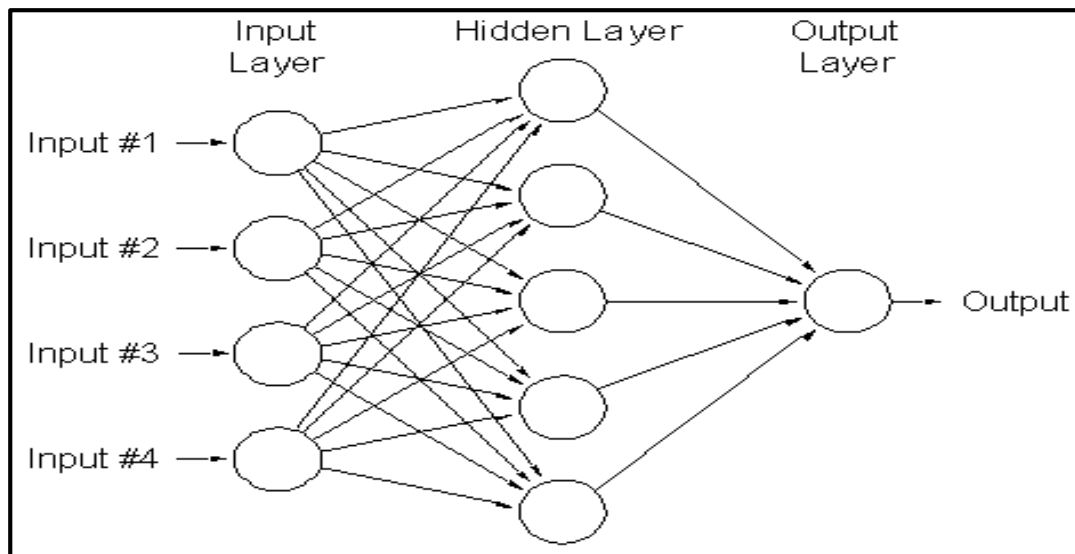


Figure 2-1 A schematic presentation for ANN methodology([Cybenko, 1989](#), [Hornik, 1991](#)).

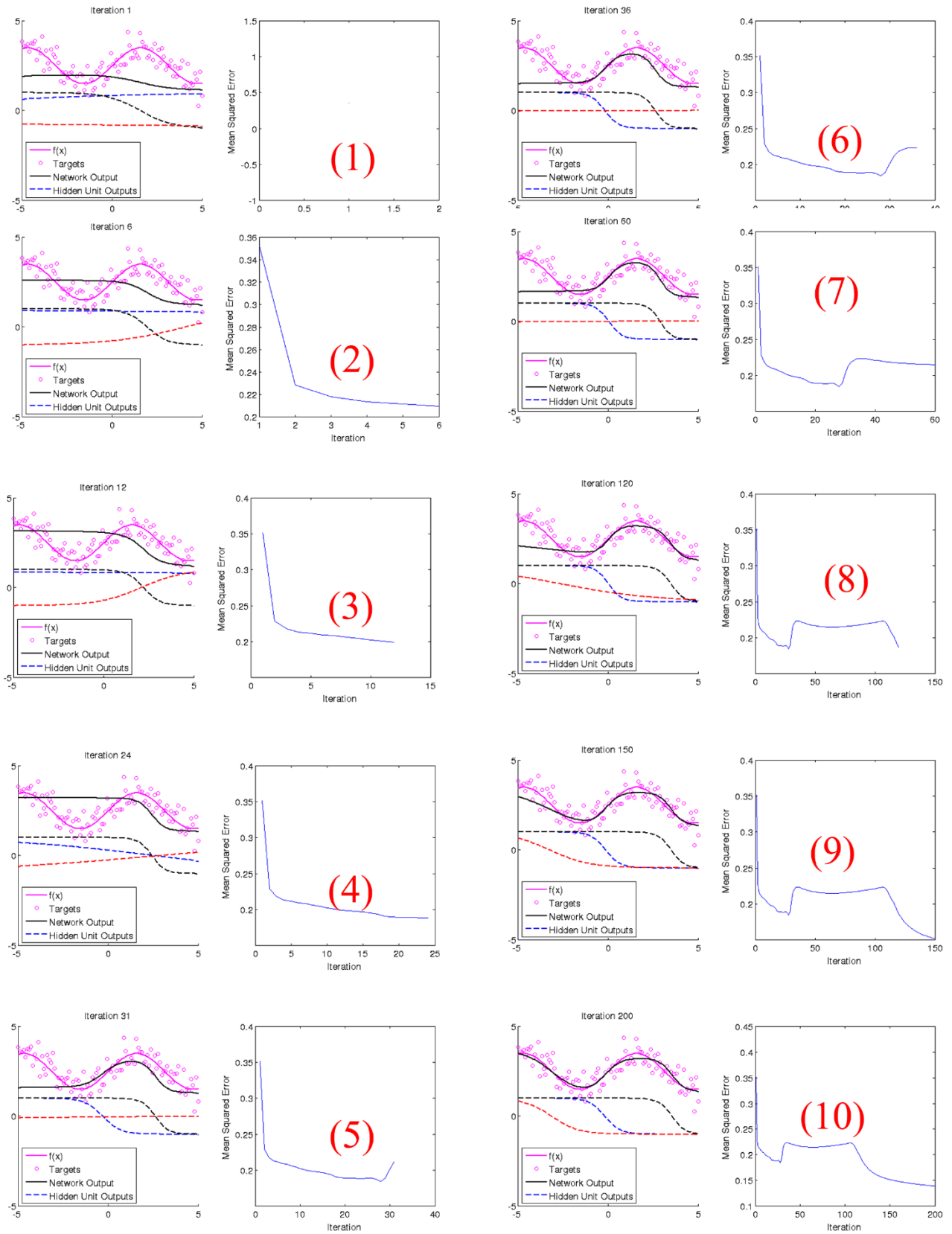


Figure 2-2 examples of ANN working methodology (Yılmaz and Yuksek, 2008)

2.4.1 ANN components

Artificial neural networks are typically composed of input layers, hidden layers and output layers, as can be summarized below:

- 1- Input Layer: The input layer of a neural network is composed of artificial input neurons, and brings the initial data into the system for further processing by subsequent layers of artificial neurons. The input layer is the very beginning of the workflow for the artificial neural network.
- 2- A hidden layer in an artificial neural network is a layer in between input layers and output layers, where artificial neurons take in a set of weighted inputs and produce an output through an activation function. It is a typical part of nearly any neural network in which engineers simulate the types of activity that go on in the human brain.
- 3- The output layer in an artificial neural network is the last layer of neurons that produce given outputs for the program. Though they are made much like other artificial neurons in the neural network, output layer neurons may be built or observed in a different way, given that they are the last “actor” nodes on the network. ([Hinton et al., 2006](#))

2.4.2 ANN and Civil engineering applications

A reliable model for any storm or sanitary network is essential in order to provide a tool for predicting its performance and to form a basis for controlling the operation of the process.

ANN Technique has the ability to build a prediction model, there are much application used ANN technique such as : rainfall intensity , coefficient of discharge ,inflow of reservoir, water quality index ([SUJANA PRAJITHKUMAR et al.](#)), sedimentation load ([Bouzeria et al., 2017](#)). It is consist of three layers input layers, hidden layers (Treatment layers), and output layers.

[Dawson and Wilby \(1998\)](#) studied the prediction of flow using actual hydrometric data in two flood-prone UK areas by using an artificial neural network (ANN). The result found the prediction similar goodness to that obtain from operational systems for the River Amber.

[Tokar and Johnson \(1999\)](#) evaluated the prediction of daily rainfall as a function of daily precipitation, temperature, and snowmelt for the Little Patuxent River watershed in Maryland by using an artificial neural network (ANN). The study concludes that prediction data from ANN more accuracy and flexibility, and the study concluded that using ANN shortens calibration data, and reduces the length of the time spent in the calibration of the models.

[Jain et al. \(1999\)](#) predicted inflow for the reservoir and operation it by using artificial neural network (ANN) in the state of Orissa, India as a case study, The study found that the ANN is using in effect for operation of reservoir and prediction of inflow of it and ANN strong device for mapping of input –output.

[Luk et al. \(2001\)](#) Studied extrapolate of the rainfall. By using artificial neural network ANN that represents a nonlinear mapping between inputs and outputs. A Case study in the western suburbs of Sydney, it concludes the result of forecasting by the realization of ANN.

[Al-Ansari et al. \(2014\)](#) Evaluated the rainfall quantity for long term(winter , spring , summer , autumn) by using an artificial neural network (ANN). The study was take Sinjar area, northwest of Iraq as a case study. The result discovers that the average rainfall decrease.

[Alfatlawi and Alshakli \(2015\)](#) forecasted coefficient of discharge for stepped morning glory spillway by using an artificial neural network (ANN). The study shows that the coefficient of discharge of stepped morning glory Spillway reduces as rising (head/length) and/or (head/radius) ratios.

Chapter Three

MODELING AND CASE STUDY**3.1 Stages of the research**

This chapter involves three main stages. In each stage, all required data, parameters, and characteristics will be discussed in next subsections.

The first stage will involve the Artificial Neural Network technology (ANN), brief description, its work methodology, and characteristics of the input parameters. The ANN technique will be performed utilizing the ANN program version. It's worth to mention that although used ANN version has stopped supporting by the created company nowadays, but it can overcome the required model. The ANN technique has approved its efficiency and accuracy in the model prediction that generated from any input multiple variables. The input parameters shall include the dependent and independent variables, the rainfall intensity represent the dependent variable while the monthly rainfall, min and max temperature, humidity, wind speed, and sunshine represent independent variables. The outcome of this stage will include one model relating to rainfall intensity and time for future periods.

While the second stage, include steps of applying the resulted model of ANN on the studied network area. The selected network components (pipes and manholes) data takes have been taken as GIS Arc Map shape file. The data have been smoothed and refined using the same program. The output data of GIS and ANN programs have been input to the Storm Water Management Model (SWMM) program to present the final results (flooding accordance and ratio).

The third stage will consist of properties of the case study like location, topography, land use, and sub-catchment area. In addition, the collected data shall be presented in this stage. The description of case study area are generated with the help of GIS ARC Map program. The methodology of the research plan can be shown in Figure (3.1)

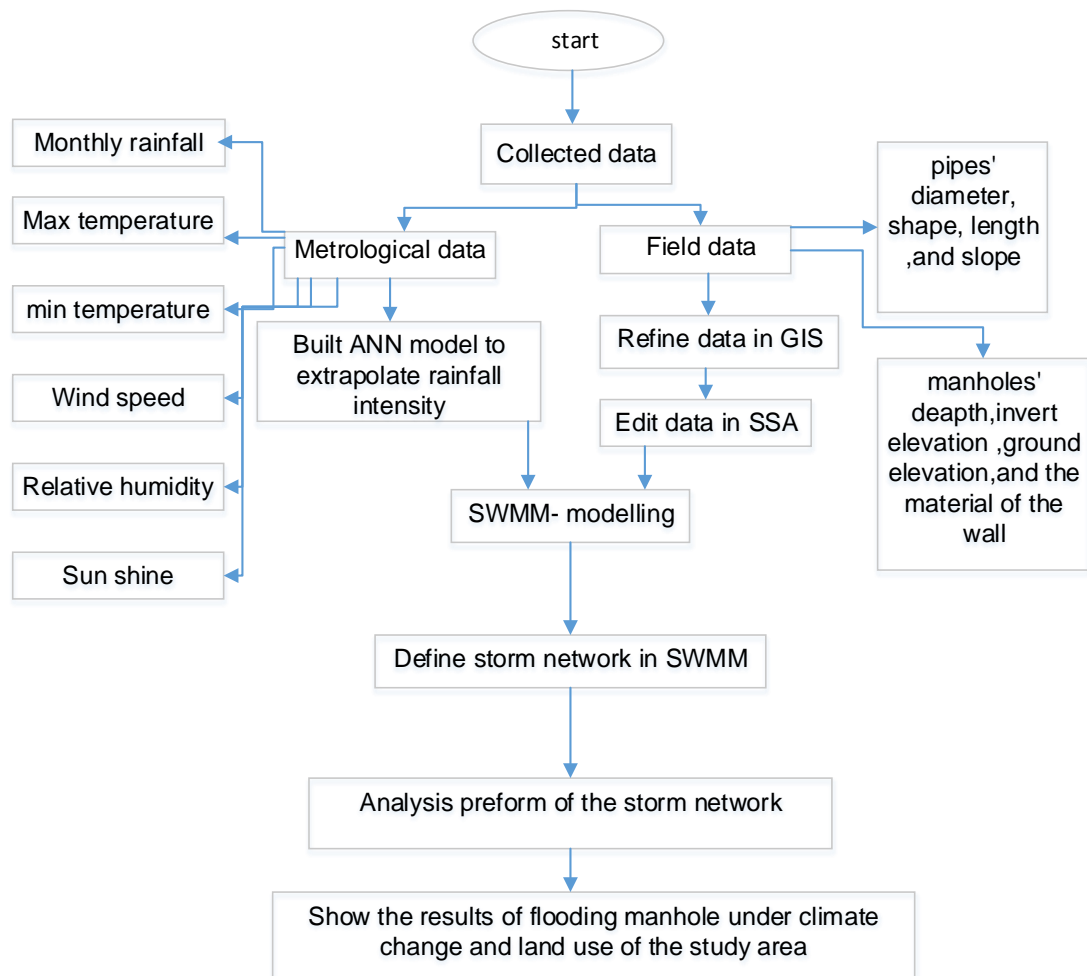


Figure 3-1 Flowchart of the research methodology.

The research plane includes two main programs: artificial neural network (ANN) and storm water management model (SWMM5.1). So, the hydraulic data analyze by ANN program and built a model to extrapolate

rainfall intensity to enter it to SWMM then made simulation and prediction the flooding of the study area.

3.2.1 Artificial neural network (ANN)

3.2.1.1 Description of ANN model

The ANN system consists of at least three main parts. The first part define as input layer. The second part describe as hidden layer which consist of at least one layer and represent the processing of the input layer,while the third part define as the output layer. The number of hidden layer depending on training(Murata et al., 1994). There are no fixed condition to choose nodes of hidden layers ,the network has difficulty generalizing to problems when the numbers of nodes too few in the hidden layer, the network takes an unacceptable period when there are too many nodes in hidden layers (Dawson and Wilby, 1998). The number of input nodes, I, and the number of output nodes, O, in an ANN are dependent on the problem to which the network is being applied. The structure of the neural network can show in Figure (3.2).

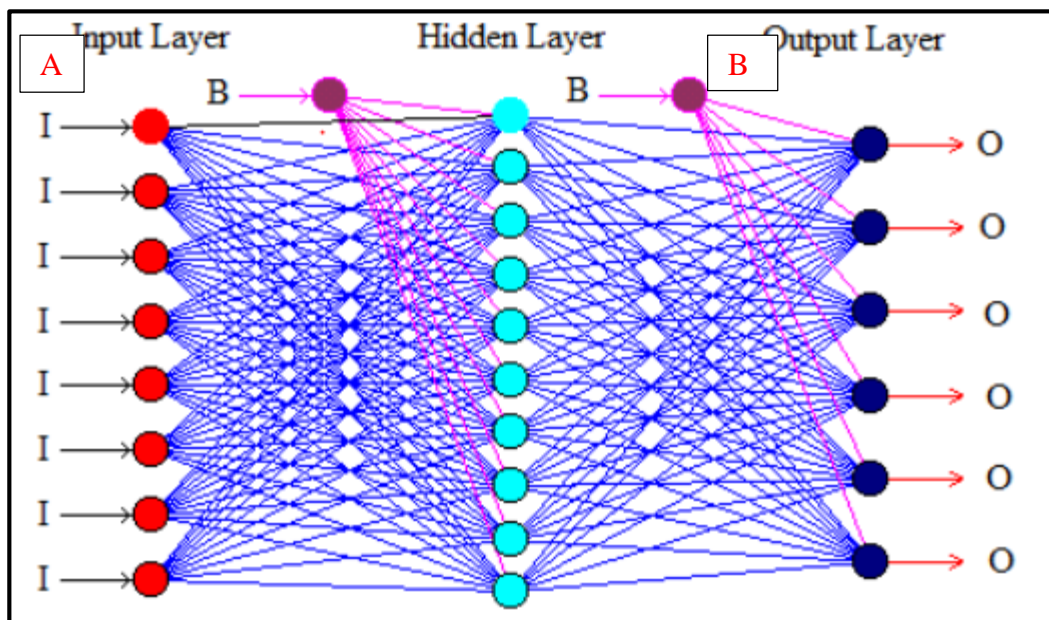


Figure 3-2 Structure of the neural network system(Dawson and Wilby, 1998).

3.2.1.2 Description of the ANN program

The data entered to ANN divided into training data 95% and testing data 5% to validation the result of the program. The program used to application ANN is neural power.

The sequence of the process in the ANN program can be standard as follows:

1. Preparing data file that involves input and output layers.
2. For learning settlements step, and to add learning files after that go to learning configuration to add hidden layers and determine node number and transfer function for each layer, there are six type of transfer function display below.

The ANN program contains several types of the transfer function in the hidden layer, and can be summarized as follows ([Giuseppe Ciaburro and September, 2017](#))

)

- 1- Sigmoid function: This function, as clarified in Equation (3.1), is frequently chosen, due to comfortable, differentiable, monotonic and limited, this mean the sigmoid function well done

$$f(x) = \frac{1}{(1+\exp(-x))} \dots \dots \dots (3.1)$$

- 2- Tanh function: as presented in equation (3.2), is comfortable, differentiable, monotonic, and limited so it is similar to sigmoid but subsequent functions don't have this properties, so this limit the use of this function.

$$f(x) = \tanh x \dots \dots \dots (3.2)$$

- 3- Gaussian function: The Gaussian function as shown in Equation (3.3) used when the input data less probably to contribute to result. Gaussian is even function so it gave the same output for input value for positive or negative

$$f(x) = \exp(-x*x) \dots\dots\dots (3.3)$$

- 4- Linear function: as demonstrated in Equation (3.4), used when the output wanted without applying any limitations, the answer gave without any further modification expect doing the input \times weight ,the linear function does not use in the hidden layer.

$$f(x) = x \dots\dots\dots (3.4)$$

- 5- Threshold linear function: as presented in Equation (3.5), need difficult limitation when the function applies the output either an exactly single value or not. So this function does not used.

$$f(x) = \mathit{if}(x < 0, 0, \mathit{if}(x > 0, 1, x)) \dots\dots\dots (3.5)$$

- 6- Bipolar linear function: as clarified in Equation (3.6), This function type has the capability to release node above limitation but it has adopted in the lower region.

$$f(x) = \mathit{if}(x < (-1), (-1), \mathit{if}(x > 1, 1, x)) \dots\dots\dots (3.6)$$

the sigmoid function is the best transfer function ,the description of all transfers function from ([MLNnotebook, 2017](#))

The error between outputs of the network and target outputs are computed at the end of each process, and then the processing continues to training until the error less than selected.

There is important factors in the learning process (Weights and biases):

Weights are a very significant factor in the ANN program to converting an input to impact the output. This function like to slope in linear regression, wherever weight is multiplied to the input to add up to form the output. Weights are numerical parameters, which determine how strongly each of the neurons affects the other.

For example, if the inputs are x_1 , x_2 , and x_3 , then the synaptic weights to be applied to them are denoted as w_1 , w_2 , and w_3 ,

The Output is:

$$y = f(x) = \sum x * w \dots\dots\dots (3.7)$$

Bias is similar the intercept added in a linear equation. It is an additional parameter, which is used to adjust the output along with the weighted sum of the inputs to the neuron.

The processing done by a neuron is thus denoted as :

$$output = sum (weight * input) + bias \dots\dots\dots (3.8)$$

The abstract of the ANN learning process can be presented in Figure (3.4).

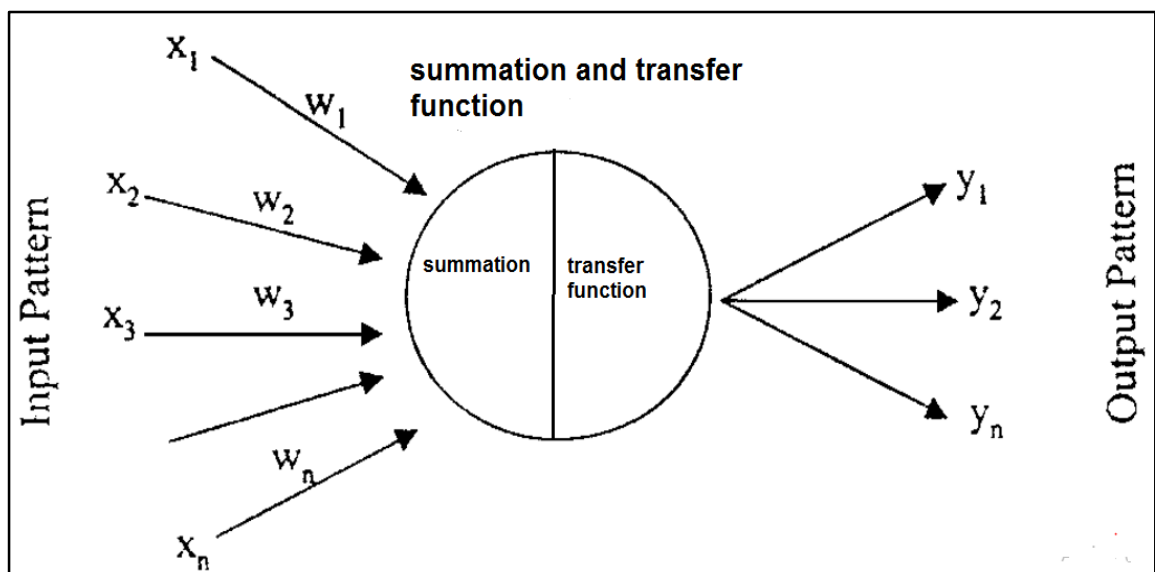


Figure 3-3 learning process of artificial neural network (X_n : input, W_n : weights, Y_n : outputs)([Cho et al., 2014](#))

3.2.1.2 Determining the number of hidden layers

When looking at the structure of dense layers, there are really two decisions to make about these hidden layers: the number of hidden layers in the neural network and the number of neurons in each of these layers. At the first, the study will look at how to determine the number of hidden layers to use with the neural network.

Before deep learning problems that require more than two hidden layers were rare .simple data sets will often require two or fewer layers. However, additional layers can be useful with complex datasets include time-series or computer vision. Table (3.1) summarizes the ability of several common layer architectures.

Table 3-1 Determining the Number of Hidden Layers([Luk et al., 2001](#)).

Number of Hidden Layers	Result
>2	Extra layers can learn complex representations of layers (a type of automatic feature geometry).
2	Can represent arbitrary decisions that are arbitrarily defined with rational activation functions and can round any smooth layout of any accuracy.
1	Round any function that contains a continuous layout from one distance to another
none	Represent only deterministic decisions or functions.

3.2.1.3 The Number of neurons in the hidden layers

Overall,for neural network structure determine the number of neurons in the hidden layers is a very important part .Although these layers do not directly react with the outer environment, they have a large influence

on the final output. Both the number of neurons and the number of hidden layers in each of these hidden layers must be carefully considered.

Underfitting will happen when the neurons in the hidden layers too few. Overfitting happened when the number of neurons in the hidden layers too many. Several problems occur with the overfitting. First, more than installation occurs when the neural network has a large amount of information processing capacity that the limited amount of information in the training group is not enough to train all the neurons in the hidden layers. A second problem can occur even when the training data is sufficient. A large number of neurons in hidden layers can increase the time it takes to train the network. The amount of training time can be increased to the extent that it is impossible to train the neural network adequately. Generally, the number of neurons should be moderate between too many and too few in the hidden layers Figure (3.3) illustrates the above mentioned problems.

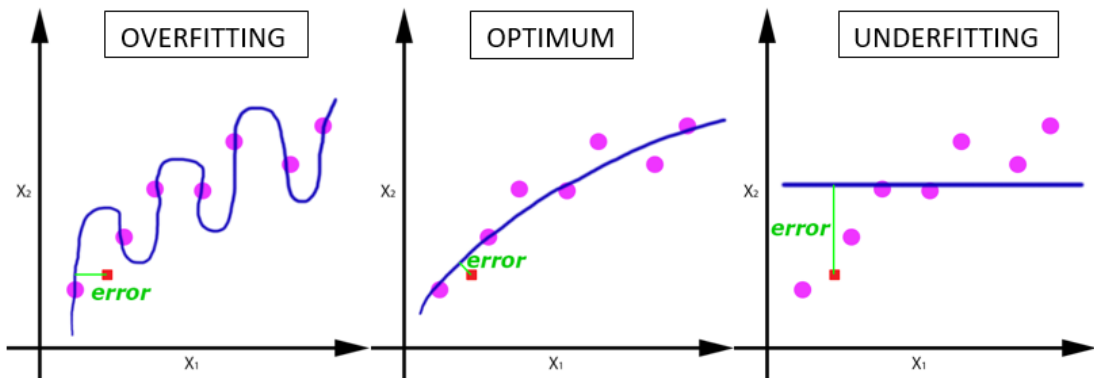


Figure 3-4 an example for the effect of a number of neurons on ANN model accuracy ([Murata et al., 1994](#)).

A few rules of thumb that suggested choosing hidden layers. There are many rule-of-thumb methods for determining an acceptable number of neurons to use in the hidden layers, such as the following:

- 1- Determining the number of neurons in the hidden layers that should be between the size of the input layer and the size of the output layer.
- 2- The number of hidden neurons should be $2/3$ the size of the input layer, plus the size of the output layer.
- 3- The number of hidden neurons should be less than two-time the size of the input layer.

It is uncertain to start throwing random numbers of layers and neurons at the network this led to very time consuming, so the selection of the layers and neurons depend on the trial and error, three rules upon providing a starting point to consider.

3.2.1.3 Building the ANN model

Artificial neural network model (ANN) building depends on input layers and output layers. Input layers include (year, month, monthly rainfall total (mm), mean max temperature (°C), mean min temperature(°C), mean relative humidity (%), mean wind speed (m/s), mean sun shine (hrs./day). Output layer includes (rainfall intensity (mm) for 1 hrs.). month and rainfall intensity(I) input to program by formula (N+1 , N-1) means for each neuron took before neuron and after neuron to determine the location of it accuracy as shown in Table(3.2).

Table 3-2: formula of data using in ANN.

y	N	N+1	N-1	R	min.tem perature	max.tem perature	hum	wind	sun.sh	I	I+1	I-1
			1									1.6
1981	1		2	12.5	5.3	17	75	2.7	6.8	1.6		2
1981	2	1	3	4.9	7.5	19.3	63	2.8	7.2	2	1.6	2
1981	3	2	4	12.8	11.1	24.7	59	3	8.3	2	2	0.7
1981	4	3	5	4.3	14.5	29.1	44	3.2	8.4	0.7	2	0
1981	5	4	6	0.001	19.2	34	36	3.6	8.8	0	0.7	0
1981	6	5	7	0.001	24.9	40.5	33	4	12.1	0	0	0
1981	7	6	8	0	28.6	44.1	27	4.5	11.9	0	0	0

The sequence of rainfall intensity prediction has been achieved using ANN which includes the following steps:

1. Building ANN model for 10 yrs. (first model) due to rainfall intensity available (output layer) from General Authority for meteorological and Seismic Observation (G.A.M.S.O) only for 10 yrs. for period (1981-1990).
2. ANN model for 10 yrs. (first model) used to predict rainfall intensity for period (1991 – 2008).
3. From Iraqi Agromet Center Data (I.A.C.D) the rainfall intensity from 2008 to 2016 was found.
4. Built ANN model (second model) for period (1981-2016).
5. SPSS program made simulation to find input layer (climate change) for future period (2017-2070).
6. Input data found from step 5 into the second model to find rainfall intensity for the period (2017-2070).

Five models were built depending on the number of hidden layers after that choosing the best depend on several statistical indexes include root mean square error RMSE and correlation coefficient Square R^2 , so the best model chosen that has least RMSE(nearest to zero) and greater R^2 (nearest to 1)

3.3 Storm water management model (SWMM)

3.3.1 Description of SWMM

Storm Water Management Model (SWMM) developed by US EPA , first developed in 1971, SWMM is a model used to simulation runoff quantity and quality from urban areas, It is used for single event or long-term (continuous). The runoff component of SWMM run on a collection of sub catchment areas that receive precipitation and produce runoff and pollutant loads, this runoff transports during a system of pipes, channels, storage/treatment devices, pumps, and regulators. SWMM5.1 keeps track of

the flow rate, flow depth, runoff volume generated within each sub-catchment, and the quality of water in each pipe and/or channel at different time steps of the simulation. SWMM Version 5.1, which is running under Windows are used in the present study as in the present study as it provides an integrated environment for editing, inputting data of the study area, running hydrologic, hydraulic and water quantity simulations, and viewing the results in a variety of formats. These include color-coded drainage area and conveyance system maps, time series graphs and tables, profile plots, and statistical frequency analyses ([Rossman, 2010](#)).

3.3.2 System flow routing

The process of determining the time and magnitude in any point of the drainage system based on known or assumed hydrographs at one or more point in upstream called the flow routing. There is three levels of sophistication used in SWMM for flow routing to solve the conservation of mass and momentum equations for conduits of open channel and this equation is the comprehensive one-dimensional ([Rossman, 2010](#)). The SWMM lets the modeller select the level of sophistication to solve the equations. The three levels of flow routing in SWMM are steady flow routing, kinematic flow routing and the dynamic flow routing. In this study, the dynamic flow routing has been used because it has the ability to account for pressurized flow, channel storage, flow reversal, backwater and entrance/exit losses so the dynamic flow routing considers the most theoretically precise consequences. In dynamic routing, the full flow closed pipe represent as Aeron pressurized flow and the flooding happens when the water depth skips the maximum available depth at the node.

For the Saint-Venant the flow can be represented by the two partial differential equations. First the momentum [eq. 3.9]:

$$\frac{1}{A} \frac{\partial q}{\partial t} + \frac{1}{A} \frac{\partial}{\partial x} \left[\frac{q^2}{A} \right] + g \frac{\partial y}{\partial x} - g [S_0 - S_f] = 0 \quad \dots [3.9]$$

Second the continuity [eq 3.10]:

$$\frac{\partial A}{\partial t} + \frac{\partial q}{\partial x} = 0 \quad \dots [3.10]$$

Where:

q = The flow rate in the system (m³/sec).

g = The acceleration due to gravity (m/s²).

y = The depth of flow (m).

S_0 = The bed slope (m/m).

S_f = The friction slope (m/m).

A = The cross-sectional area (m²).

x = The distance along the channel (m).

and t = The time (sec) ([Pitt et al., 1999](#)).

The terms in the momentum equation describe as follow:

$\frac{1}{A} \frac{\partial q}{\partial t}$ = The change in momentum due to the change in velocity over time.

$\frac{1}{A} \frac{\partial}{\partial x} \left[\frac{q^2}{A} \right]$ = The change in momentum due to the change in velocity along the channel.

$g \frac{\partial y}{\partial x}$ = the change in the water depth along the channel.

$g [S_0 - S_f]$ = gravity force term, proportional to the bed slope and friction force term, proportional to the friction slope.

While the terms in the continuity equations represent as follow: -

$\frac{\partial A}{\partial t}$ = The rate of change of area with time.

$\frac{\partial q}{\partial x}$ = The rate of change of channel flow width distance.

The two partial differential equations solve numerically as done for runoff surface routing. The dynamic flow routing used the manning equation to determine flow rate [Q]. the Hazen-Williams or Darcy-Weisbach equation

is used for circular force main shapes under pressurized flow ([Rossman, 2010](#)).

3.3.3 Infiltration model

The infiltration in SWMM can model in three different formulas Horton, Green-Ampt and SCS curve number method. In this research, the Green-Ampt model has been used. There is no unified vision for preference one way for others and the Green-Ampt model is more physically-based ([Gironás et al., 2009](#)) The Green -Ampt method is a simplify, empirical model to represent the infiltration process. It develops from the application of Darcy's law and the law of conservation of mass. Green-Ampt suppose that a sharp wetting front exists in the soil column separating the soil where the above wetting front is fully saturated and the soil below is at the initial moisture content ([Rawls et al. \(1983\)](#)). This method is a function of the soil's hydraulic conductivity, soil suction head, porosity and initial moisture deficit of the soil. The general [eq.3.11,3.112] of the Green-Ampt is given below ([Rawls et al., 1983](#)):

$$f = K * \left\{ \left[\frac{\Psi * n}{F} \right] + 1 \right\} \quad \dots [3.11]$$

$$F = K * t + \Psi * n * \ln \left\{ 1 + \left[\frac{F}{\Psi * n} \right] \right\} \quad \dots [3.12]$$

Where:

f = Infiltration capacity [mm/h].

K = Saturated hydraulic conductivity [mm/h].

Ψ = Suction head [mm].

n = Available porosity which is calculated as the effective porosity [θ_e] minus initial soil water content saturated [θ_i] for initially dry soil or it is the difference between the soil's porosity [ϕ] and its field capacity [**FC**] for

completely drained soil [where θ_e estimate as the total porosity[ϕ] minus residual saturation, θ_r].

F = Accumulative infiltration [mm].

Rawls et al. (1983) have been considered these equations was under the assumption that the depth of ponding on the soil surface is negligible and analyzed approximately 5000 soils samples through the United States and published values for the Green-Ampt parameters as shown in Table (3.3):

Table 3-3 Parameters of Green-Ampt for different soil type, Rawls et al. (1983).

Soil texture class	K	Ψ	Φ	FC	WP wilting point
Sand	4.74	1.93	0.437	0.062	0.024
Loamy Sand	1.18	2.4	0.437	0.105	0.047
Sandy Loam	0.43	4.33	0.453	0.19	0.085
Loam	0.13	3.5	0.463	0.232	0.116
Silt Loam	0.26	6.69	0.501	0.284	0.135
Sandy Clay Loam	0.06	8.66	0.398	0.244	0.136
Clay Loam	0.04	8.27	0.464	0.31	0.187
Silty Clay Loam	0.04	10.63	0.471	0.342	0.21
Sandy Clay	0.02	9.45	0.43	0.321	0.221
Silty Clay	0.02	11.42	0.479	0.371	0.251
Clay	0.01	12.6	0.475	0.378	0.265

3.3.4 Building SWMM model

The result of the climate change scenario represent as rainfall intensity from (ANN) model for predict period (2017-2070) were used on Al-Abbas section in Karbala city.

So, the following steps are followed in SWMM to model rainfall intensity on a study area:

1. Collection the field data for the Al-Abbas section from Directorate of the Sewage of Karbala (D.S.K) include pipe and manhole and its properties.
2. Assign set of option and properties of an object were used as default.
3. Refine data in GIS.
4. Edit data and connect the area to a nearest manhole in a storm and sanitary Analysis (SSA), which as program of AutoCAD civil3d Package.
5. Enter in SWMM and make analysis performs.
6. Show the results of the simulation.

3.4 Study area and data

In this subsection, a description of the study area, land use, topography of the case study, field and metrological data shall be presented with details. It worth to mention that the raster map of GIS has been provided by the Ministry of Construction, Housing, Municipalities and Public Works (M.C.H.M.PW). The map has been captured in the year 2016, which is the last version has been taken for the study area.

3.4.1 Description of the study area

Geographically, the study area (Al-Abbas quarter) is located to the north-east of the center of Karbala city , Iraq, between latitudes $32^{\circ}37'56.7''\text{N}$ - $32^{\circ}38'15.9''\text{N}$, and longitudes $44^{\circ}02'39.8''\text{E}$ - $44^{\circ}03'08.9''\text{E}$, as shown in Figure (3.5). The distance is 2 km between the center of the study area and center of Karbala city. The total area approximately is 0.373 km^2 , total impervious area approximately is 0.257 km^2 , (70% of total area) including (roofs and paved area), the previous area approximately is 0.116 km^2 , (30% of total area) including (green area and unpaved area). It is a flat surface with low slopes and sandy, clay soil. Regional elevations range from 28 m to 43 m above sea level. The network of the case study is storm water network divided into 64 sub-catchment. Some new developments are

expected to take place surrounding the case study according to Kerbela master plan. The climate of the case study shown in Table (3.4).

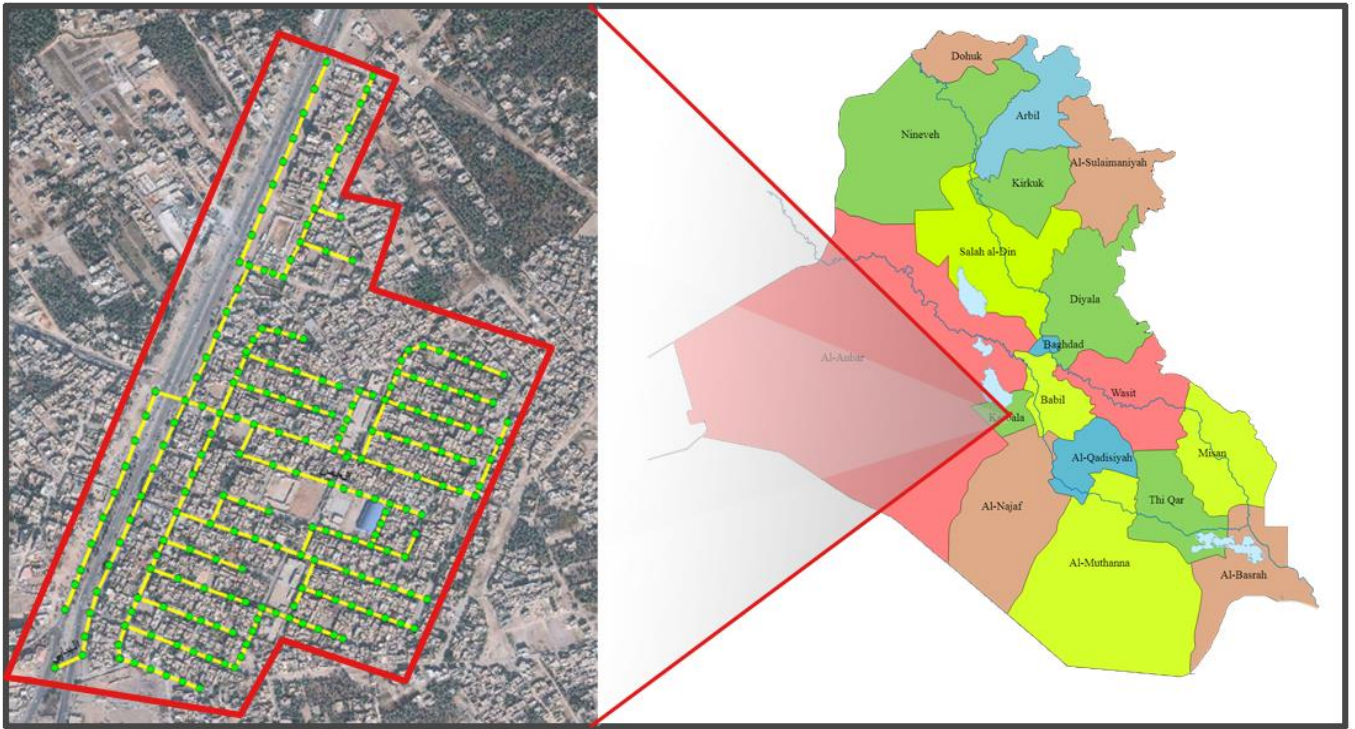


Figure 3-5 Geographical location of the study area according to Iraqi map (M.C.H.M.PW).

Table 3-4 clarify min and max value of climate of the case study ([Meehl et al., 2007](#)).

Climate	Min value	Max value
Temperature (c°)	1.6	46
Monthly rainfall (mm)	0	48
Humidity (%)	23	83
Wind speed (m/s)	1.9	5.2
Sun shine (hrs./day)	5.2	12.6

3.4.2 Land use

Identifying characteristics of land use of a specific location is necessary to assign a quantity of water runoff that cannot be absorbed by land media. Land use area of the case study divided into three main parts; paved area, gardens and service building, and houses. The paved area occupied about 8% of total land use area, which considers the smallest portion. The second part, which occupies about 12% of total land use area, consists of gardens and service buildings, such as schools and hospitals. While the third part, which occupied by houses, forming about 80% of total land use area. Figure (3.6), clarifies land use area of the selected case study. It worth to mention that the aforementioned figure has been created utilizing ARCMAP program of GIS package.



Figure 3-6 land use of Al-Abbas quarter (M.C.H.M.P.W).

3.4.3 The topography

The contour map of the study area has been generated a 0.5 meter contour interval using GIS (geographic information system) software. The map has been created utilizing from the DEM (Digital elevation model) surface raster file provided from the USGS (U.S Geological survey) ([USGS, 2018](#)). After importing the DEM file in GIS (ARC MAP V10.4.1), random points have been generated for the study area only, after that, the Z elevation was extracted from the DEM file to the generated Radom points. The resulted processes were point's data with XYZ information. Finally, the

contour map has been generated utilizing ARC tool box that provided as a package with the GIS software. It is worth to mention that Karbala city has a flat ground and the earth topography is ranged from 28-34 m of the steady area. This illustrates in Figure (3.7).

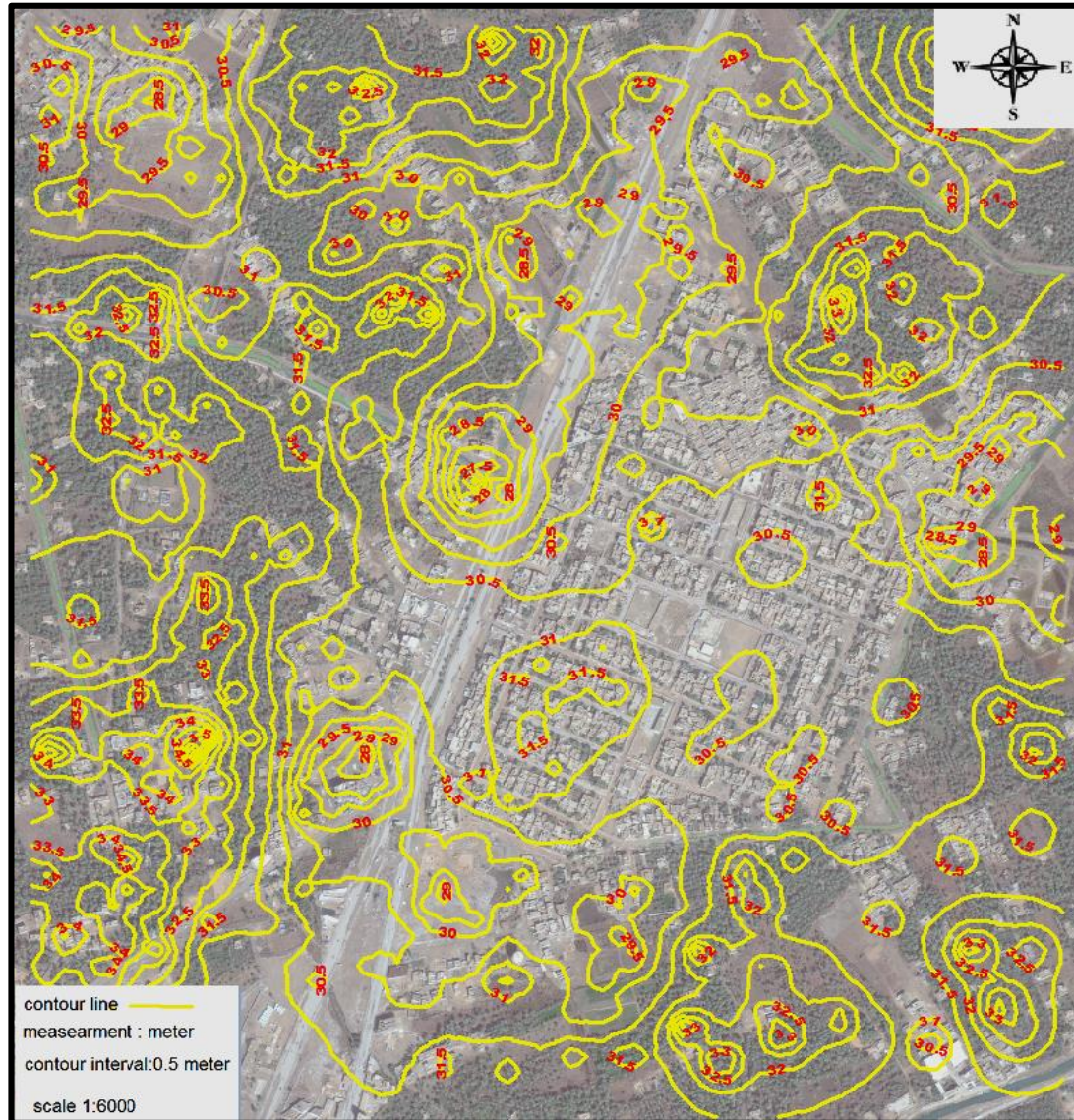


Figure 3-7 topography of the study area ([USGS, 2018](#)).

3.4.4 Sub catchment

Sub catchments divided into pervious and impervious sub areas. Surface runoff of the pervious subarea can Infiltrate into the upper soil zone, but not through the impervious subarea. Impervious areas can be divided into two types: sub catchment have depression storage and sub catchment do not

contain depression storage. Runoff flow either routed from sub area in sub catchment to another sub area, or both sub catchment can drain to the sub catchment outlet. The total area approximately to 0.373 km² and the area divided into 64 sub catchments as shown in Figure (3.8).

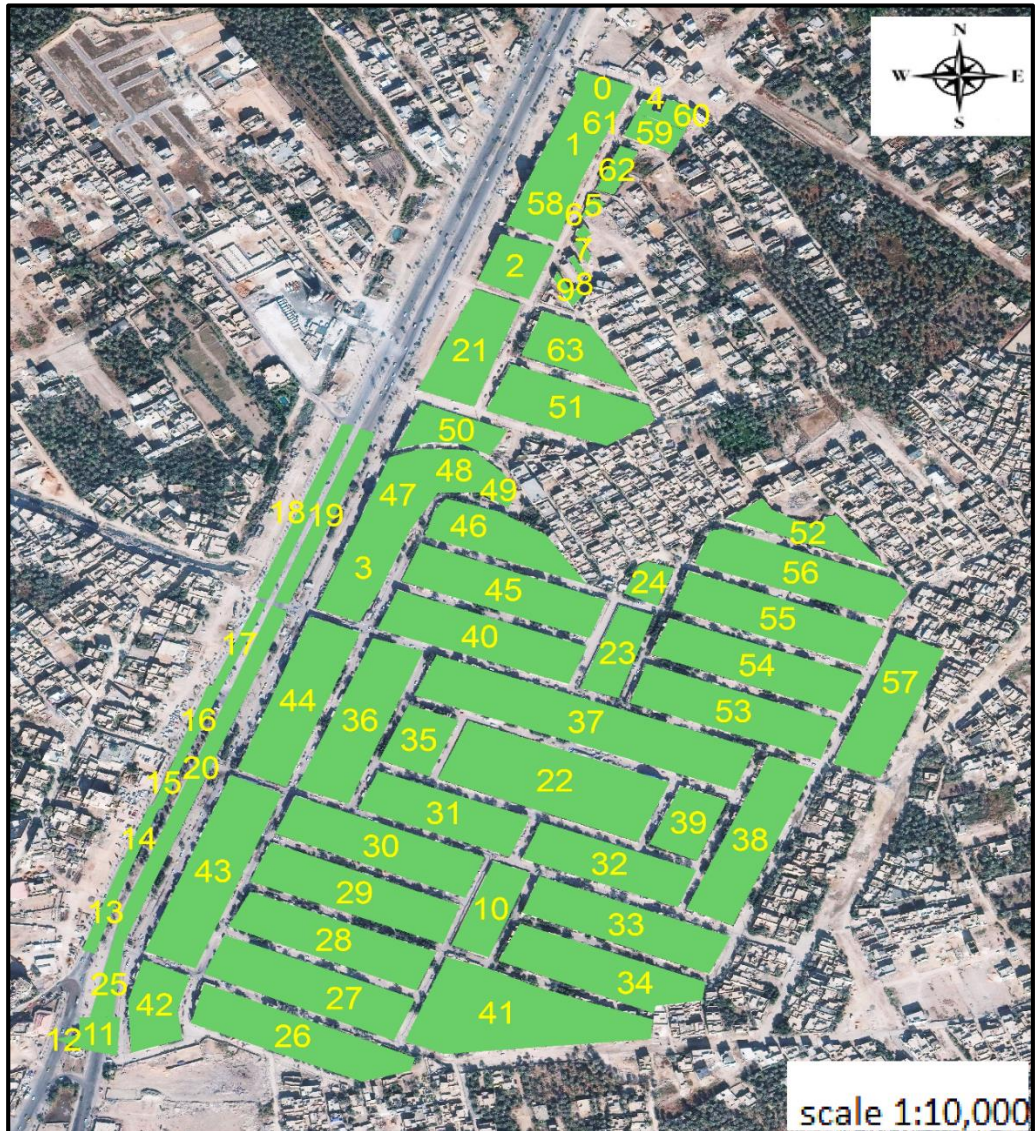


Figure 3-8 the distribution of sub catchment areas in the study area (M.C.H.M.P.W.).

3.4.5 Field data

Field data collection for the case study Al-Abbas quarter from (D.S.K) includes pipe and manhole and their properties. The collected data

has been drawn in GIS ARCMAP as point and line shape files. After drawing and refining data, the network has been imported to SWMM program.

3.4.5.1 Pipes properties

The pipe is a type of Conduits that is used to transfer water from one node to another in the conveyance system. The spatial distribution and the upstream and downstream altitude must be a supply for each pipe in the model to gain the slope and to set the flow direction of the fluid. The study area contain 222 pipes that have circular shape, the length of the pipes between (2-68) m and the diameter of the pipe of the network between (315-600) mm as shown in Figure (3.9) The pipes made from polyvinyl chloride [PVC] and the Manning roughness coefficient values for the pipes are shown in the Table (3.5) below where the manning value for the PVC pipe [plastic pipe] is 0.011.

Table 3-5 Values of Manning roughness coefficients for different materials of pipes([Rothman et al., 1998](#)).

The material of the pipe	N
Plastic pipe	0.009
Well-planed timber evenly laid	0.009
Neat cement. Very smooth pipe	0.01
Unplanned timber. Cast-iron pipe of ordinary roughness	0.012
Well-laid brick work. Good concrete. Riveted steel pipe. Well-laid vitrified clay pipe	0.013
Vitrified tile and concrete pipe poorly jointed and unevenly settled. Average brick work	0.015
Rough brick. Tuberculation iron pipe	0.017
smooth earth or firm gravel	0.02
Ditches and rivers in good order , some stones and weeds	0.03
Ditches and rivers with rough bottoms and much vegetation	0.04

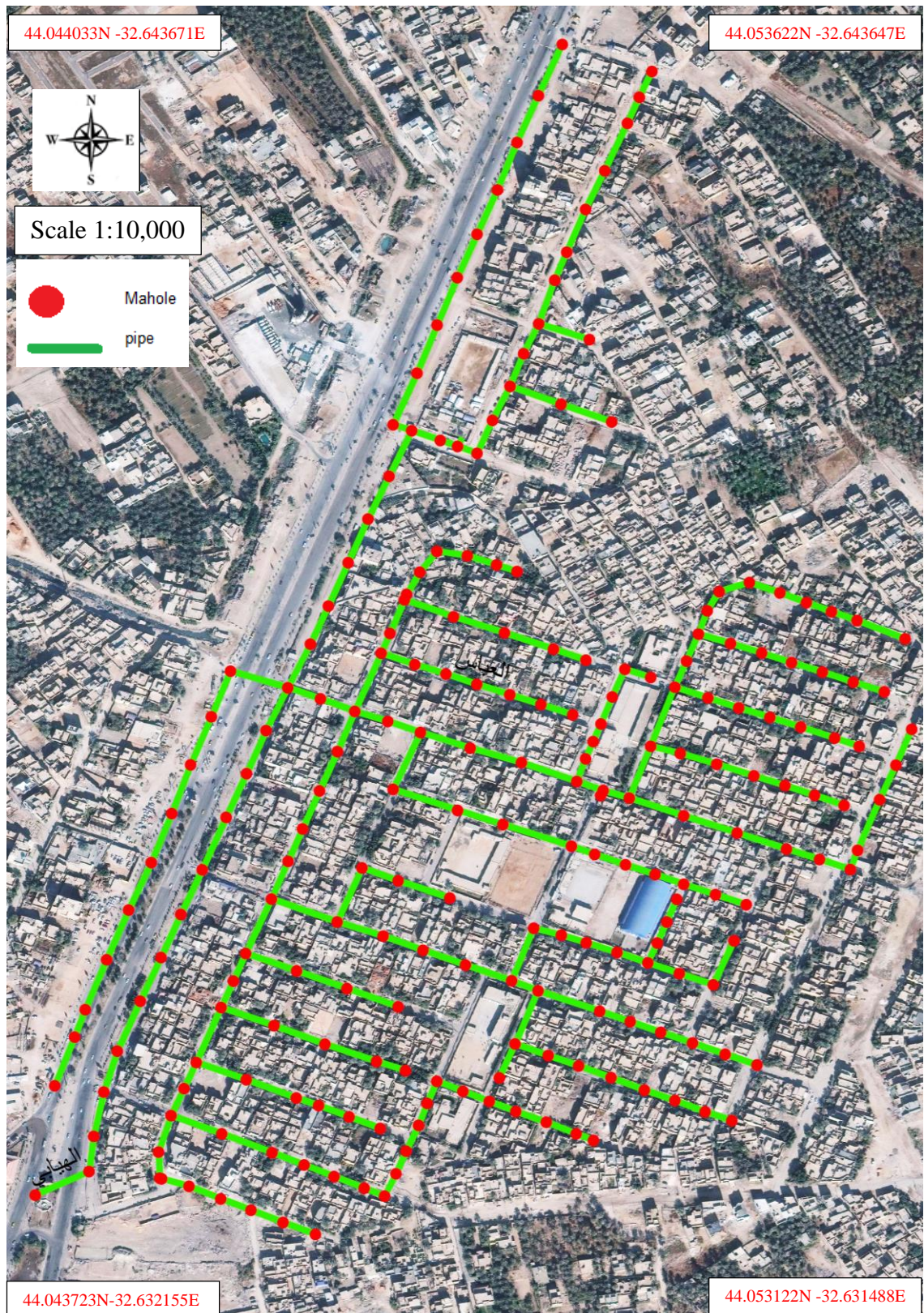


Figure 3-9 the storm drainage network of Al-Abbas quarter(M.C.H.M.PW)..

3.4.5.2 Manholes typies

The Wall of the manholes has been made with concrete materials. The maximum depth of manholes is 3.632 m, and the maximum invert elevation is 27.225 m. Maximum ground elevation of the manholes is 28.81 m. three types of manholes shapes were found in the network and summarized below (D.S.K):

- AS type: a rectangular manhole shape having dimensions 150 cm length and 110 cm width. It is used for shallow depths and it can connected with 250 mm pipes diameter.
- BS type: has a circular cross section area of 110 cm, used for medium depths. Three pipes diameters can be connected to such manhole are 250 mm, 315 mm, and 400 mm.
- CD type: has a circular cross section area of 150 cm, used for deep cases. Four pipes diameters can be connected to such manhole are 400 mm, 600 mm, and 715 mm.

3.4.6 Metrological data

metrological data has been collected from the (G.A.M.S.O) for period from 1980 to 2016 including; monthly rainfall (mm), mean maximum temperature (°C), mean minimum temperature (°C), mean relative humidity (%), mean wind speed (m/s), mean sun shine (hr. /day). While the collected data for the period from 1981 to 1990 included rainfall intensity for Karbala station in (mm) for 1 hour. This data use in ANN program. Figures (3.10) through (3.16) shows the average of (monthly rainfall, mean max temperature, mean min temperature, mean relative humidity ,mean wind speed, mean sun shine) for 36 yrs., and the average of rainfall intensity for 10 yrs, consequently.

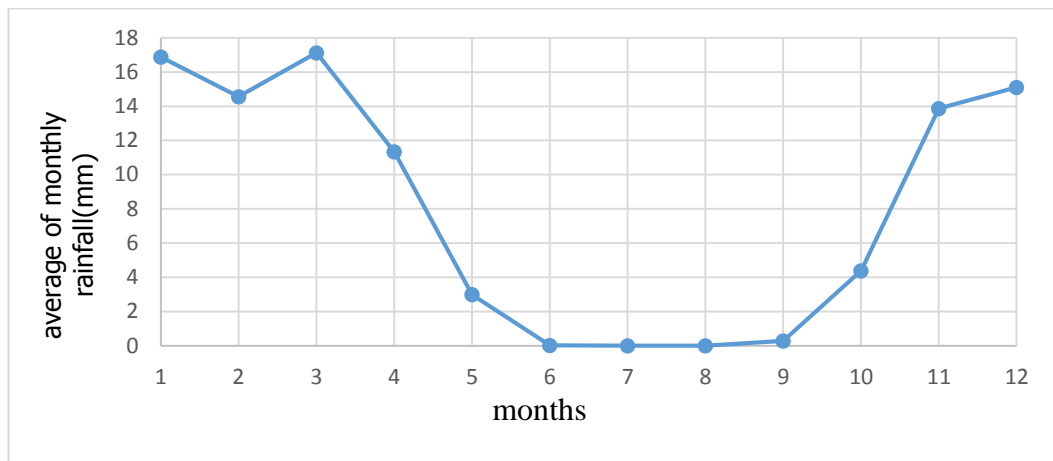


Figure 3-10 the average of montly rainfall for period (1980-2016).

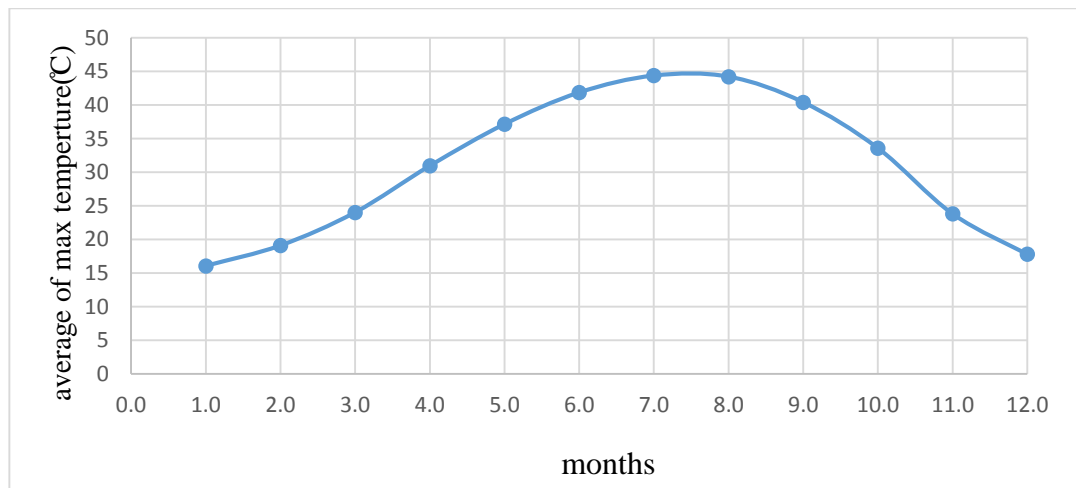


Figure 3-11 the average of max temperture for period(1980-2016).

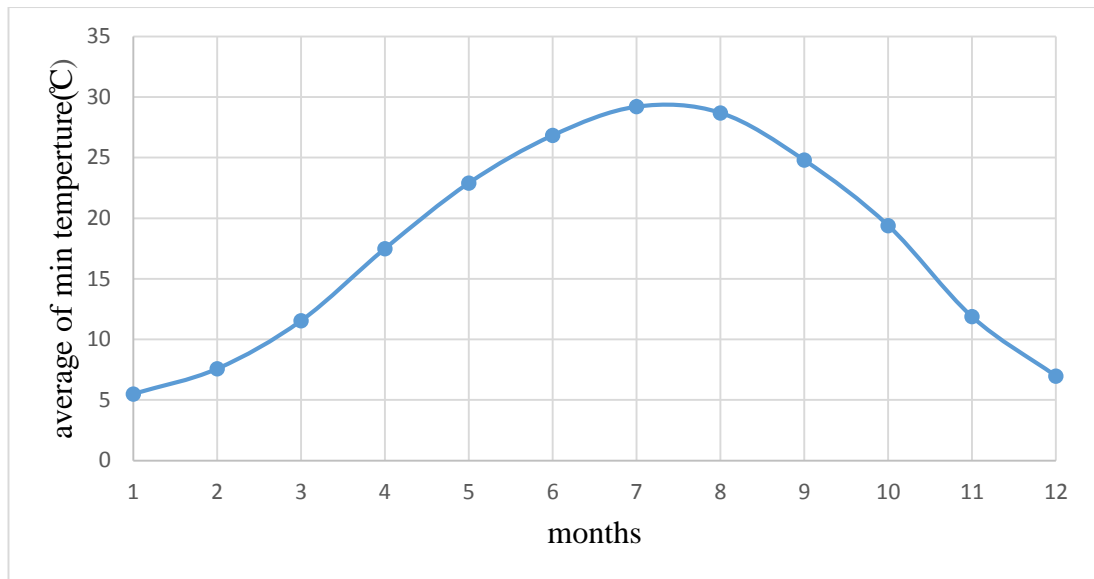


Figure 3-12 average of min temperture for period(1980-2016).

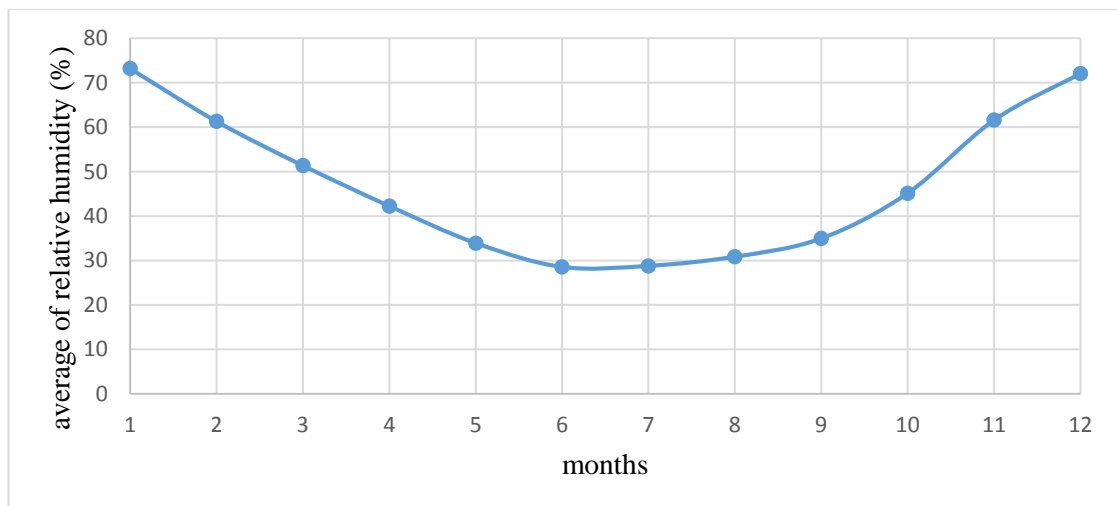


Figure 3-13 average of relative humidity for period(1980-2016).

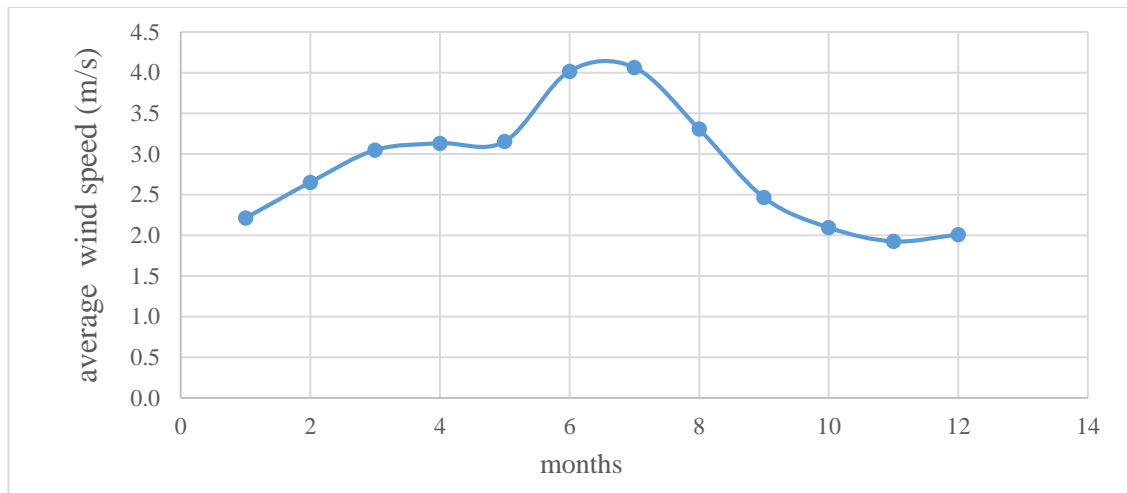


Figure 3-14 average of wind speed for period(1980-2016).

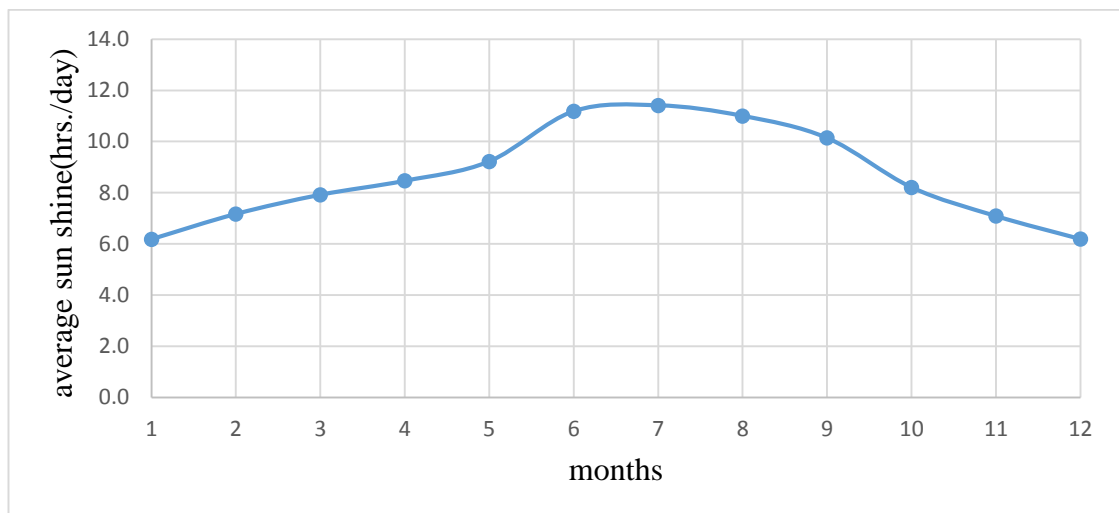


Figure 3-15 average of sun shine for period(1980-2016).

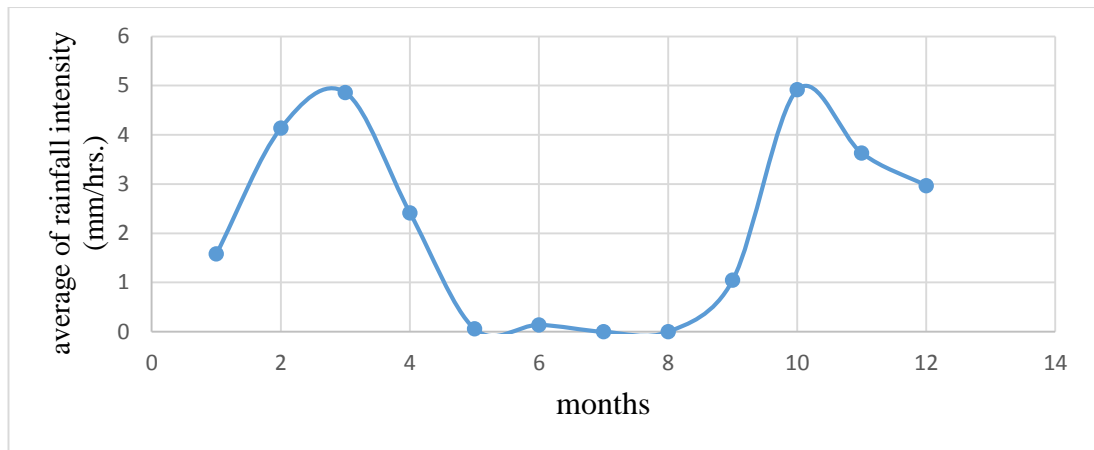


Figure 3-16 average of rainfall intensity for period (1981-1990).

3.5 Suggestion scenario

Land use is an important factor that should be taken into account for future prediction of flooding occurrence, in addition to the change of rainfall intensity. Therefore, In case of forecasting period of the study plan until 2070, any developed area within the study area should be taken into account. The previous analysis of flooding occurrence has been considered only the current land use area.

In the previously suggested scenario, the rational method has been used to calculate flooding discharge. It is the simplest method to determine peak discharge from drainage basin runoff. Equation (3.13) describe rational method parameters:

$$Q=CIA..... (3.13)$$

Where:

Q = Peak discharge, liter/sec

c = Rational method runoff coefficient from Table (3.6)

i = Rainfall intensity, mm/hrs.

A = Drainage area, hectar

Table 3-6 Rational Method Runoff Coefficients([Kadioglu and ŞEN, 2001](#)).

Ground Cover	Runoff Coefficient, c
Lawns	0.05 - 0.35
Forest	0.05 - 0.25
Cultivated land	0.08-0.41
Meadow	0.1 - 0.5
Parks, cemeteries	0.1 - 0.25
Unimproved areas	0.1 - 0.3
Pasture	0.12 - 0.62
Residential areas	0.3 - 0.75
Business areas	0.5 - 0.95
Industrial areas	0.5 - 0.9
Asphalt streets	0.7 - 0.95
Brick streets	0.7 - 0.85
Roofs	0.75 - 0.95
Concrete streets	0.7 - 0.95

Chapter Four

RESULTS AND DISCUSSION**4.1 Topics of search results**

The discussion of search result divided into three parts: the first parts display the result of rainfall intensity model and its calibration, the second parts display the results of flooding model and calibration of it, and the third parts display suggestion scenario by calculation the effect of future land use on the storm network of region studied.

4.2 ANN Rainfall intensity model

This part display calibration of ANN model, weight distribution, and effect of climate change on the ANN model.

4.2.1 Learning process of ANN models functions

Learning the ANN program to predict rainfall intensity function requires several input parameters. One of the most important parameters is, type of transfer function and number of hidden layers. No universal accepted criteria for selecting the type of transfer data or number of hidden layers, but several researchers adopted sigmoid function in their research since it can learn faster, and gives optimum results.

In this study, and to ensure that sigmoid function works correctly in the test for training data, several trials have been made for years from (1981-1990) to predict some missing data. Different functions types such as sigmoid, Tanh, Gaussian, and bipolar has been testes to select the best one. Also, for each trialled function, the optimum number of the hidden layer was also checked out, as can be seen in Table (4.1).

Table 4-1 present effect different training function and the number of hidden layers on the strength of the correlated function.

function type	No. hidden layer	R (correlation coefficient)	RMSE (root mean square error)	R ² (determination coefficient)	average R	average RMSE	average DC
Sigmoid	1	0.922	1.285	0.849	0.97475	0.849	0.9515
Sigmoid	2	0.997	0.26	0.97			
Sigmoid	4	0.996	0.267	0.993			
Tanh	1	0.959	1.25	0.92	0.95525	0.95675	0.919
Tanh	2	0.985	0.587	0.97			
Tanh	3	0.977	0.53	0.975			
Tanh	4	0.9	1.46	0.811			
Gaussian	1	0.646	2.4	0.42	0.646	2.4	0.42
Gaussian	2	N/A	N/A	N/A			
Gaussian	3	N/A	N/A	N/A			

*N/A : no accepted

From the previous table, it can be noticed that the average R and RMSE parameters for sigmoid function type, is higher than other types, as mentioned previously by the researchers. It should be noticed that the lowest value of RMSE reflected the best results. Also, the correlated function is highly dependent on a number of hidden layers, for each type of trailed function. It can be noticed that 2 hidden layers for sigmoid function gave better results than others. While increasing hidden layers more than 2 was insufficient in term of time cost and performance of network learning, and this called overfitting.

Therefore, and base on the previous data results, it has been selected sigmoid function with 2 hidden layers as constant parameters for others to test model learning from (1981-2016).

Figure (4.1), (4.2), and (4.3) clarify ANN learning process of a sigmoid- 2 hidden layers incorporated 9 neurons per layer, the relation between observed and correlated data set for the same period, and behavior of RMSE function, respectively. The same consequences are presented in Figures (4.4), (4.5), and (4.6).

For both cases, the learned function tends to fit the observed function through adjusting the node weights process. The weights are modified in each iteration process. So, after a numerous number of iterations, finally the function had been learned successfully (the red color function), and with 0.97 and 0.706 of R and RMSE values for Figure (4.1) and the weights have been reached the stability limit. These results are the best reached and has been taken for testing, as can be seen in the next subsection (calibration model). The same explanation can be adopted for Figure (4.4).

For the RMSE function as presented in Figure (4.3) and (4.6), it has been noticed a continuous reduction in RMSE values with a higher number of iterations. This behavior is reasonable, and sometimes after a certain time of the process, the values begin to slight increase and decrease for a specific limit without any noticeable improvement achieved.

Overall, the maximum values of R and the minimum values of RMSE, have been taken as the main criteria for accepting models.

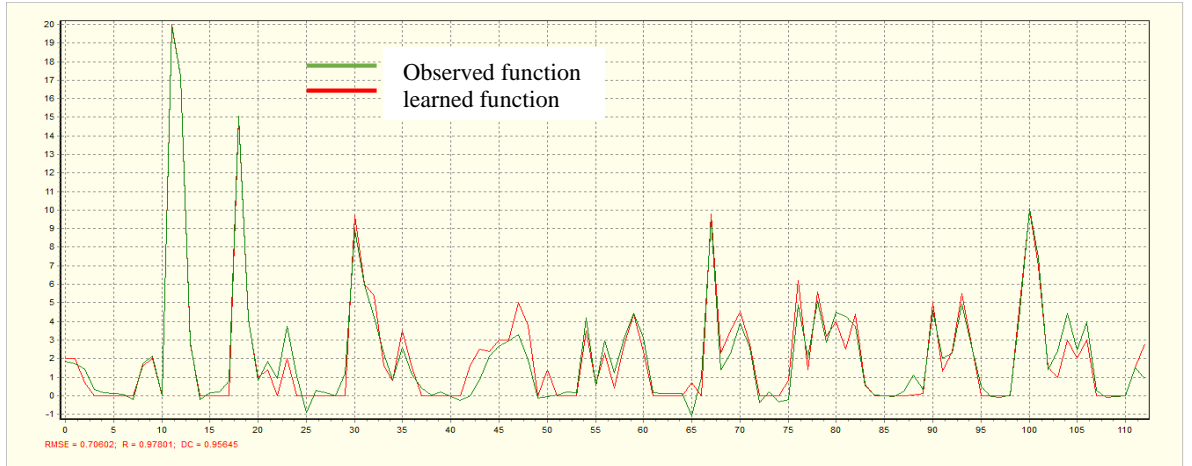


Figure 4-1 ANN learning process of a ten years testing data.

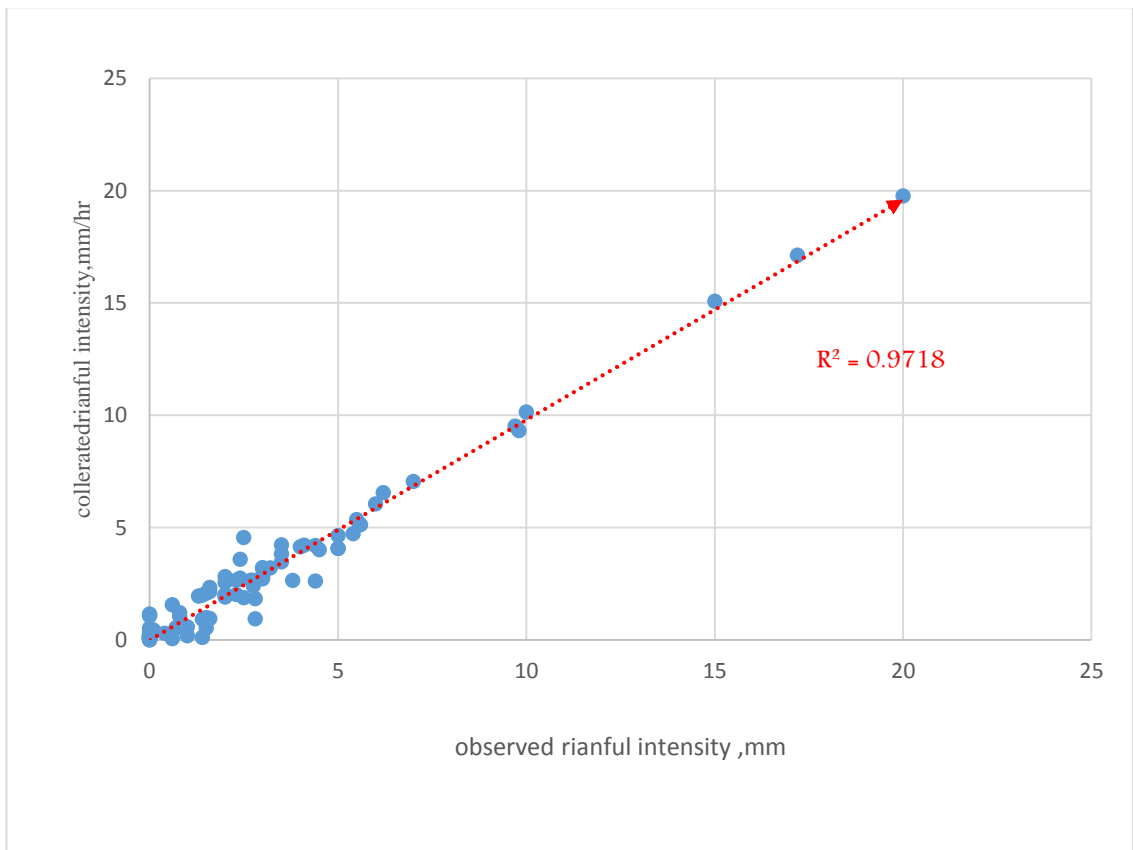


Figure 4-2 Correlation strength of the fitting line between observed and learned data for 10 years.

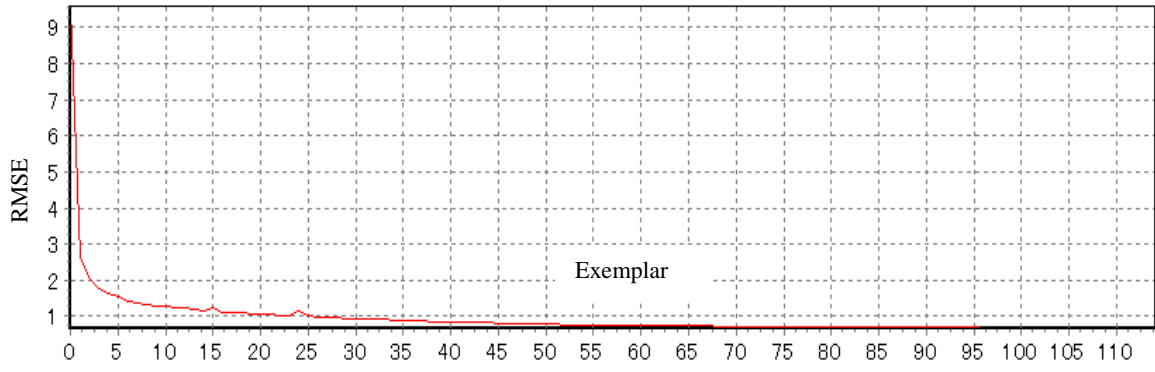


Figure 4-3 RMSE function behavior during the function learning process.

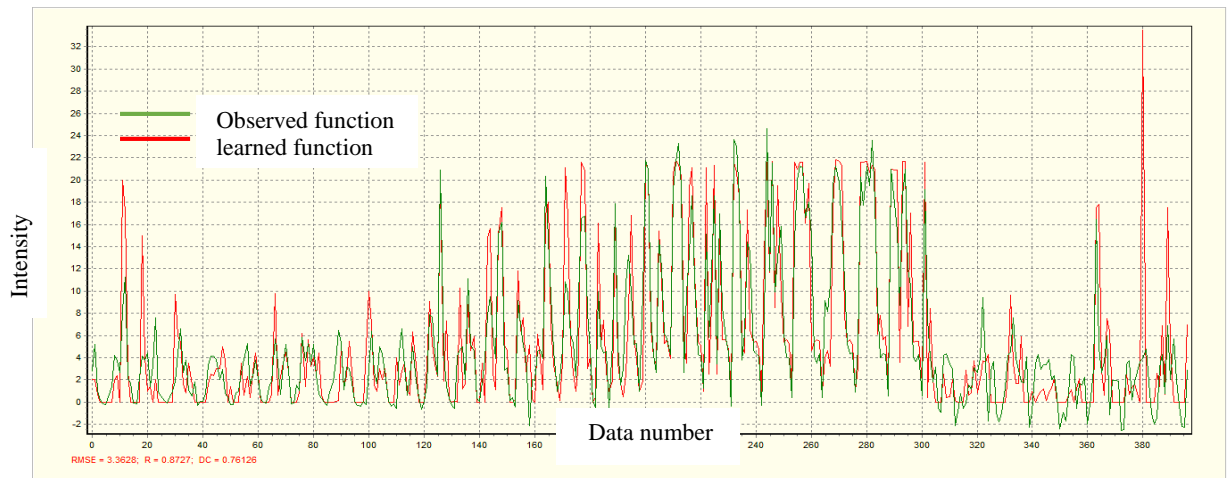


Figure 4-4 ANN learning process for 36 years testing data.

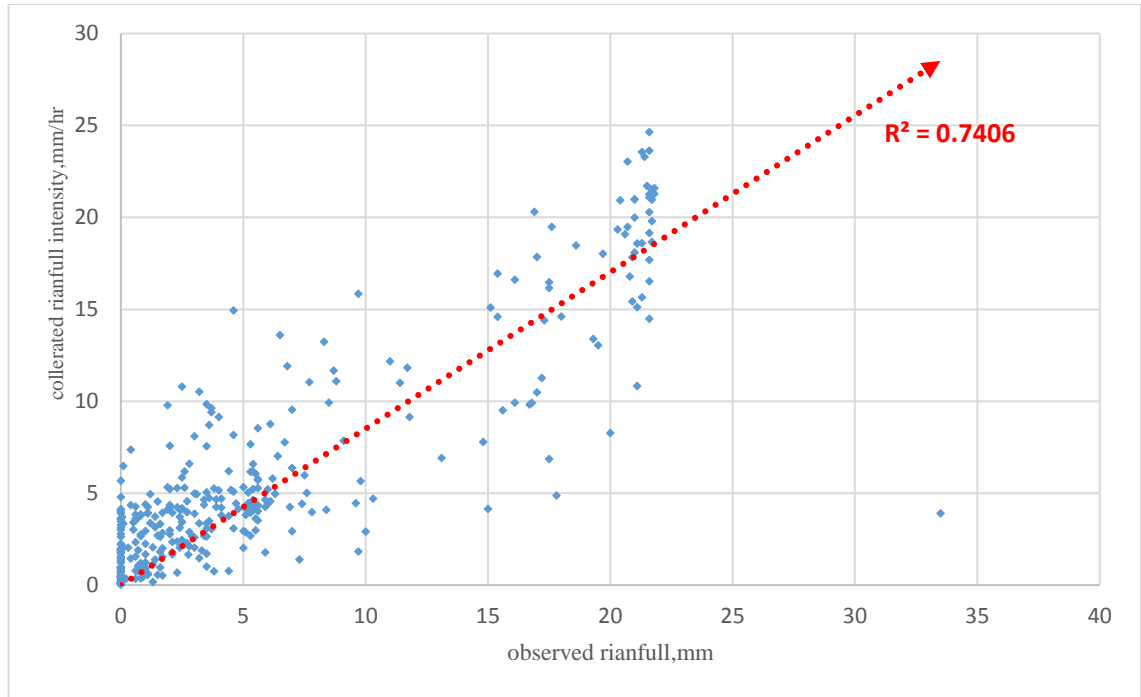


Figure 4-5 Correlation strength of the fitting line between observed and learned data for 36 years.

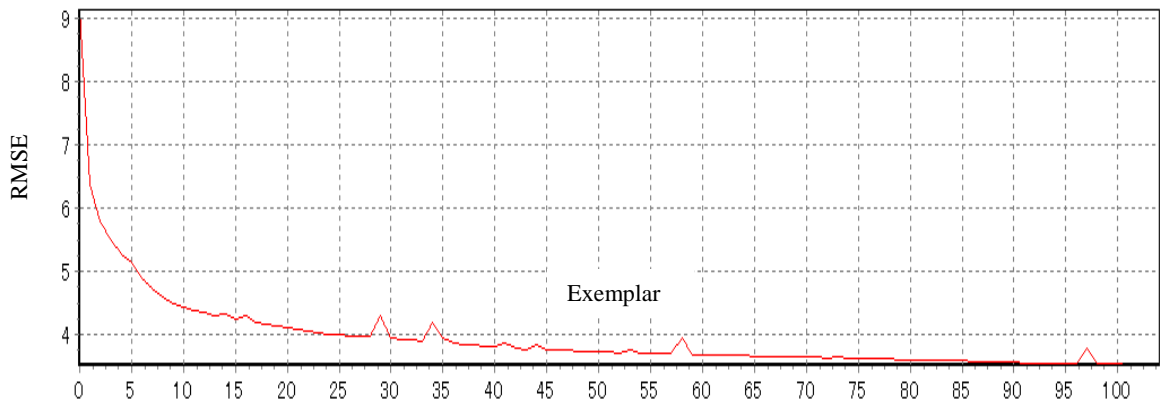


Figure 4-6 RMSE function behavior during the function learning process.

4.2.2 Weights distributions of models

Weight is the most important factor in the learning process. Each input parameter is connected to all nodes in the first hidden layer, and each node in a hidden layer connected to the nodes of the second hidden layer, also, each output layer is connected to the nodes of the last hidden layer. In

addition to bias number. The total mentioned connections refer to the number of weights. Figure (4.7) illustrates layers connections between them of two different cases.

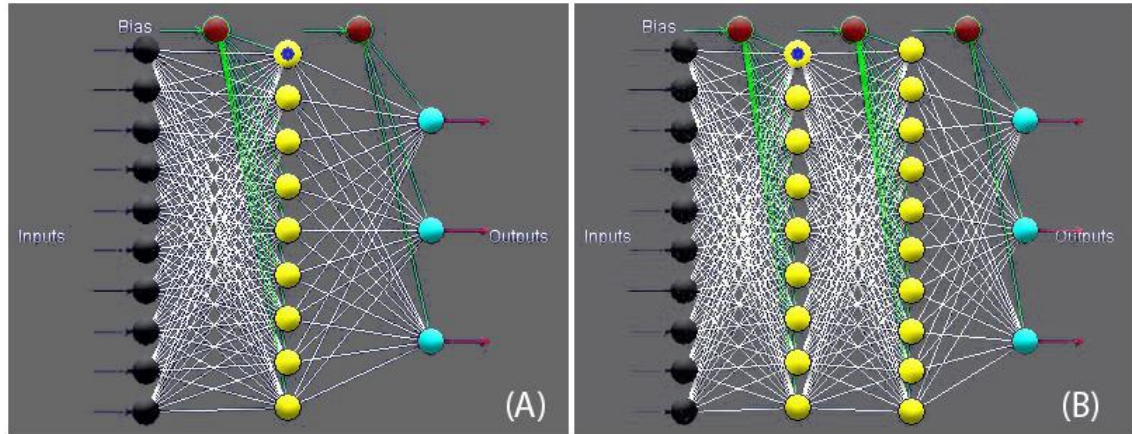


Figure 4-7 weight distribution process, A- for 1 hidden layer contains 9 nodes, B- for 2 hidden layers contains 19 nodes.

The number of weight, maximum and minimum value of it varies from ANN model to another. Figure (4.8) show weight distribution of model 1, the total number of weights are 232 and the most effective value of weight is (33). It should be noted that the horizontal axis refers to a number of weights, and the vertical axis refers to a weight value, for all weight distribution figures.

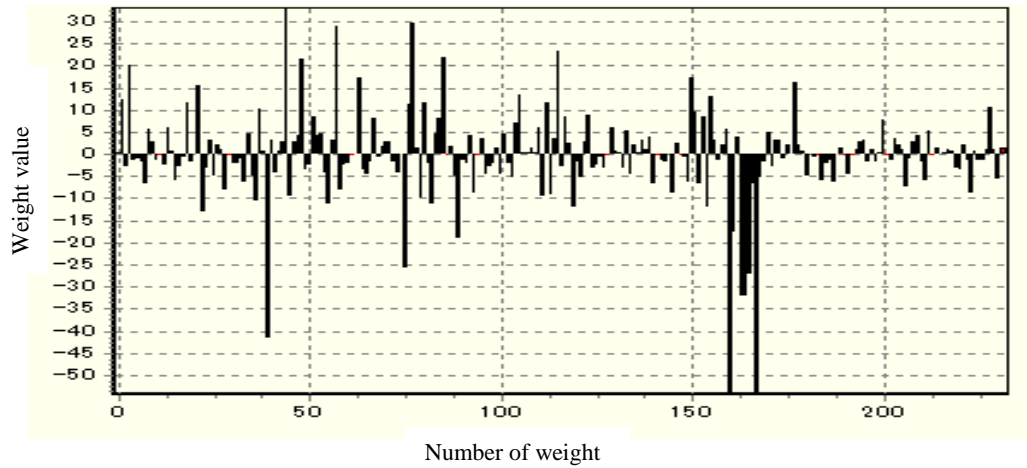


Figure 4-8 show the distribution of the weights of model 1.

Figure (4.9) clarifies weight distribution for model 2, the number of weights connection is 356 and the most effective value of weight is (77).

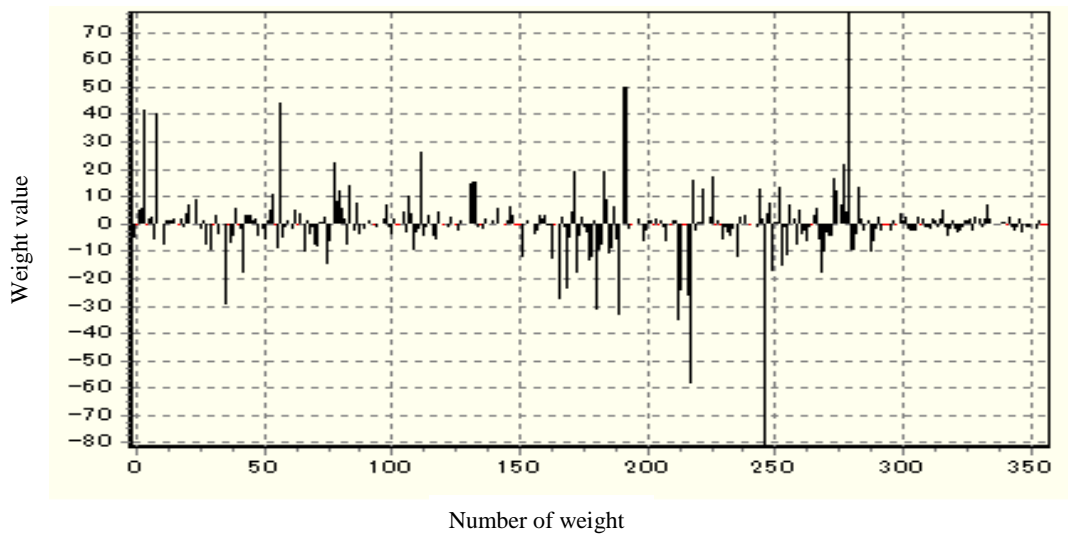


Figure 4-9 show the distribution of the weights of model 2.

Figure (4.10) illustrates the weight distribution for model 3, the number of weights connection is 232 and the most effective value of weight is (89).

Figure (4.11) illustrated weight distribution for model 4, the number of weights connection is 129 and the most effective value of weight is (94)

Figure (4.12) show the weight distribution for model 5, the number of weights connection is 356 and the most effective value of weight is (80).

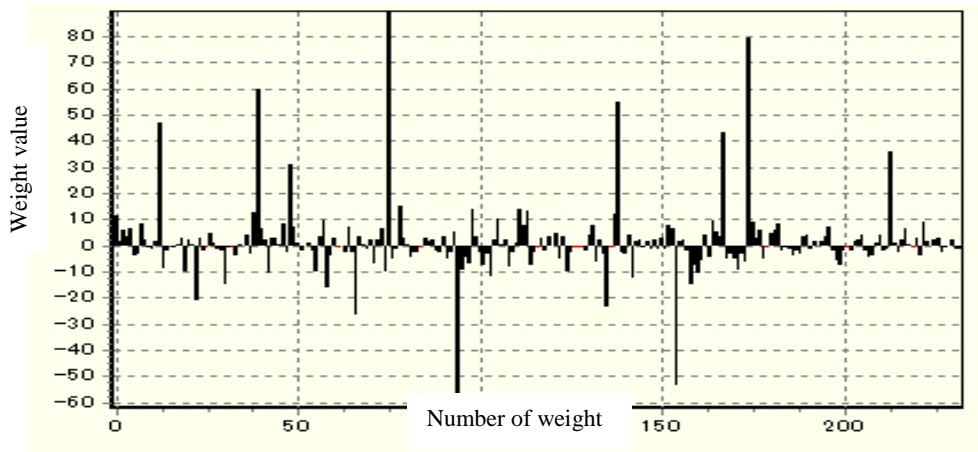


Figure 4-10 show distribution of the weights of model 3.

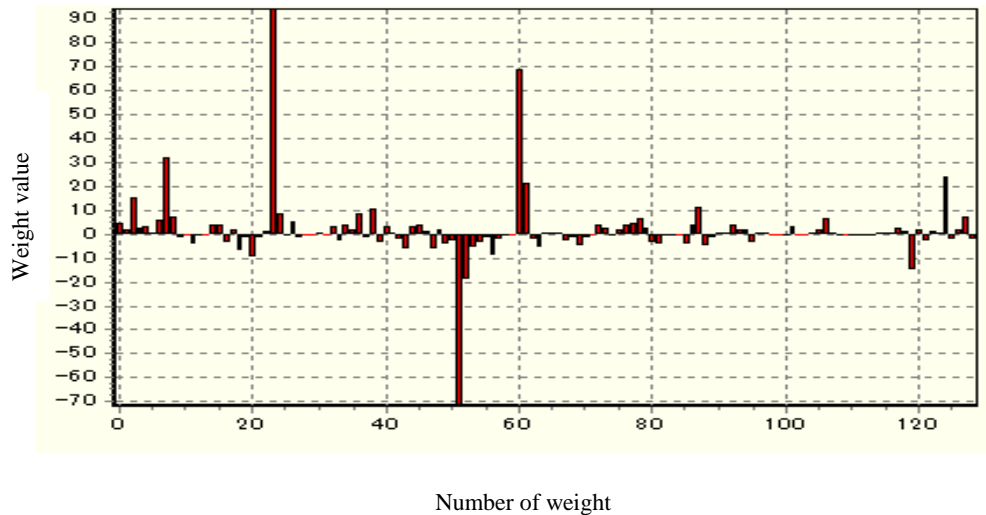


Figure 4-11 show the distribution of the weights of model 4.

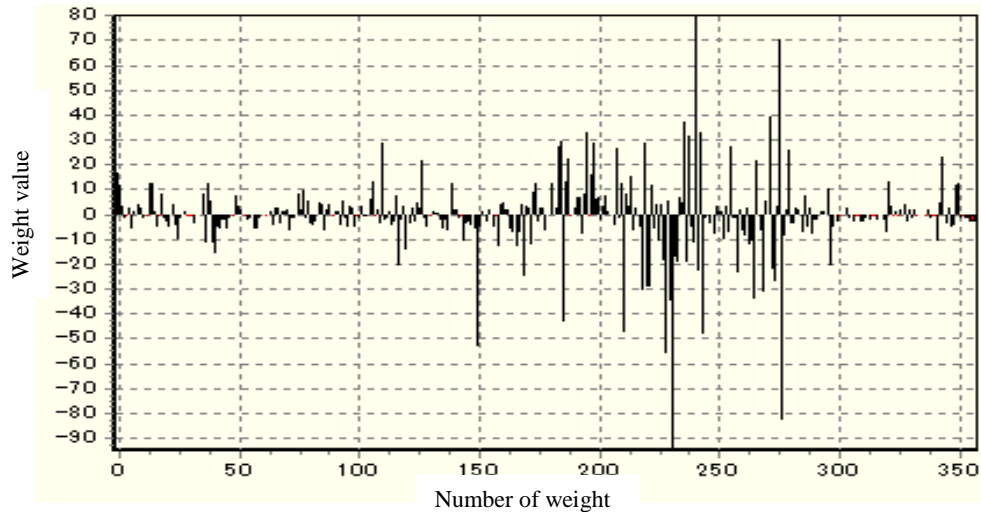


Figure 4-12 show the distribution of the weights of model 5.

4.2.3 Calibration of the ANN model

The prediction of rainfall intensity is difficult because it is a non-continuous function daily such as temperature and depends on the seasons and rainy periods. After selecting the ANN parameters (function type, number of hidden layers, and number of neurons each layer), Table(4.2) show number of the models, number of hidden layers, R^2 , RMSE for ANN models that used to prediction the rainfall intensity in the study area. Model 1 was the first model chose and model 3 was the second model chose, since they have minimum RMSE values (1.67, 3.46), and maximum R^2 values (0.722, 0.64), respectively.

Table 4-2 The model description, number of hidden layers, and its parameter.

number of model	Description	Number of hidden layers	R²	RMSE
Model 1	First model for 10 years for period (1981-1990)	2	0.722	1.67
Model 2	First model for 10 years for period (1981-1990)	3	0.684	2.68
Model 3	Second model for 36 years for period (1981-2016)	2	0.64	3.46
Model 4	Second model for 36 years for period (1981-2016)	1	0.62	3.68
Model 5	Second model for 36 years for period (1981-2016)	3	0.41	5.25

It is worth to mention that the used data in the ANN model has been selected randomly by SPSS program. About 95% of the data set has been selected randomly for generating the training function process, and about 5% of the data set has been taken for validation (testing) process. Figures (4.13, 4.14, and 4.15) illustrates the result of the calibration process between the observed and the predicted rainfall intensity data for models 3, 4, and 5 respectively.

In Figure (4.13), it can be clarified that the mathematical model was able to predict values to an acceptable limit, and can be used to predict in the coming years with some ratios of errors.

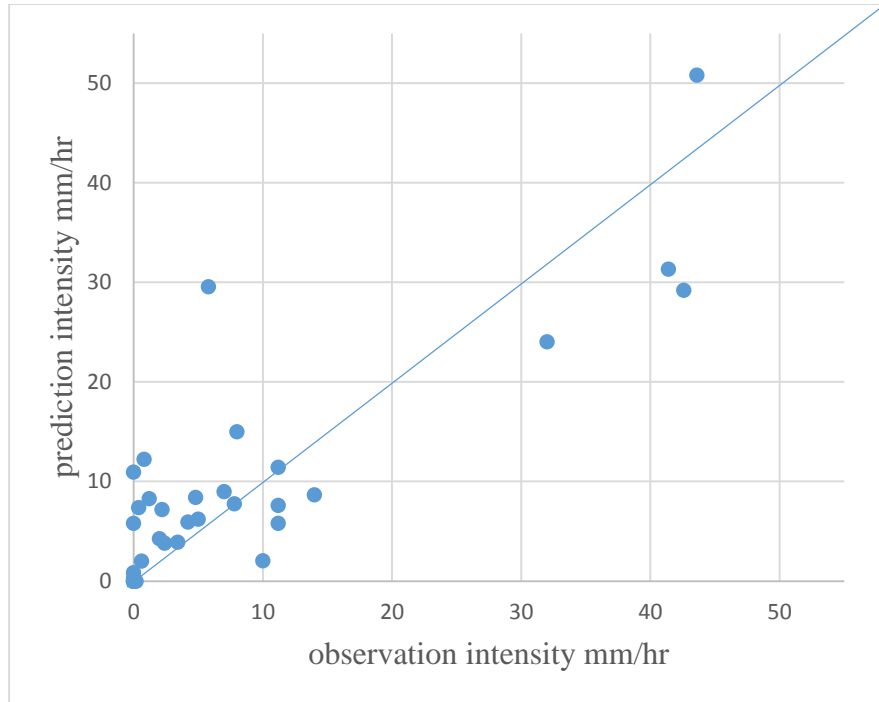


Figure 4-13 predict versus observation intensity values of model 3 (($R^2=0.640$, $RMSE=3.460$)).

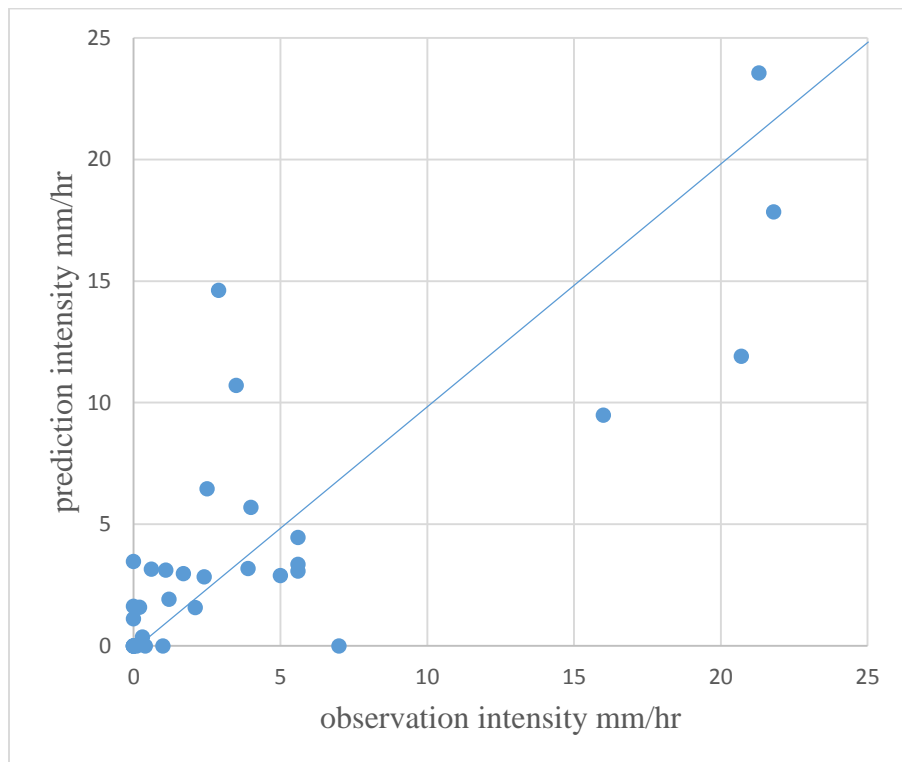


Figure 4-14 Predict versus observation intensity values of model 4 ($R^2=0.620$, $RMSE=3.680$).

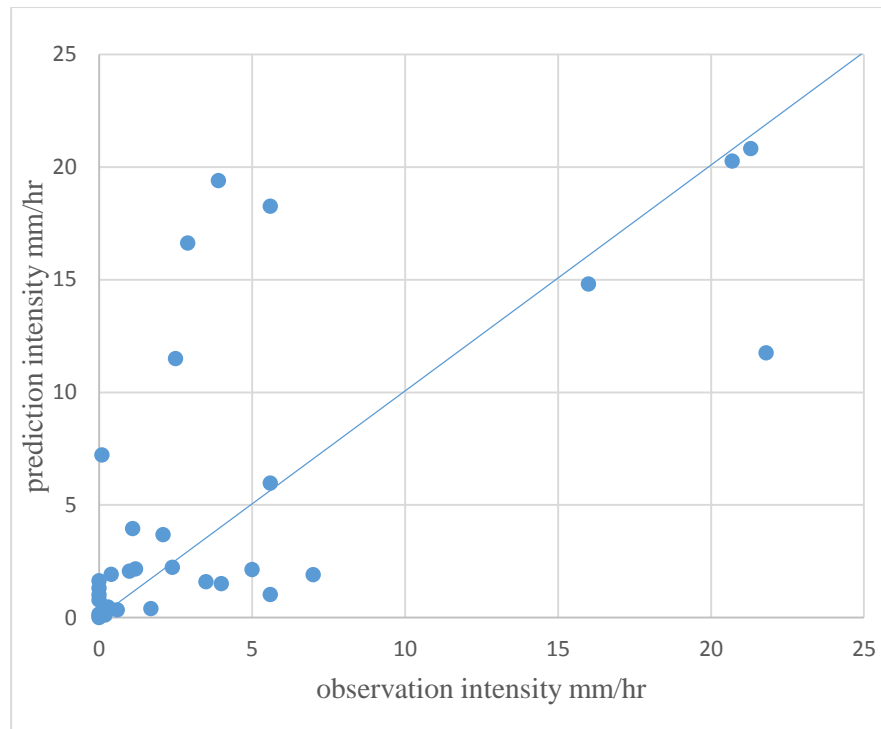


Figure 4-15 predict versus observation intensity for model 5 ($R^2=0.410$, RMSE=5.25).

Figure (4.16) shows the intensity value for three periods from 1981-1990 which gated from the General Authority for metrological and Seismic Observations ([G.A.A.S.O, 2018](#)), second period (1991-2008) which predicted from the model 1 and the third period (2008-2016) which gated from ([I.A.C.D, 2018](#)) the trend line of the intensity increase with the progress of time in general. Using model 3 to predicted rainfall intensity from 2017-2070, in general, the trend line of the prediction increase with the progress of time this illustrates in Figure (4.17), the maximum value of each year from Figure (4.17) enter to the SWMM. Model 3 can be used to predict rainfall intensity at any period due to it is developed depend on climate change of 36 years.

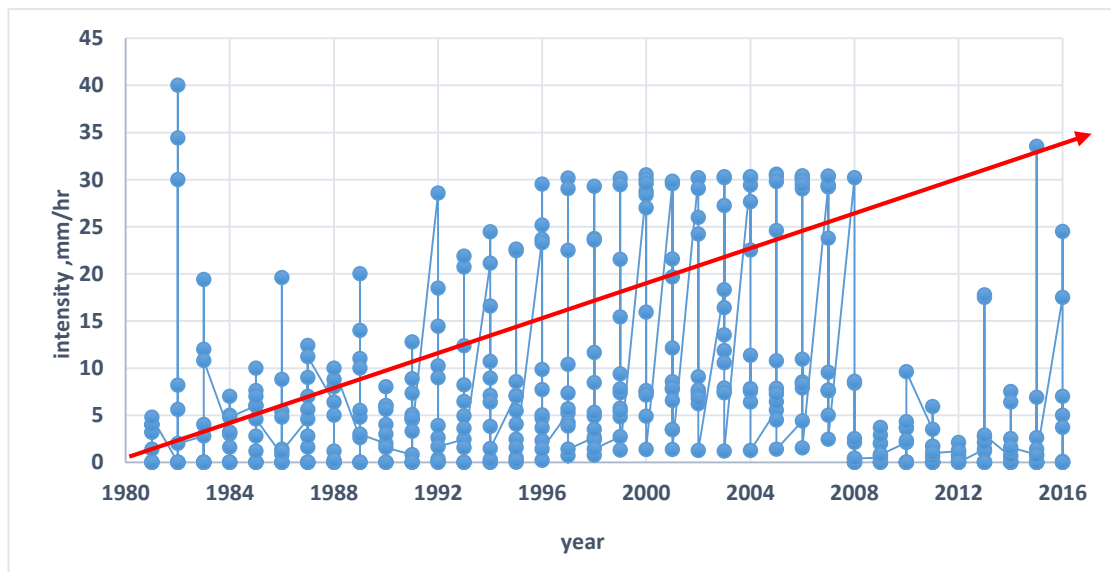


Figure 4-16 observation data of rainfall intensity.

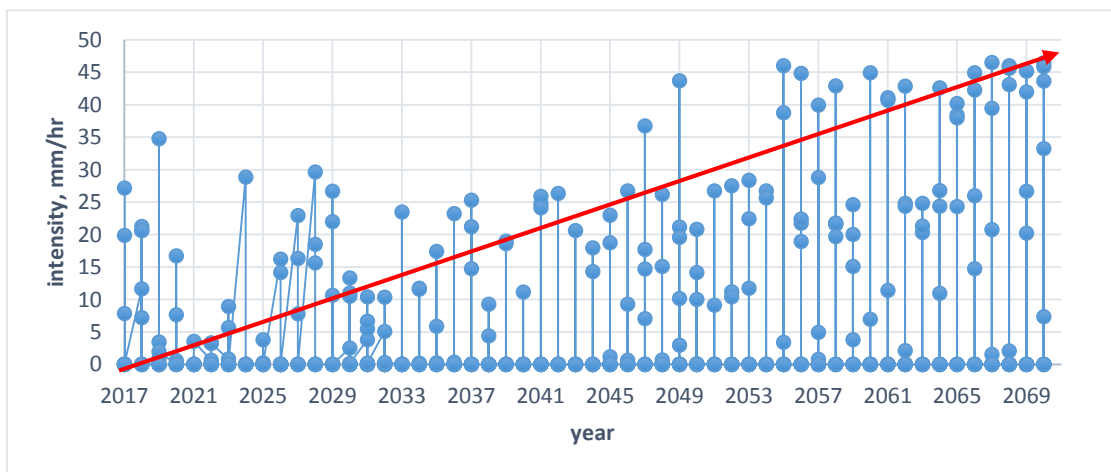


Figure 4-17 Prediction of rainfall intensity by ANN model (model 3).

4.2.4 Effect of climate change on the ANN model

Many factors of climate use to build ANN models include rainfall, max temperature, min temperature, wind speed, humidity, and sun shine. From ANN models it has been concluded that the rainfall more factor effect on the modelling. Rainfall, wind speed, sunshine, min temperature, max temperature, and humidity the sequence of climate factor that effect on

model 1. Rainfall, wind speed, sun shine, min temperature, humidity, and max temperature. The sequence of climate factor effect on model 3.

In each model generation, the priority of climate parameter changing according to their effects. For example, model 1 has a parameter priority that differs from model 3. But, it should be noted that rainfall parameter is still dominant among others. Figures (4.18 and 4.19) illustrate model importance of data parameters.

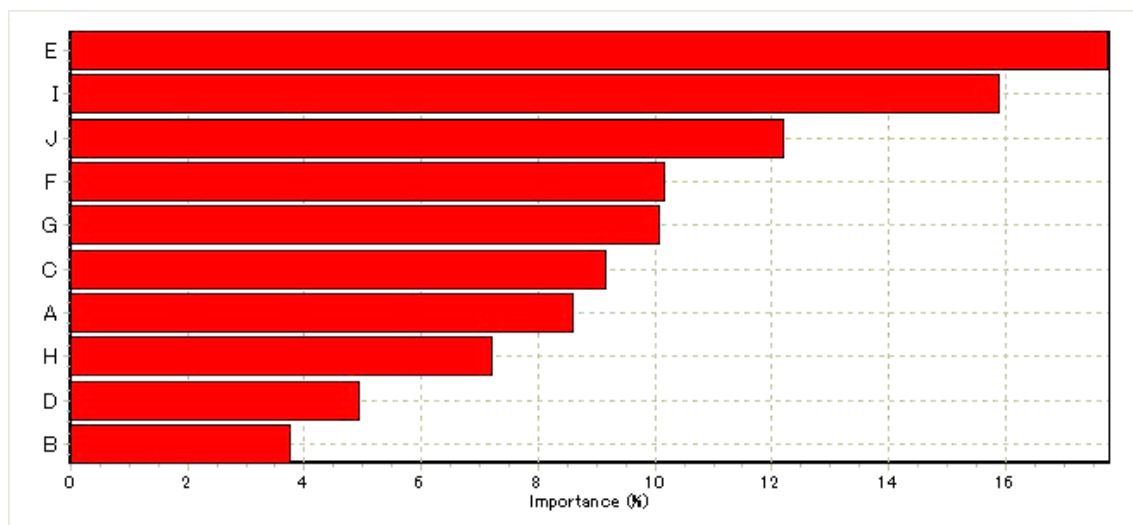


Figure 4-18 model importance distribution parameters of model 1.

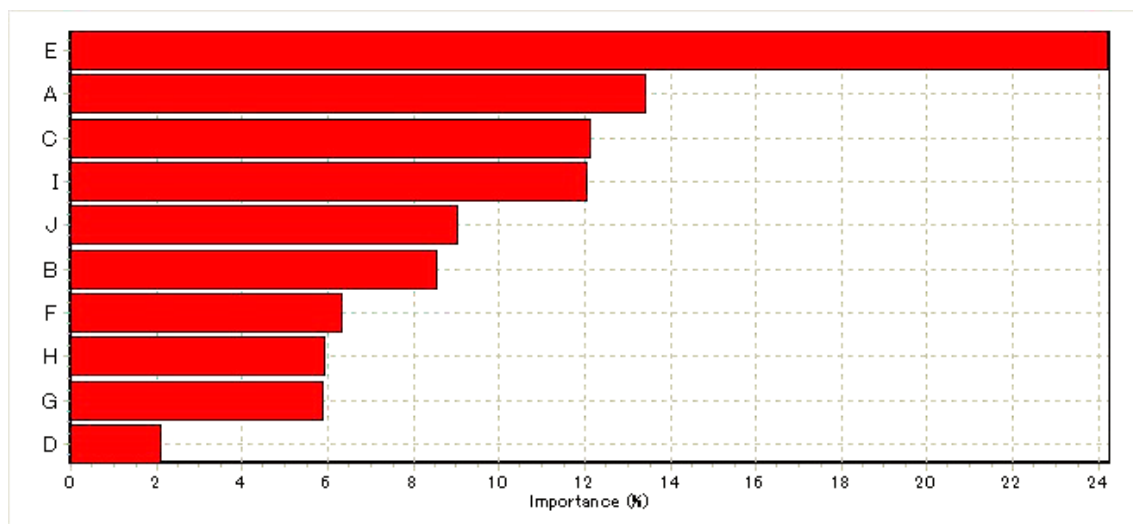


Figure 4-19 model importance distribution parameters of model 3.

Where:

A: is the number of years parameter

B: number of data N

C: is N-1 parameter

D: is N-1 parameter

E: rainfall intensity parameter

F: minimum temperature parameter

G: Maximum temperature parameter

H: Humidity parameter

I: wind speed parameter

J: is a sunshine parameter

4.3 Flooding model

The process of Simulation flooding occurrence is not simple since many different numbers of parameters should be considered during this step. After generating the ANN model and prediction of data for different future periods, and preparing the network geometry and its related parameters, it can be said that the simulation process is ready with SWMM. First, SWMM model shall be calibrated with currently available data. Also, Simulation process shall cover different time periods.

4.3.1 Model calibration

A manual trial and error method has been used to calibrate the simulation model of storm drainage network of the study area. There was a lack of data that need to calibrate the model. There are six months available as observation data: January 2017, February 2017, November 2017, January 2018, March 2018, and April 2018. Rainfall intensity is using: (7.86, 27.5, 19.86, 11.66, 21.28, and 7.24) mm/h. The result of calibration shown in figure (4.20).

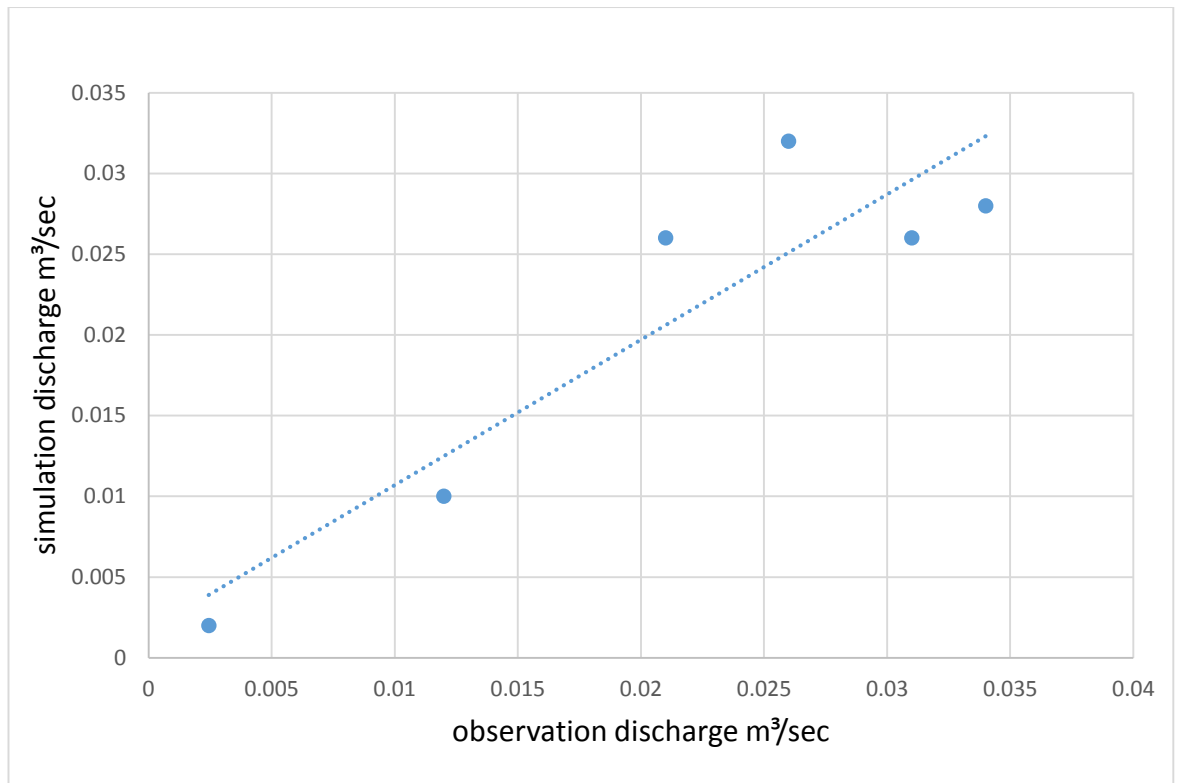


Figure 4-20 model calibration result under different rainfall intensity

In order to check the validity of all the input parameters in the model and estimation of model parameters, cross-validation is carried out on the data. The cross validation results show that the mean square error (MSE) for all events are very close to zero (0.000021). Moreover, root means square error (RMSE) is very low as compared to the variance of the observed data for all events (0.0045). The correlation coefficient (R^2) equal to (0.83). The model can be used after the calibration with acceptable result and with the error rate indicated in the Table (4.3).

Table 4-3 the result of calibration of SWMM

Observed data(m ³ /sec)	Simulation results(m ³ /sec)	MSE	RMSE	R ²	error
0.031	0.026	0.000021	0.0045	0.83	16.1%
0.026	0.032				23%
0.021	0.026				23.8%
0.012	0.01				16.6%
0.034	0.028				17.6%
0.0024	0.002				18.36%

4.3.2 Climate change simulation results by SWMM

The storm drainage network in the Al-Abbas quarter had been designed for a rainfall intensity of 13 mm/h and 2-year return period (D.S.K and 2018). However, the study area has been exposed to the impacts of climate change represent an increase in rainfall intensity reach max percent in 2067 is three times of design intensity. The study area is exposed to flooding due to an increase in rainfall intensity. The climate change of the case study has been simulated for the rainy event (a maximum month in each year) for the future period from (2017 to 2070). The flooding discharge amount of the manholes divided into five stages as follows:

- Stage1 [no flooding] range from [0 to 0.001 m³/sec].
- stage2 [very light flooding] range from [greater than 0.001 to 0.01 m³/sec],
- stage3 [medium flooding] range from [greater than 0.01 to 0.05 m³/sec]
- stage4 [high flooding] range from [greater than 0.05 to 0.12 m³/sec],
- Stage 5 [very high flooding] for [greater than 0.12 m³/sec].

In order to study this effect on rain intensity change, a set of expected rain intensities will be applied in the next years on the network in

the study area. The focus will be on the high intensities expected to determine the extent of the network's ability to deal with these intensities.

Figure (4.21) shows the behavior of the storm network in winter 2017 with rainfall intensity equal to 27.5mm/h, this value of rainfall intensity greater than design rainfall intensity with ratio equal to 111%.78% of the manhole had no flooding (stage 1) and 16% of the manhole had very light flooding (stage 2), 3% of the manhole had medium flooding (stage 3), 3% of the manhole flooding had high flooding (stage 4). So, the behavior of the network looks somewhat good for the duration of flooding 50 min.

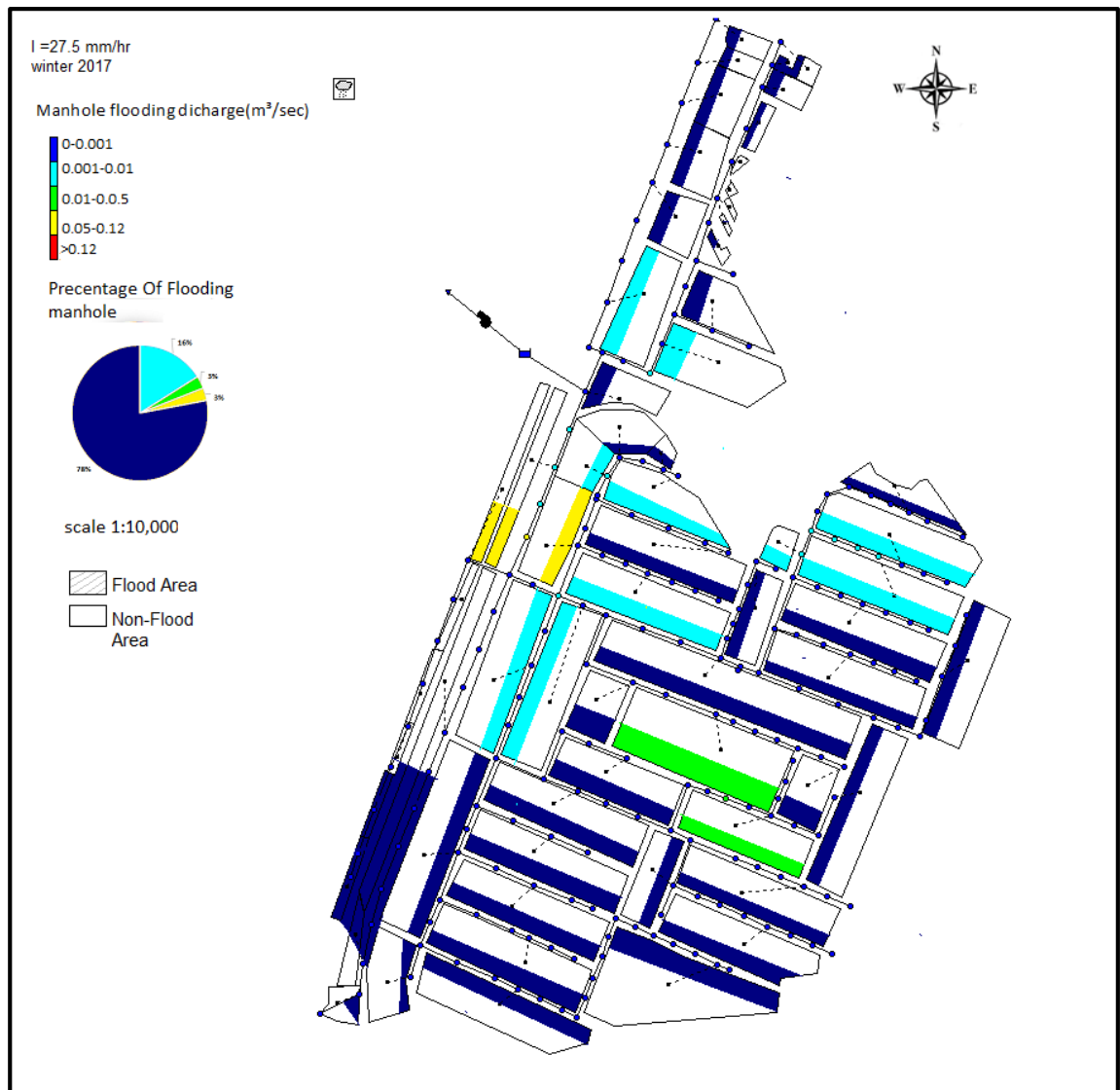


Figure 4-21 The flooding manhole under rainfall intensity (27.5 mm/h) at peak time in winter 2017.

Figure (4.22) show the behavior of the storm network in winter 2019 with rainfall intensity equal to 34.47mm/h, this value of rainfall intensity greater than design rainfall intensity with ratio equal to 165%.64% of the manhole had no flooding (stage 1) and 16% of the manhole had very light flooding (stage 2) , 10% of the manhole had medium flooding (stage 3), 10% of the manhole flooding had high flooding (stage 4). So the behavior of the network consider good, the duration of flooding is 45 min.

Also, from the same Figure, it can be observed that flooding discharge condition for the year 2019 decrease stage 1 with a rate about 21.8%, stage

2 has no change , stage 3 and stage 4 increase with double compared to the year 2017. No significant change has occurred during this interval since the period too close.

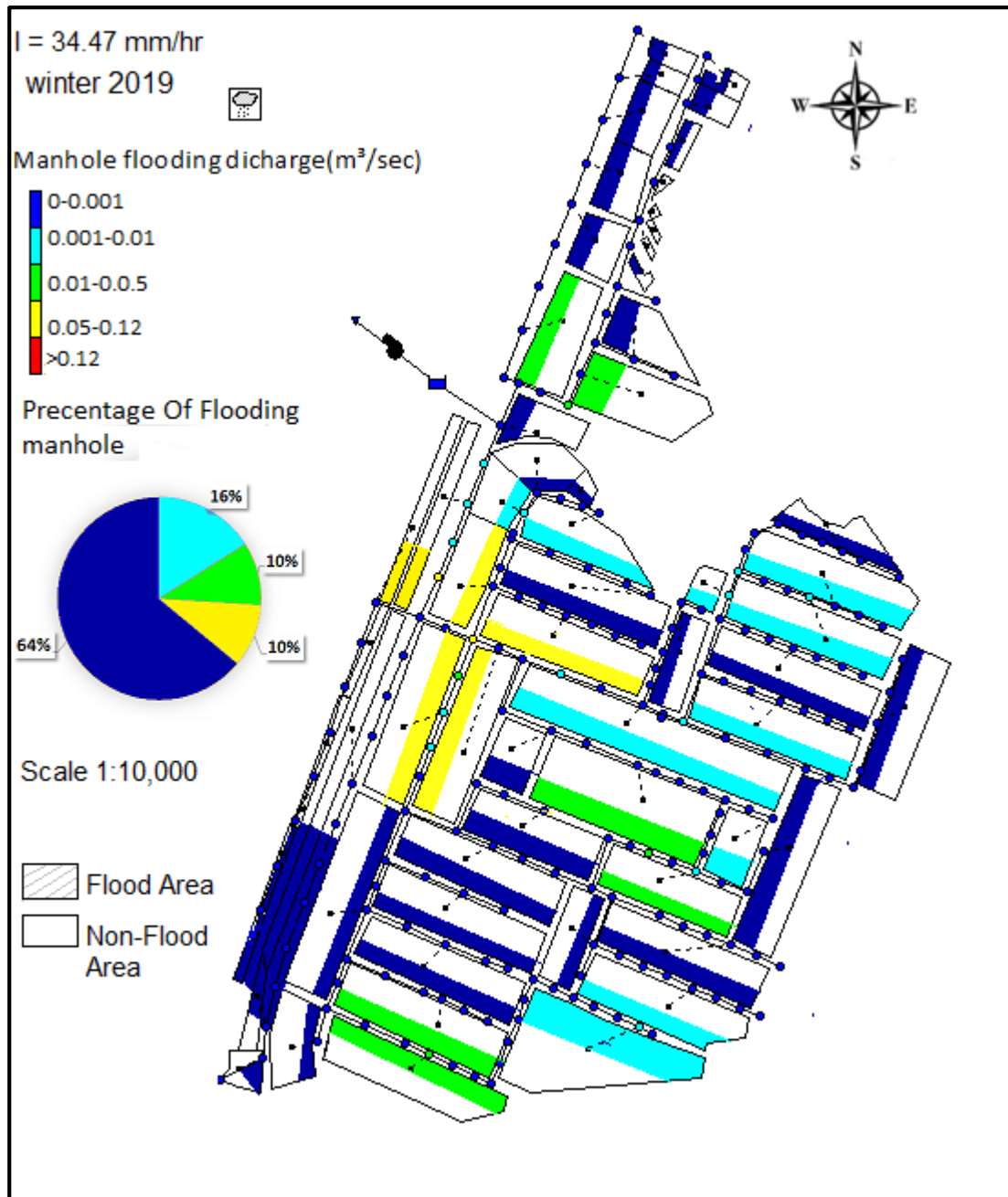


Figure 4-22 The flooding manhole under rainfall intensity (34.74 mm/h) at peak time in winter 2019.

Figure (4.23) Show the behavior of the storm network in winter 2024 with rainfall intensity equal to 28.82mm/h, this value of rainfall intensity greater than design rainfall intensity with a ratio equal to 121%. 73% of the

manhole had no flooding (stage 1),14% of the manhole flooding had very light flooding (stage 2), 3% of the manhole had medium flooding (stage 3), and 10% of the manhole flooding had high flooding (stage 4) , the duration of flooding is 45 min .

Also, from the same Figure, it can be observed that flooding discharge condition for the year 2024 increase stage 1 with a rate about 14%, stage 2 has been decreasing with a rate about 14.2%, stage 3 decrease to double and stage 4 had no change compared to the year 2019.

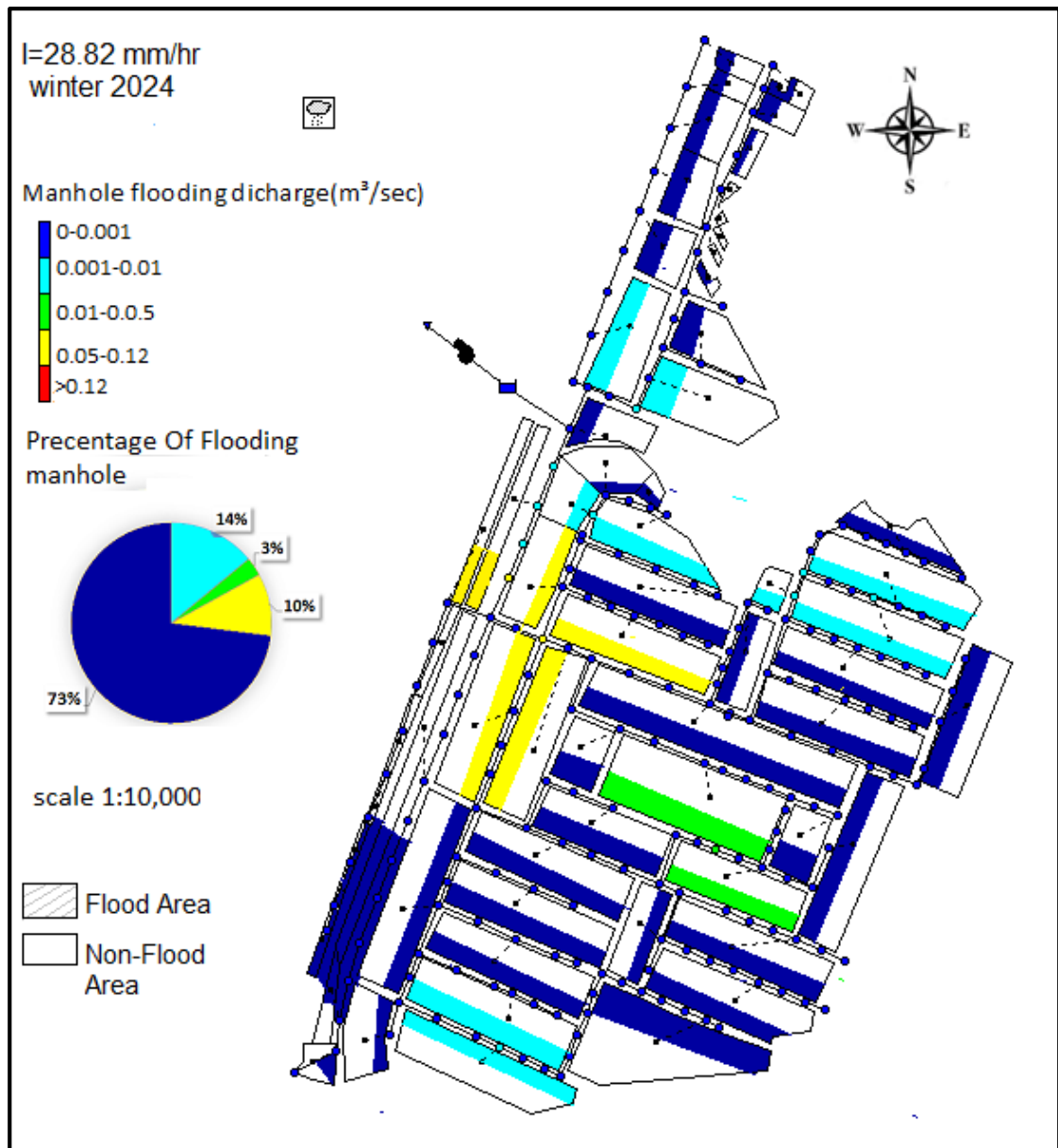


Figure 4-23 The flooding manhole under rainfall intensity (28.82 mm/h) at peak time in winter 2024.

Figure (4.24) Show the behavior of the storm network in winter 2028 with rainfall intensity equal to 29.62mm/h, this value of rainfall intensity greater than design rainfall intensity with a ratio equal to 127%. 74% of the manhole had no flooding (stage 1), 13% of the manhole flooding had very light flooding (stage 2) ,3% of the manhole had medium flooding (stage 3), and 10% of the manhole flooding had high flooding (stage 4), the duration of flooding is 50 min.

Also, from the same Figure, it can be observed that flooding discharge condition for the year 2028 increase stage 1 with a rate about 1.3%, stage 2 has been decreasing with a rate about 7.6% , stage 3 and stage 4 had no change compared to the year 2024. No significant change has occurred during this interval since the period too close.

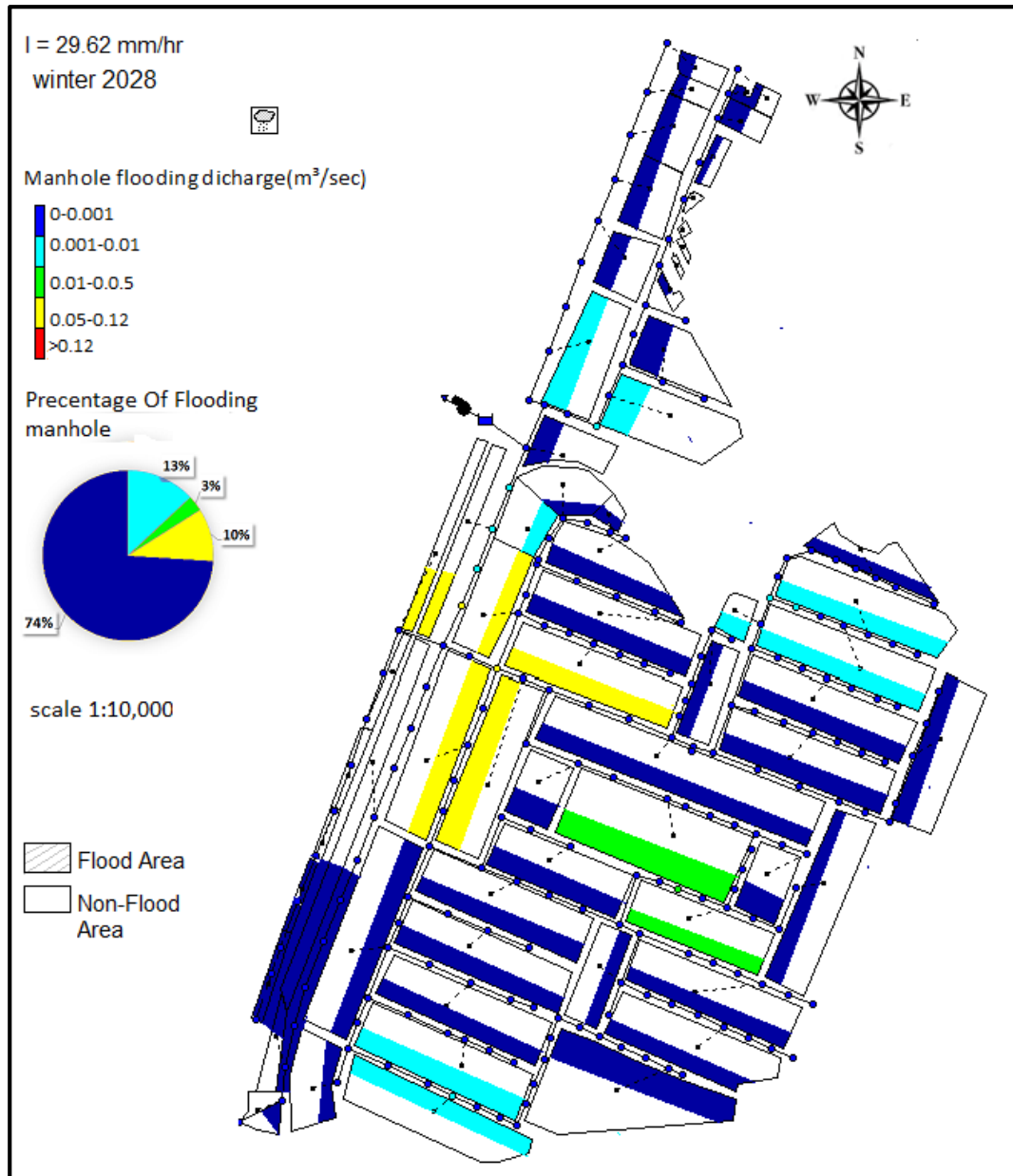


Figure 4-24 The flooding manhole under rainfall intensity (29.62 mm/h) at peak time in winter 2028.

Figure (4.25) show the behavior of the storm network in winter 2037 with rainfall intensity equal to 25.28mm/h, this value of rainfall intensity greater than design rainfall intensity with a ratio equal to 94%. 74% of the manhole had no flooding (stage 1), 13% of the manhole had had very light flooding (stage 2) ,8% of the manhole had medium flooding (stage 3)and, 5% of the manhole had very high flooding (stage 5) ,the duration of flooding is 50 min.

Also, from the same Figure, it can be observed that flooding discharge condition for year 2037increase stage 1, stage 2 have been no change , stage 3 has increasing with rate about 1.6%, and stage 4 has been decreasing once time to the year 2028. No significant change has occurred during this interval since the period too close.

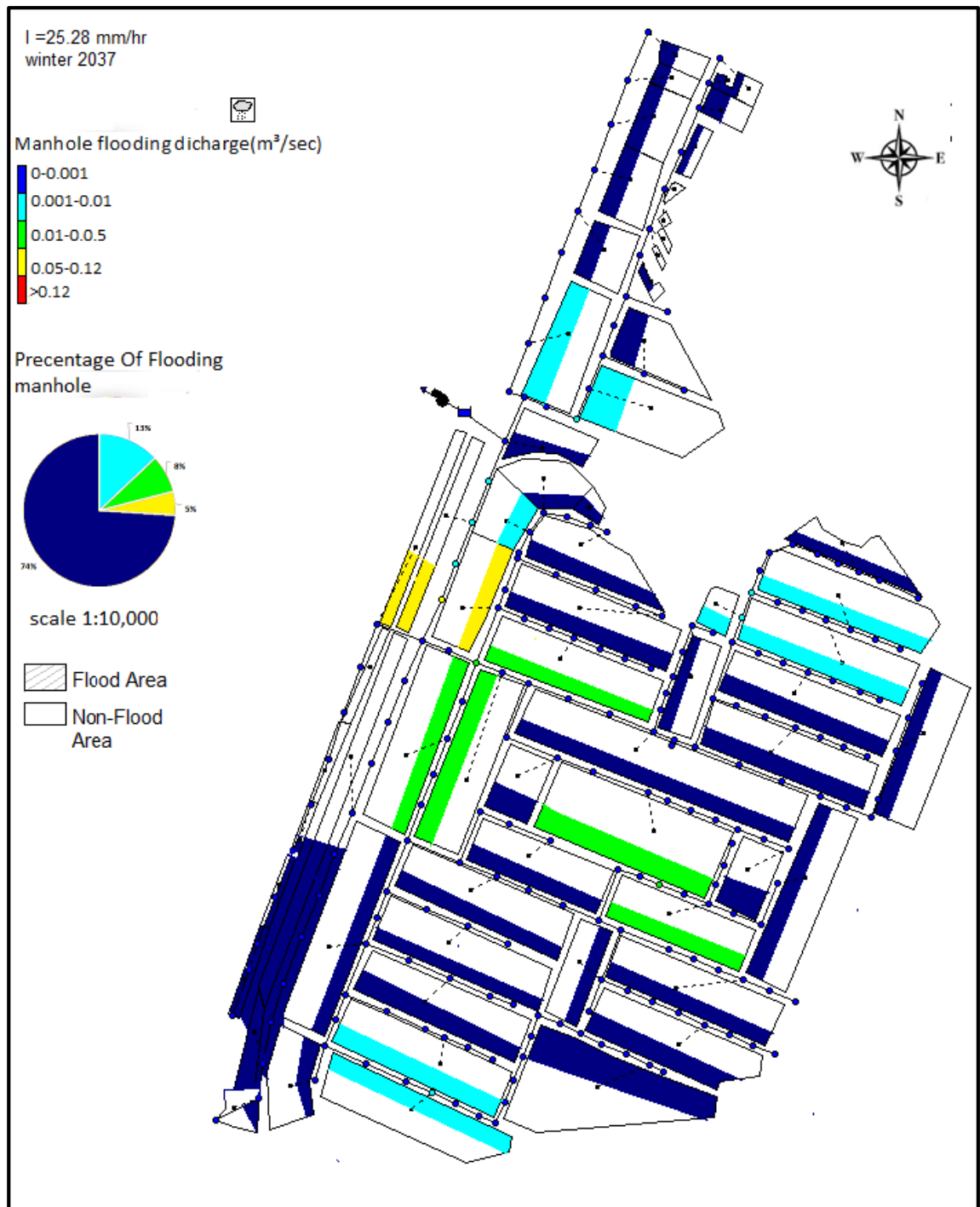


Figure 4-25 The flooding manhole under rainfall intensity (25.28 mm/h) at peak time in winter 2037.

Figure (4.26) show the behavior of the storm network in winter 2042 with rainfall intensity equal to 26.34mm/h, this value of rainfall intensity greater than design rainfall intensity with a ratio equal to 103%. 76% of the manhole had no flooding (stage 1), 11% of the manhole had had very light flooding

(stage 2) ,8% of the manhole had medium flooding (stage 3)and, 5% of the manhole had very high flooding (stage 5) ,the duration of flooding is 45 min.

Also, from the same Figure, it can be observed that flooding discharge condition for the year 2042 increase stage 1 with a rate about 2.7%, stage 2 has been decreasing with a rate about 18.1%, stage 3 and stage 4 had no change compared to the year 2037. No significant change has occurred during this interval since the period too close.

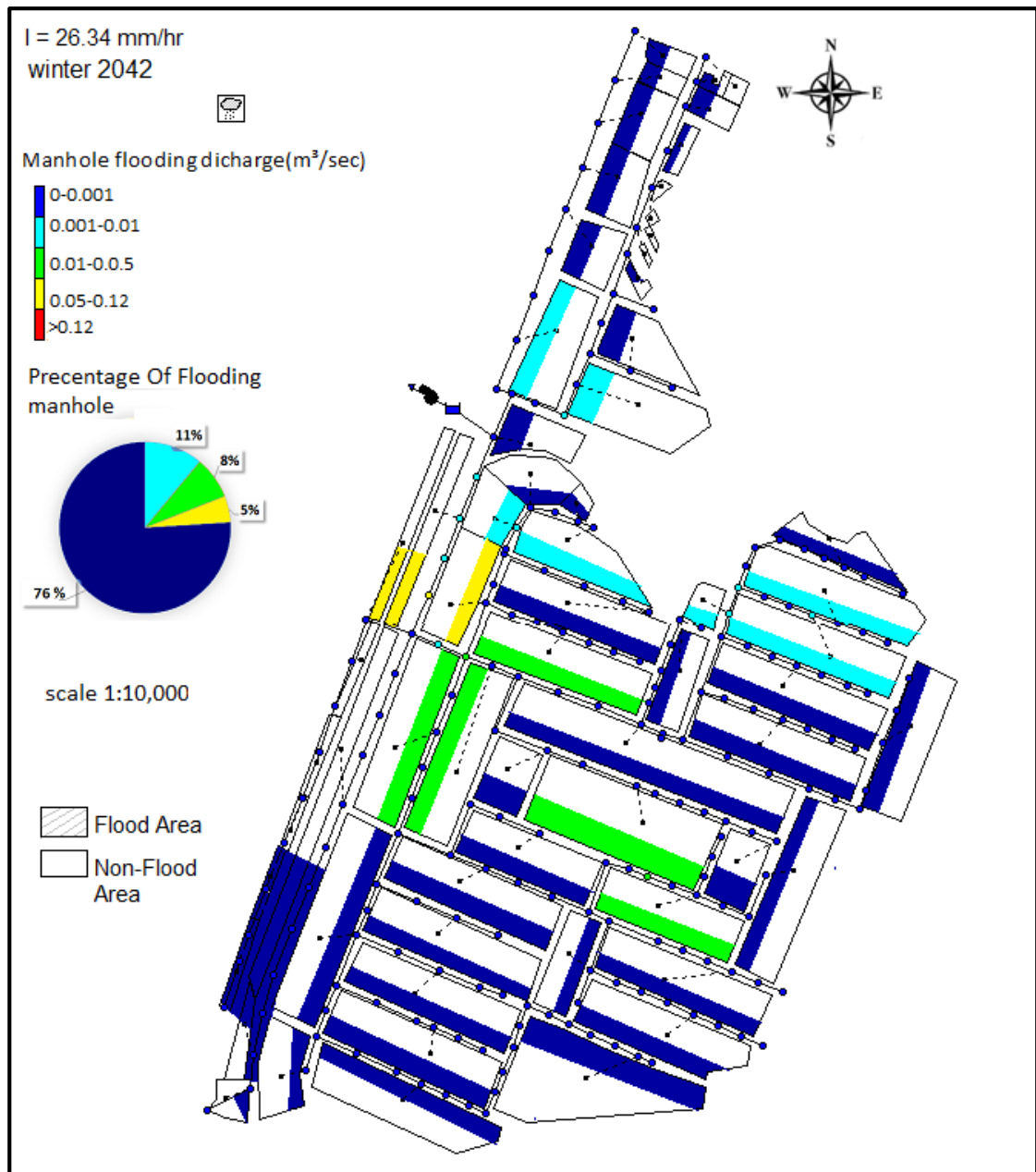


Figure 4-26 The flooding manhole under rainfall intensity (26.34 mm/h) at peak time in winter 2042.

Figure (4.27) shows the behavior of the storm network in winter 2055 with rainfall intensity equal to 45.98mm/h, this value of rainfall intensity greater than design rainfall intensity with ratio equal to 254%.56% of the manhole had no flooding (stage 1), 14% of the manhole had very light flooding (stage 2), 21% of the manhole had medium flooding (stage 3), 3% of the manhole flooding had high flooding (stage 4) and, 6% of the manhole had very high flooding (stage 5), the duration of flooding is 20 min.

In addition, from the same Figure, it can be observed that flooding discharge condition for year 2055 decreasing stage 1 with a rate about 35.7%, stage 2 has been increasing with rate about 27.2% , stage 3 has been increasing with rate about 1.6 time , stage 4 has been decreased with a rate about 66.6%,and stage 5 has been increased with a rate about 6% compared to the year 2042.

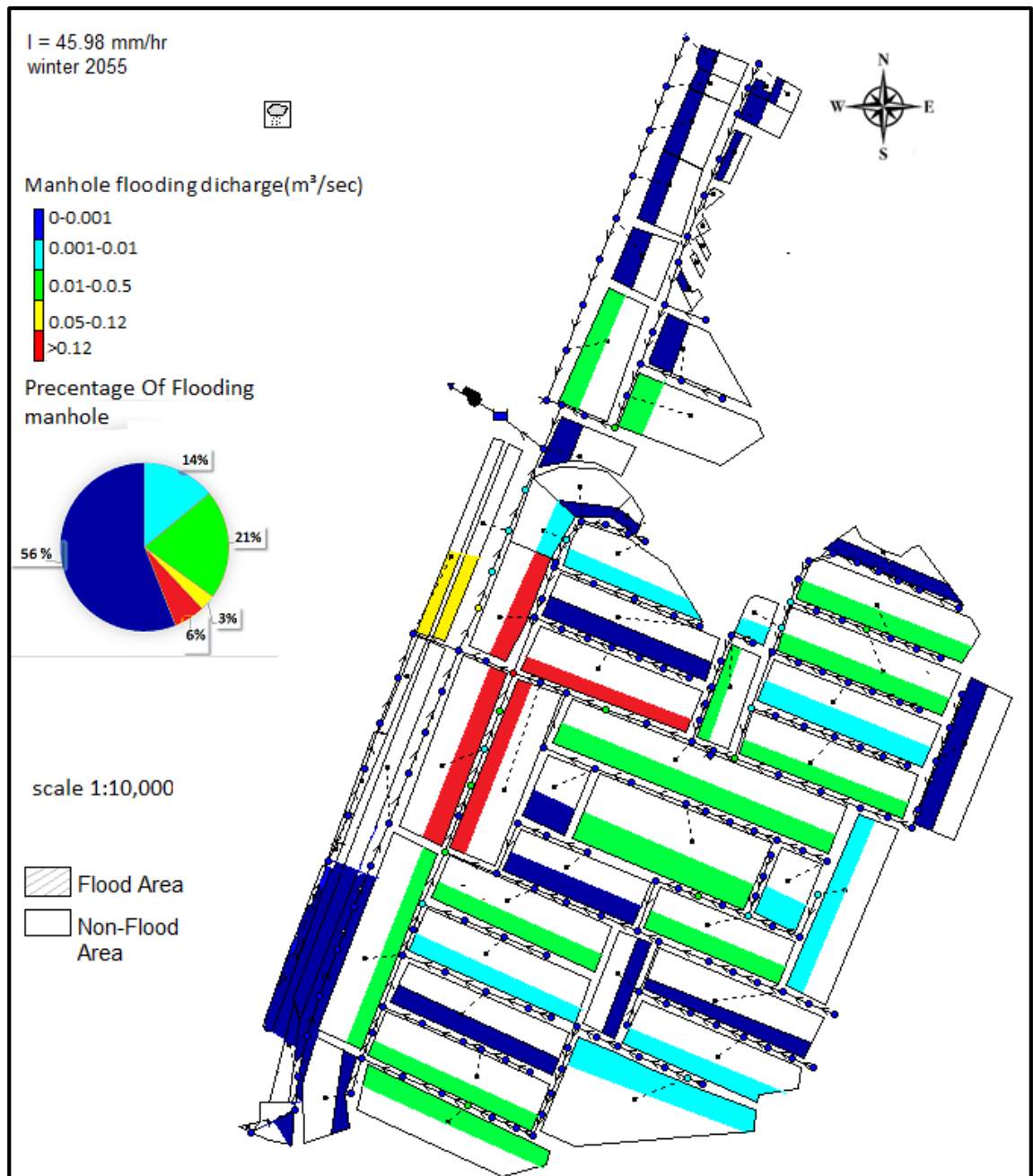


Figure 4-27 The flooding manhole under rainfall intensity (45.98 mm/h) at peak time in winter 2055.

Figure (4.28) shows the behavior of the storm network in winter 2060 with rainfall intensity equal to 44.9 mm/h. This value of rainfall intensity is greater than the design rainfall intensity with a ratio equal to 245%. 60% of the manholes had no flooding (stage 1), 11% of the manholes had very light flooding (stage 2), 20% of the manholes had medium flooding (stage 3), 3% of the

manhole flooding had high flooding (stage 4) ,and, 6% of the manhole had very high flooding (stage 5) ,the duration of flooding is 35min.

Also, from the same Figure, it can be observed that flooding discharge condition for year2060 increasing stage 1 with a rate about 6.1%, stage 2 has been decreased with rate about 27.2%, stage 3 has been decreased with a rate about 5%, stage 4 has been increased about once time, and stage 5 has been decreased about 6% once time compared to the year 2055.

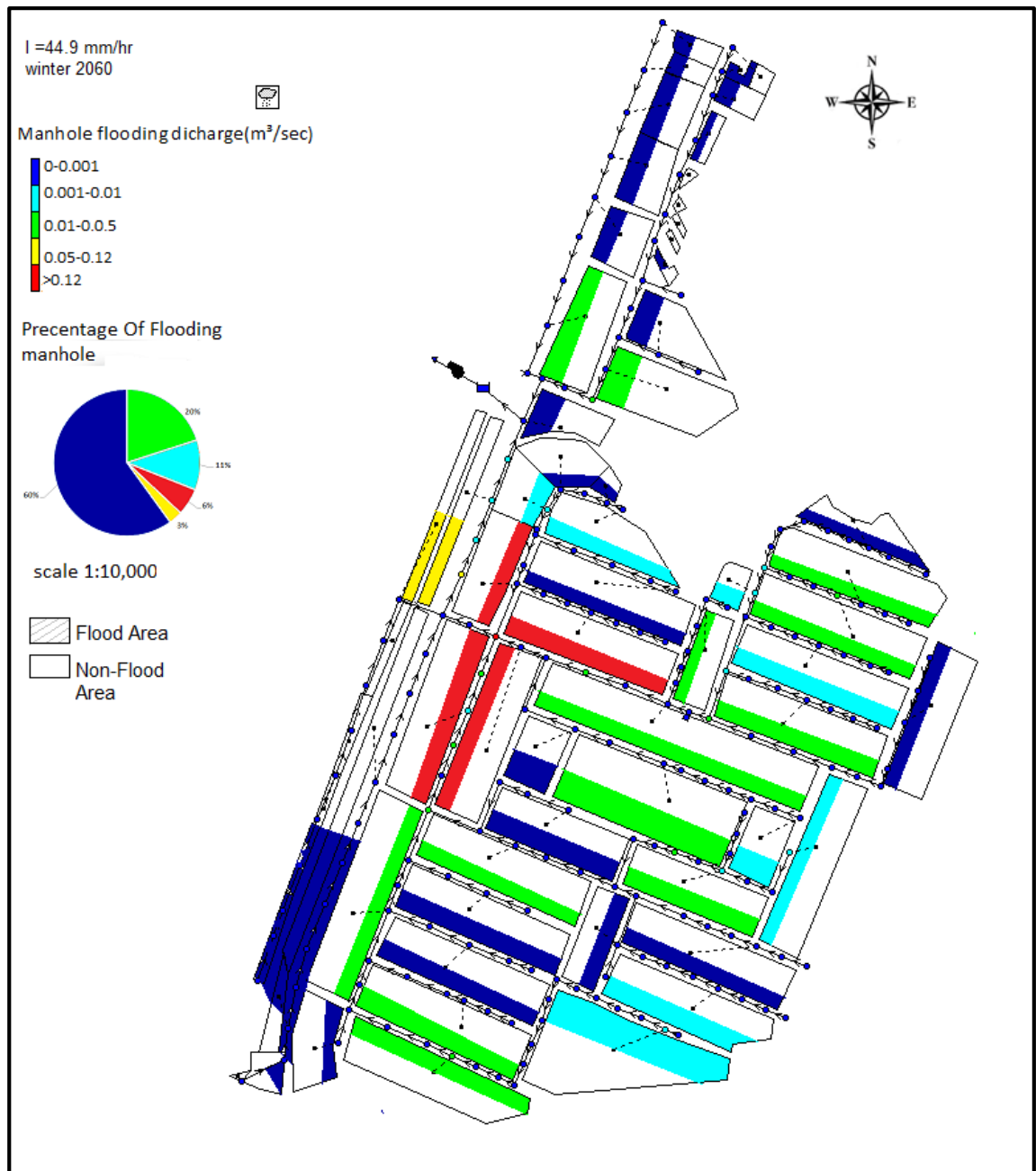


Figure 4-28 The flooding manhole under rainfall intensity (44.9 mm/h) at peak time.

Figure (4.29) shows the behavior of the storm network in winter 2067 under maximum rainfall intensity equal to 46.48 mm/h. This value of rainfall intensity is greater than the design rainfall intensity with a ratio equal to 257%. 56% of manholes have no flooding (stage 1), whereas 14% of the manholes have very light flooding (stage 2). Furthermore, 21% of manholes have medium flooding (stage 3), 3% of the manhole flooding had high

flooding (stage 4). Finally, 6% of the manholes have very high flooding (stage 5). The duration of flooding for this study is 45 min.

Also, in the same Figure, it can be observed that flooding discharge condition for year 2067 decreasing (stage 1) with a rate about 7.1%. stage 2 has been increased with a rate about 27.2%, stage 3 has been increased with a rate about 5%, stage 4 has been decreased about one time, and stage 5 has been increased about once time compared to year 2060.

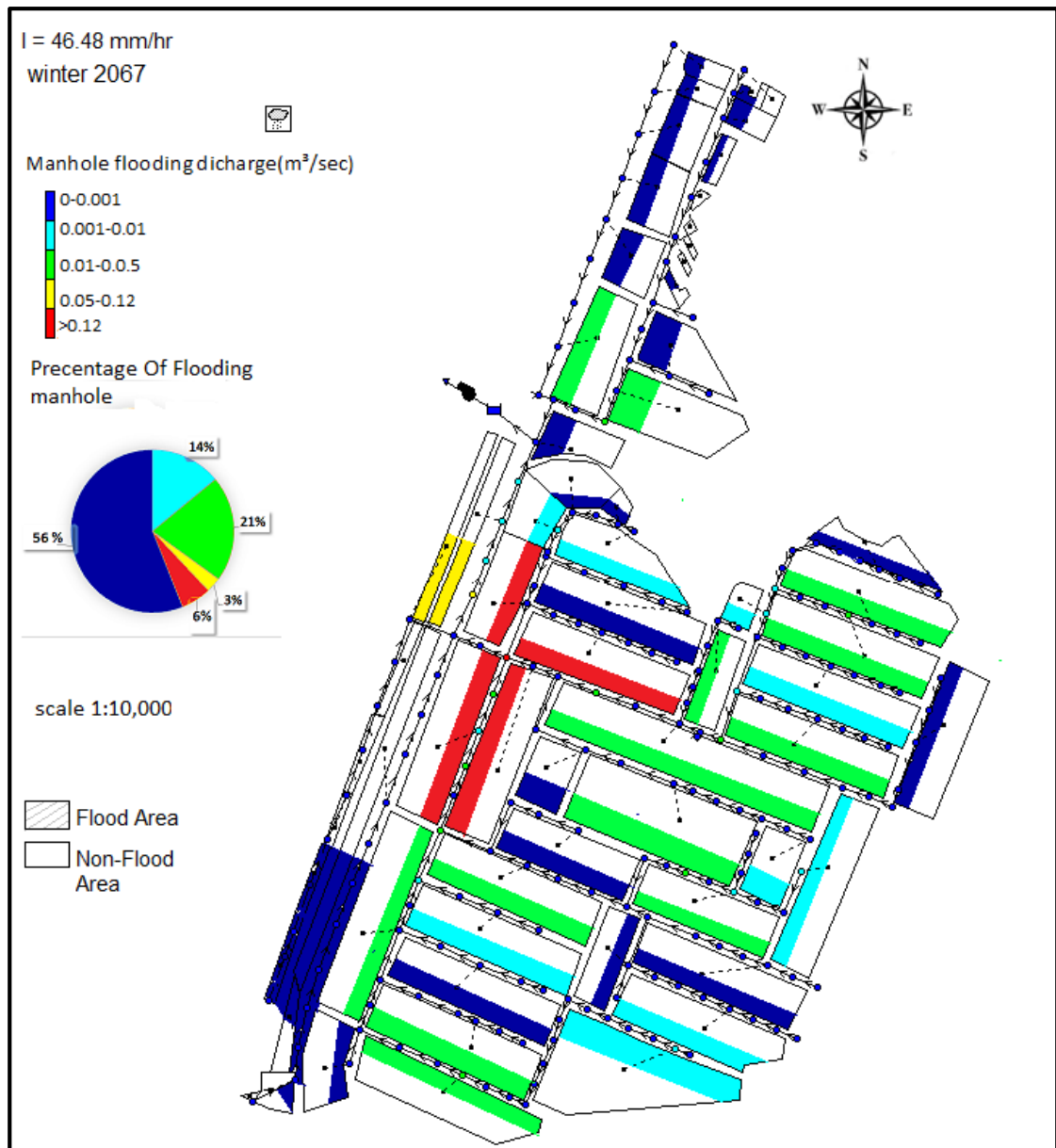


Figure 4-29 The flooding manhole under maximum rainfall intensity (46.48 mm/h) at peak time in winter2067 .

Figure (4.30) shows the behavior of the storm network in winter 2070 with rainfall intensity equal to 46.42mm/h. This value of rainfall intensity greater than the design rainfall intensity with ratio equal to 257%.56% of the manhole had no flooding (stage 1), 14% of the manhole had very light flooding (stage 2), 21% of the manhole had medium flooding (stage 3), 3% of the manhole flooding had high flooding (stage 4) and, 6%

of the manhole had very high flooding (stage 5), the duration of flooding is 45 min.

In addition, from the same Figure, it can be observed that flooding discharge condition for the year 2070 decrease stage 1, stage 2, stage 3, stage 4, and stage 5 have been no change compared to the year 2067. No significant change has occurred during this interval since the period too close.

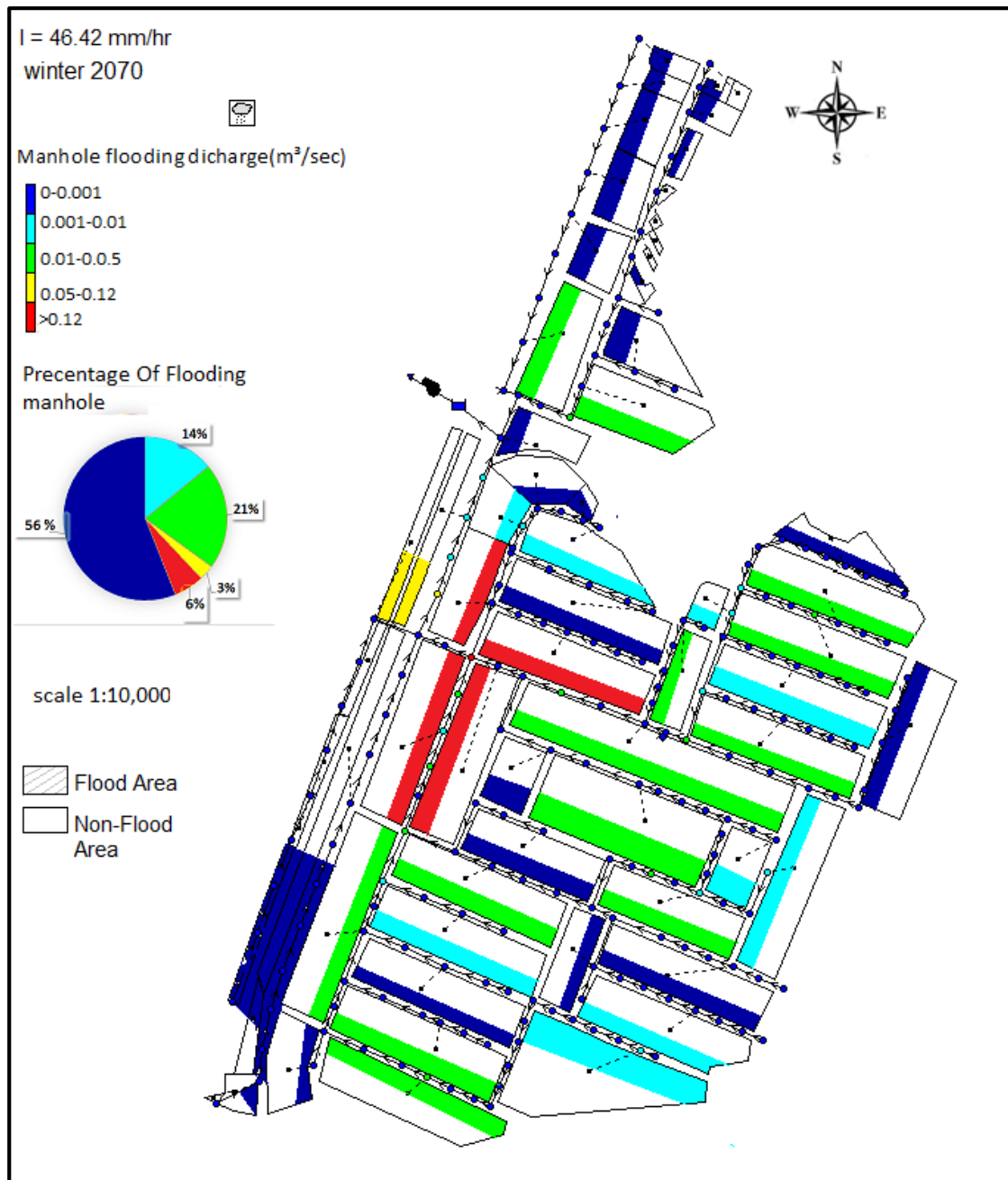


Figure 4-30 The flooding manhole under rainfall intensity (46.42 mm/h) at peak time in winter 2070.

For the cases above there are decrease and increase in the flooding discharge manhole rate with progress of time, but originally flooding discharge increase when compared the end design period (2070) with beginning design period (2017) stage 1 has been decreasing with rate about 39.2%, stage 2 has been increasing with rate about 14.2%, stage3 has

increase about 6 times, stage 4 has no change, and stage 5 increase with a rate about 6%.

4.4 Result of Suggested scenario

The result of suggestion will cover the future additional land use area (up to 2070) that surrounding the end life span of Karbala master plan (2050). Figure (4.31) clarifies the proposed future additional land use area and flooding discharge.

Figure (4.31) contains variation of flooding discharge from 2017 until 2070, in addition to current flooding discharge. The current flooding discharge (2017) is about 2.75 m³/sec. The value of flooding discharge manhole at the end period of master plan (2050) reach 11.48 m³/sec, which is increasing almost three times of the current flooding discharge (2017). At the end of design period (2070) the value of flooding discharge manhole reach 16.83 m³/sec, the rate of increase reach five time the current one.

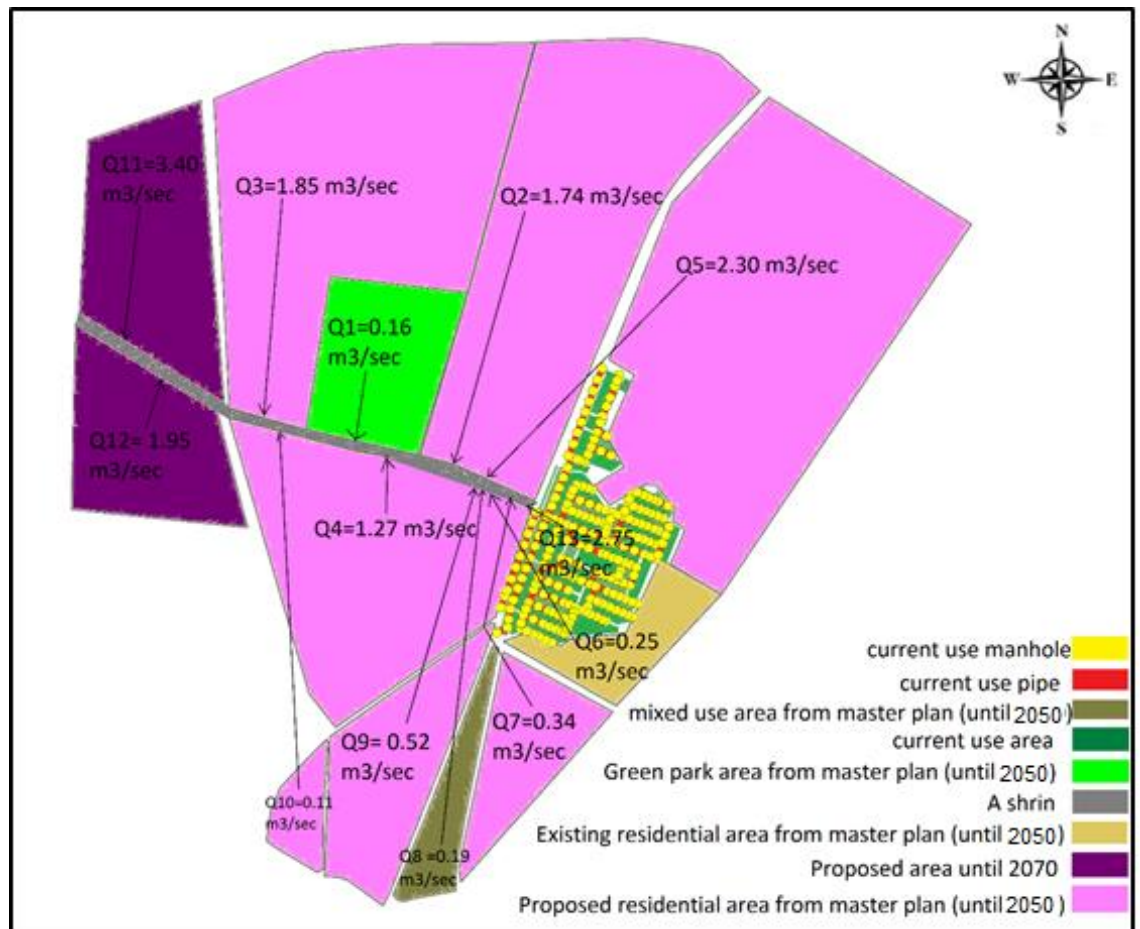


Figure 4-31 suggestion scenario for future flooding occurrence forecasting (2070).

Chapter Five

CONCLUSION AND FUTURE RECOMMENDATIONS**5.1 Introduction**

This study artificial neural network ANN model and predict the rainfall intensity for the next 53 years. The expected resulted intensity can be applied on the storm water network design for the study area by using SWMM model to estimate the flooding ratio.

5.2 Conclusion

The conclusions depended on the result can be summarized below:

1. The calibration of ANN model depend on R^2 and RMSE, the best models would have least RMSE ,and greater R^2 .Model 1 has RMSE equal to (1.67) , R^2 equal to (0.722) and model 3 has RMSE equal to (3.46) , R^2 equal to (0.64).
2. The result of ANN model indicates that the rainfall intensity increase with progress of time reach 46.48 mm/h in winter 2067.
3. many factor of climate change may effect on the ANN model such as: rainfall , wind speed , sun shine , humidity , min and max temperature , but the rainfall is the most effective factor on the climate change.
4. SWMM model was very effective in the analysis of the flooding problem. The calibration of SWMM model for six rainfall events with rainfall intensity (7.86 ,27.5, 19.86, 11.66, 21.28, and

7.24)mm/hr was good where the cross validation results show that the mean square error (MSE) for all events are very close to zero (0.000021). Moreover, root mean square error (RMSE) is very low as compared to the variance of the observed data for all events (0.0045).The correlation coefficient (R^2) equal to (0.83).

5. The SWMM analysis storm drainage system meet rainfall intensity greater than design intensity (13 mm/h) with peak rainfall intensity equal to 29.62 mm/h in winter 2028, with flooding duration 50 min and reach stage 4 (from 0.05-0.12) m³/s with ratio 1%.
6. The SWMM analysis storm drainage system meet rainfall intensity greater than design intensity (13 mm/h) with peak rainfall intensity equal to 45.98 mm/h in winter 2055, with flooding duration 20 min and reach to stage 5 (greater than 0.12) m³/s with ratio 6%.
7. The SWMM analysis storm drainage system meet rainfall intensity greater than design intensity (13 mm/h) with peak rainfall intensity equal to 44.9 mm/h in winter 2060, with flooding duration 35 min and reach stage 5 (greater than 0.12) m³/s with ratio 6%.
8. The SWMM analysis storm drainage system meet rainfall intensity greater than design intensity (13 mm/h) with peak rainfall intensity equal to 46.48 mm/h in winter 2067, that maximum intensity happened in future period (2017-2070), with flooding duration 45 min and reach stage 5 (greater than 0.12) m³/s with ratio 6%.
9. The percentage of flooding manhole at 2017 reach stage 4 (0.05-0.12) m³/s with ratio 3% while the percentage of flooding manhole at 2070 reach stage 5 (greater than 0.12) m³/s with ratio 6%.

5.3 Recommendations:

The proposed mechanism deal with the flood situation are:

1. Increase the diameter of the pipes to increase the capacity of water quantity.
2. Add second outlet to rid network from the flooding.

5.4 Recommendations for future studies:

1. Using another program to analysis the climate change to predict rainfall intensity.
2. Take another case study in kabala city.

List of Reference

- AL-ANSARI, N., ABDELLATIF, M., ALI, S. S. & KNUTSSON, S. 2014. Long term effect of climate change on rainfall in northwest Iraq. *Central European Journal of Engineering*, 4, 250-263.
- ALFATLAWI, T. J. & ALSHAKLI, H. I. 2015. Prediction the Coefficient of Discharge for Stepped Morning Glory Spillway Using ANN and MNLN Approaches.
- BIJLSMA, L., EHLER, C., KLEIN, R., KULSHRESTHA, S., MCLEAN, R., MIMURA, N., NICHOLLS, R., NURSE, L., NIETO, H. P. & STAKHIV, E. 1996. Coastal zones and small islands. Cambridge University Press, Cambridge, United Kingdom and New York, NY, USA.
- BOIX, A. P. 2017. toward sustained cities through an environmental ,economic and eco-efficiency and drainage system
- BOUZERIA, H., GHENIM, A. N. & KHANCHOUL, K. 2017. Using artificial neural network (ANN) for prediction of sediment loads, application to the Mellah catchment, northeast Algeria. *Journal of Water and Land development*, 33, 47-55.
- CHO, K., VAN MERRIËNBOER, B., GULCEHRE, C., BAHDANAU, D., BOUGARES, F., SCHWENK, H. & BENGIO, Y. 2014. Learning phrase representations using RNN encoder-decoder for statistical machine translation. *arXiv preprint arXiv:1406.1078*.
- CYBENKO, G. 1989. Approximation by superpositions of a sigmoidal function. *Mathematics of control, signals and systems*, 2, 303-314.
- DAWSON, C. W. & WILBY, R. 1998. An artificial neural network approach to rainfall-runoff modelling. *Hydrological Sciences Journal*, 43, 47-66.
- DENAULT, C., MILLAR, R. G. & LENCE, B. J. 2006. Assessment of possible impacts of climate change in an urban catchment. *JAWRA Journal of the American Water Resources Association*, 42, 685-697.
- EVANS, J. P. 2009. 21st century climate change in the Middle East. *Climatic Change*, 92, 417-432.

LIST OF REFERENCES

G.A.A.S.O 2018. General Authority for Aeronautical and Seismic Observations

GIRONÁS, J., ROESNER, L. A., DAVIS, J., ROSSMAN, L. A. & SUPPLY, W. 2009. *Storm water management model applications manual*, National Risk Management Research Laboratory, Office of Research and Development, US Environmental Protection Agency Cincinnati, OH.

GIRONÁS, J., ROESNER, L. A., ROSSMAN, L. A. & DAVIS, J. 2010. A new applications manual for the Storm Water Management Model (SWMM). *Environmental Modelling & Software*, 25, 813-814.

GIUSEPPE CIABURRO, B. V. & SEPTEMBER 2017
Neural network with R

HASSAN, W. H., NILE, B. K. & AL-MASODY, B. A. 2017. Study the climate change effect on storm drainage networks by storm water management model [SWMM].

HINTON, G. E., OSINDERO, S. & TEH, Y.-W. 2006. A fast learning algorithm for deep belief nets. *Neural computation*, 18, 1527-1554.

HORNIK, K. 1991. Approximation capabilities of multilayer feedforward networks. *Neural networks*, 4, 251-257.

HOUGHTON, J. T. 1996. *Climate change 1995: The science of climate change: contribution of working group I to the second assessment report of the Intergovernmental Panel on Climate Change*, Cambridge University Press.

HUONG, H. & PATHIRANA, A. 2013. Urbanization and climate change impacts on future urban flooding in Can Tho city, Vietnam. *Hydrology and Earth System Sciences*, 17, 379-394.

I.A.C.D 2018. Iraqi Agromet Center Data

JAIN, S., DAS, A. & SRIVASTAVA, D. 1999. Application of ANN for reservoir inflow prediction and operation. *Journal of water resources planning and management*, 125, 263-271.

JENG, D., CHA, D. & BLUMENSTEIN, M. Application of neural network in civil engineering problems. Proceedings of the International Conference on Advances in the Internet, Processing, Systems and Interdisciplinary Research, 2003.

LIST OF REFERENCES

- JIANG, L., CHEN, Y. & WANG, H. 2015. Urban flood simulation based on the SWMM model. *Proceedings of the International Association of Hydrological Sciences*, 368, 186-191.
- JUNG, M., KIM, H., MALLARI, K., PAK, G. & YOON, J. 2015. Analysis of effects of climate change on runoff in an urban drainage system: a case study from Seoul, Korea. *Water Science and Technology*, 71, 653-660.
- KADIOGLU, M. & ŞEN, Z. 2001. Monthly precipitation-runoff polygons and mean runoff coefficients. *Hydrological Sciences Journal*, 46, 3-11.
- LUK, K. C., BALL, J. E. & SHARMA, A. 2001. An application of artificial neural networks for rainfall forecasting. *Mathematical and Computer modelling*, 33, 683-693.
- MEEHL, G. A., T.F. STOCKER, W.D. COLLINS, P. FRIEDLINGSTEIN, A.T. GAYE, J.M. GREGORY, A. KITO, R. KNUTTI, J.M. MURPHY, A. NODA, S.C.B. RAPER, I.G. WATTERSON, A.J. WEAVER AND & ZHAO, Z.-C. 2007. *Global Climate Projections. In: Climate Change 2007: The Physical Science Basis. Contribution of Working Group I to the Fourth Assessment Report of the Intergovernmental Panel on Climate Change [Solomon, S., D. Qin, M. Manning, Z. Chen, M. Marquis, K.B. Averyt, M. Tignor and H.L. Miller (eds.)]* [Online]. Cambridge, United Kingdom and New York, NY, USA: Cambridge University Press
- MLNNOTEBOOK 2017. A Simple Neural Network - Transfer Functions. 08 Mar 2017.
- MURATA, N., YOSHIZAWA, S. & AMARI, S.-I. 1994. Network information criterion-determining the number of hidden units for an artificial neural network model. *IEEE Transactions on Neural Networks*, 5, 865-872.
- NIE, L., LINDHOLM, O., LINDHOLM, G. & SYVERSEN, E. 2009. Impacts of climate change on urban drainage systems—a case study in Fredrikstad, Norway. *Urban Water Journal*, 6, 323-332.
- NIRUPAMA, N. & SIMONOVIC, S. P. 2007. Increase of flood risk due to urbanisation: a Canadian example. *Natural Hazards*, 40, 25.
- OSMAN, Y. 2017. Climate Change and Future Precipitation in Arid Environment of Middle East: Case study of Iraq: Climate Change and Future Precipitation in Arid Environment of Middle East: Case study of Iraq. *Journal of Environmental Hydrology*, 25, 1-18.
- PITT, R., LILBURN, M., NIX, S., DURRANS, S., BURIAN, S., VOORHEES, J. & MARTINSON, J. 1999. Guidance Manual for Integrated Wet Weather Flow

LIST OF REFERENCES

- (WWF) Collection and Treatment Systems for Newly Urbanized Areas (New WWF Systems). *Current and Future Design Practices*.
- RAWLS, W. J., BRAKENSIEK, D. L. & MILLER, N. 1983. Green-ampt Infiltration Parameters from Soils Data. *Journal of Hydraulic Engineering*, 109, 62-70.
- REYNARD, N. S., PRUDHOMME, C. & CROOKS, S. M. 2001. The flood characteristics of large UK rivers: potential effects of changing climate and land use. *Climatic change*, 48, 343-359.
- ROSSMAN, L. A. 2010. *Storm water management model user's manual, version 5.0*, National Risk Management Research Laboratory, Office of Research and Development, US Environmental Protection Agency Cincinnati.
- ROTHMAN, L. S., RINSLAND, C., GOLDMAN, A., MASSIE, S., EDWARDS, D., FLAUD, J., PERRIN, A., CAMY-PEYRET, C., DANA, V. & MANDIN, J.-Y. 1998. The HITRAN molecular spectroscopic database and HAWKS (HITRAN atmospheric workstation): 1996 edition. *Journal of quantitative spectroscopy and radiative transfer*, 60, 665-710.
- SAGHAFIAN, B., FARAZJOO, H., BOZORGY, B. & YAZDANDOOST, F. 2008. Flood intensification due to changes in land use. *Water resources management*, 22, 1051-1067.
- SANSOM, J. & RENWICK, J. A. 2007. Climate change scenarios for New Zealand rainfall. *Journal of Applied Meteorology and Climatology*, 46, 573-590.
- SCHREIDER, S. Y., SMITH, D. & JAKEMAN, A. 2000. Climate change impacts on urban flooding. *Climatic Change*, 47, 91-115.
- SEMADENI-DAVIES, A., HERNEBRING, C., SVENSSON, G. & GUSTAFSSON, L.-G. 2008. The impacts of climate change and urbanisation on drainage in Helsingborg, Sweden: Suburban stormwater. *Journal of hydrology*, 350, 114-125.
- SUJANA PRAJITHKUMAR, D., VERMA, S. & MAHAJAN, B. Application of ANN model for the prediction of Water Quality Index. *International Journal of Engineering Research and General Science*, 3.
- TOKAR, A. S. & JOHNSON, P. A. 1999. Rainfall-runoff modeling using artificial neural networks. *Journal of Hydrologic Engineering*, 4, 232-239.
- USGS 2018. U.S. Geological Survey

LIST OF REFERNCES

YILMAZ, I. & YUKSEK, A. 2008. An example of artificial neural network (ANN) application for indirect estimation of rock parameters. *Rock Mechanics and Rock Engineering*, 41, 781-795.

APPENDIX A – GIS STORM NETWORK DATA

OBJECTID	Upstream In	Downstream	Diameter	Slope	Install Date	Sector No_H	Length	القضا	sector	SHAPE_Length
1	25.93	25.8	315	0.003175	1/1/2007	العباس	50	المركز	باب بغداد	49.99999
2	25.96	25.8	315	0.003175	1/1/2007	العباس	41	المركز	باب بغداد	40.99996
3	26.1	25.96	315	0.003175	1/1/2007	العباس	28	المركز	باب بغداد	28.00003
4	0	0	315	0.003175	1/1/2007	العباس	2	المركز	باب بغداد	1.99995
5	26.05	25.93	315	0.003175	1/1/2007	العباس	50	المركز	باب بغداد	49.99998
6	25.8	25.71	400	0.0025	1/1/2007	العباس	31.2	المركز	باب بغداد	31.20007
7	25.71	25.625	400	0.0025	1/1/2007	العباس	30.3	المركز	باب بغداد	30.30004
8	25.83	25.625	315	0.003175	1/1/2007	العباس	49.2	المركز	باب بغداد	49.19996
9	25.951	25.83	315	0.003175	1/1/2007	العباس	49.4	المركز	باب بغداد	49.40001
10	25.625	25.536	400	0.0025	1/1/2007	العباس	63	المركز	باب بغداد	63.00004
11	25.646	25.536	315	0.003175	1/1/2007	العباس	51.8	المركز	باب بغداد	51.79998
12	25.736	25.646	315	0.003175	1/1/2007	العباس	50.6	المركز	باب بغداد	50.60004
13	25.856	25.736	315	0.003175	1/1/2007	العباس	50.3	المركز	باب بغداد	50.29999
14	25.926	25.856	315	0.003175	1/1/2007	العباس	28	المركز	باب بغداد	27.99997
15	25.536	25.466	400	0.0025	1/1/2007	العباس	30.6	المركز	باب بغداد	30.60002
16	25.466	25.4	400	0.0025	1/1/2007	العباس	31.6	المركز	باب بغداد	31.59998
17	25.561	25.4	315	0.003175	1/1/2007	العباس	50	المركز	باب بغداد	50
18	25.691	25.561	315	0.003175	1/1/2007	العباس	49.5	المركز	باب بغداد	49.50003
19	25.841	25.691	315	0.003175	1/1/2007	العباس	50.6	المركز	باب بغداد	50.59999
20	25.4	25.226	400	0.0025	1/1/2007	العباس	63	المركز	باب بغداد	62.99995
21	25.326	25.226	500	0.002	1/1/2007	العباس	64.5	المركز	باب بغداد	64.49996
22	25.49	25.326	400	0.0025	1/1/2007	العباس	62.2	المركز	باب بغداد	62.20001
23	25.61	25.49	400	0.0025	1/1/2007	العباس	35.7	المركز	باب بغداد	35.70002
24	25.72	25.61	400	0.0025	1/1/2007	العباس	50.3	المركز	باب بغداد	50.29995
25	25.496	25.326	400	0.0025	1/1/2007	العباس	44.4	المركز	باب بغداد	44.39997
26	25.566	25.496	400	0.0025	1/1/2007	العباس	39.2	المركز	باب بغداد	39.20005
27	25.661	25.566	400	0.0025	1/1/2007	العباس	42	المركز	باب بغداد	42.00002
28	25.906	25.661	315	0.003175	1/1/2007	العباس	44.8	المركز	باب بغداد	44.80004
29	26.046	25.906	315	0.003175	1/1/2007	العباس	60	المركز	باب بغداد	59.97993
30	25.996	25.906	315	0.003175	1/1/2007	العباس	26.4	المركز	باب بغداد	26.4
31	26.086	25.996	315	0.003175	1/1/2007	العباس	60.1	المركز	باب بغداد	60.11929
32	26.166	25.996	315	0.003175	1/1/2007	العباس	60.7	المركز	باب بغداد	60.65559
33	26.336	26.166	315	0.003175	1/1/2007	العباس	39.3	المركز	باب بغداد	39.34447
34	25.226	25.156	500	0.002	1/1/2007	العباس	43.2	المركز	باب بغداد	43.20001
35	25.156	25.101	500	0.002	1/1/2007	العباس	37.3	المركز	باب بغداد	37.30004

36	25.101	25.041	500	0.002	1/1/2007	العباس	43.7	المركز	باب بغداد	43.7
37	25.041	24.961	500	0.002	1/1/2007	العباس	45.2	المركز	باب بغداد	45.20002
38	24.961	24.889	500	0.002	1/1/2007	العباس	46	المركز	باب بغداد	45.99997
39	24.889	24.759	500	0.002	1/1/2007	العباس	34	المركز	باب بغداد	34.00004
40	24.759	24.629	500	0.002	1/1/2007	العباس	32	المركز	باب بغداد	32.00004
41	24.889	24.675	500	0.002	1/1/2007	العباس	32	المركز	باب بغداد	32.00001
42	24.813	24.675	500	0.002	1/1/2007	العباس	32	المركز	باب بغداد	32.00003
43	25.159	24.813	315	0.003175	1/1/2007	العباس	66	المركز	باب بغداد	66.00006
44	25.27	25.159	315	0.003175	1/1/2007	العباس	62.6	المركز	باب بغداد	62.59998
45	25.385	25.27	315	0.003175	1/1/2007	العباس	43.7	المركز	باب بغداد	43.70003
46	25.52	25.385	315	0.003175	1/1/2007	العباس	66.4	المركز	باب بغداد	66.36421
47	24.973	24.813	400	0.0025	1/1/2007	العباس	48	المركز	باب بغداد	48
48	25.119	24.973	400	0.0025	1/1/2007	العباس	49	المركز	باب بغداد	49.00001
49	25.279	25.119	400	0.0025	1/1/2007	العباس	54	المركز	باب بغداد	54.00003
50	25.413	25.279	315	0.003175	1/1/2007	العباس	26	المركز	باب بغداد	25.99996
51	0	0	315	0.003175	1/1/2007	العباس	6	المركز	باب بغداد	5.999977
52	25.479	25.413	315	0.003175	1/1/2007	العباس	25	المركز	باب بغداد	24.99997
53	25.619	25.479	315	0.003175	1/1/2007	العباس	53	المركز	باب بغداد	52.99999
54	25.729	25.619	315	0.003175	1/1/2007	العباس	52	المركز	باب بغداد	51.99998
55	25.831	25.729	315	0.003175	1/1/2007	العباس	48	المركز	باب بغداد	48.00002
56	25.61	25.479	315	0.003175	1/1/2007	العباس	59	المركز	باب بغداد	59.00006
57	25.056	24.966	400	0.0025	1/1/2007	العباس	22.6	المركز	باب بغداد	22.58902
58	25.126	25.056	400	0.0025	1/1/2007	العباس	38.5	المركز	باب بغداد	38.49996
59	24.965	24.629	500	0.002	1/1/2007	العباس	50	المركز	باب بغداد	49.99999
60	25.05	24.965	500	0.002	1/1/2007	العباس	49.5	المركز	باب بغداد	49.50005
61	25.13	25.05	500	0.002	1/1/2007	العباس	50.5	المركز	باب بغداد	50.50003
62	25.23	25.13	500	0.002	1/1/2007	العباس	60.6	المركز	باب بغداد	60.59996
63	25.31	25.23	500	0.002	1/1/2007	العباس	51.7	المركز	باب بغداد	51.70002
64	25.41	25.31	500	0.002	1/1/2007	العباس	49.5	المركز	باب بغداد	49.5
65	25.5	25.41	500	0.002	1/1/2007	العباس	50.7	المركز	باب بغداد	50.70002
66	25.58	25.5	500	0.002	1/1/2007	العباس	57.6	المركز	باب بغداد	57.60005
67	25.66	25.58	500	0.002	1/1/2007	العباس	45.5	المركز	باب بغداد	45.50002
68	25.75	25.66	500	0.002	1/1/2007	العباس	48.4	المركز	باب بغداد	48.40001
69	25.83	25.75	500	0.002	1/1/2007	العباس	38	المركز	باب بغداد	38.00002
70	25.9	25.83	500	0.002	1/1/2007	الهيابي	55	المركز	باب بغداد	54.99997
71	25.885	24.629	315	0.003175	1/1/2007	العباس	55	المركز	باب بغداد	54.99997
72	25.955	25.885	315	0.003175	1/1/2007	العباس	52	المركز	باب بغداد	52.00002
73	26.136	25.955	315	0.003175	1/1/2007	العباس	55	المركز	باب بغداد	54.99997
74	26.318	26.136	315	0.003175	1/1/2007	العباس	55	المركز	باب بغداد	55.00003

75	26.499	26.318	315	0.003175	1/1/2007	العباس	56	المركز	باب بغداد	55.99999
76	26.681	26.499	315	0.003175	1/1/2007	العباس	55	المركز	باب بغداد	55.00002
77	26.862	26.681	315	0.003175	1/1/2007	العباس	57	المركز	باب بغداد	57.00001
78	27.044	26.862	315	0.003175	1/1/2007	العباس	57	المركز	باب بغداد	57.00001
79	27.225	27.044	315	0.003175	1/1/2007	العباس	31	المركز	باب بغداد	30.99999
80	25.196	25.126	400	0.0025	1/1/2007	العباس	48.3	المركز	باب بغداد	48.29996
81	25.306	25.196	315	0.003175	1/1/2007	العباس	49	المركز	باب بغداد	48.99995
82	25.456	25.306	315	0.003175	1/1/2007	العباس	48	المركز	باب بغداد	48.00003
83	25.595	25.456	315	0.003175	1/1/2007	العباس	31.5	المركز	باب بغداد	31.50002
84	0	0	400	0.0025	1/1/2007	العباس	6	المركز	باب بغداد	5.999984
85	23.886	23.738	315	0.003175	1/1/2007	العباس	38	المركز	باب بغداد	37.99998
86	24.253	23.886	315	0.003175	1/1/2007	العباس	40	المركز	باب بغداد	39.99998
87	24.633	24.253	315	0.003175	1/1/2007	العباس	50	المركز	باب بغداد	49.99997
88	24.783	24.633	315	0.003175	1/1/2007	العباس	50	المركز	باب بغداد	50.00001
89	24.376	24.253	315	0.003175	1/1/2007	العباس	37	المركز	باب بغداد	37.00006
90	24.496	24.376	315	0.003175	1/1/2007	العباس	35	المركز	باب بغداد	35.00003
91	25.046	24.496	315	0.003175	1/1/2007	العباس	49	المركز	باب بغداد	48.99994
92	24.606	24.496	315	0.003175	1/1/2007	العباس	49	المركز	باب بغداد	48.99996
93	24.746	24.606	315	0.003175	1/1/2007	العباس	32	المركز	باب بغداد	31.99995
94	24.856	24.746	315	0.003175	1/1/2007	العباس	49	المركز	باب بغداد	49.00003
95	25	24.856	315	0.003175	1/1/2007	العباس	45	المركز	باب بغداد	44.99999
96	25.185	25	315	0.003175	1/1/2007	العباس	55	المركز	باب بغداد	54.99996
97	25.355	25.185	315	0.003175	1/1/2007	العباس	30	المركز	باب بغداد	29.99995
98	25.495	25.355	315	0.003175	1/1/2007	العباس	30	المركز	باب بغداد	30.00002
99	25.68	25.645	315	0.003175	1/1/2004	العباس	18.1	المركز	باب بغداد	18.0791
100	25.83	25.68	315	0.003175	1/1/2007	العباس	59.4	المركز	باب بغداد	59.42456
101	25.98	25.83	315	0.003175	1/1/2007	العباس	55	المركز	باب بغداد	55.00003
102	26.13	25.98	315	0.003175	1/1/2007	العباس	54	المركز	باب بغداد	53.99998
103	26.28	26.13	315	0.003175	1/1/2007	العباس	50	المركز	باب بغداد	50.00002
104	26.4	26.28	315	0.003175	1/1/2007	العباس	51	المركز	باب بغداد	50.99999
105	26.56	26.4	315	0.003175	1/1/2007	العباس	54	المركز	باب بغداد	53.99995
106	26.725	26.56	315	0.003175	1/1/2007	العباس	54	المركز	باب بغداد	53.99996
107	26.87	26.725	315	0.003175	1/1/2007	العباس	59	المركز	باب بغداد	59.00001
126	0	0	315	0.003175	1/1/2007	العباس	32	المركز	باب بغداد	31.99999
127	0	0	315	0.003175	1/1/2004	العباس	30	المركز	باب بغداد	30.00001
128	0	0	315	0.003175	1/1/2004	العباس	30	المركز	باب بغداد	30.00004
129	0	0	315	0.003175	1/1/2004	العباس	20.4	المركز	باب بغداد	20.37663
130	0	0	315	0.003175	1/1/2004	العباس	26	المركز	باب بغداد	25.99998
131	0	0	315	0.003175	1/1/2004	العباس	26	المركز	باب بغداد	25.99998

132	0	0	315	0.003175	1/1/2004	العباس	30	المركز	باب بغداد	30.00004
133	0	0	315	0.003175	1/1/2004	العباس	25	المركز	باب بغداد	25.00001
134	0	0	315	0.003175	1/1/2004	العباس	25	المركز	باب بغداد	25
135	0	0	315	0.003175	1/1/2004	العباس	26	المركز	باب بغداد	25.99997
136	0	0	315	0.003175	1/1/2004	العباس	26	المركز	باب بغداد	25.99999
137	0	0	315	0.003175	1/1/2004	العباس	26.5	المركز	باب بغداد	26.50003
138	0	0	315	0.003175	1/1/2004	العباس	30	المركز	باب بغداد	29.99995
139	0	0	315	0.003175	1/1/2004	العباس	30	المركز	باب بغداد	30.00001
140	0	0	315	0.003175	1/1/2004	العباس	17	المركز	باب بغداد	17.00001
141	0	0	315	0.003175	1/1/2007	العباس	32.4	المركز	باب بغداد	32.39996
142	0	0	315	0.003175	1/1/2004	العباس	30	المركز	باب بغداد	29.99997
143	0	0	315	0.003175	1/1/2004	العباس	32	المركز	باب بغداد	31.99998
144	0	0	315	0.003175	1/1/2004	العباس	33	المركز	باب بغداد	33.00002
145	0	0	315	0.003175	1/1/2004	العباس	30	المركز	باب بغداد	30.00004
146	0	0	315	0.003175	1/1/2004	العباس	30	المركز	باب بغداد	29.99999
147	0	0	315	0.003175	1/1/2004	العباس	26	المركز	باب بغداد	26.00005
148	0	0	315	0.003175	1/1/2004	العباس	31	المركز	باب بغداد	31.00002
149	0	0	315	0.003175	1/1/2004	العباس	32	المركز	باب بغداد	32.00001
150	0	0	315	0.003175	1/1/2004	العباس	31	المركز	باب بغداد	30.99997
151	0	0	315	0.003175	1/1/2004	العباس	30	المركز	باب بغداد	30.00011
152	0	0	315	0.003175	1/1/2004	العباس	30	المركز	باب بغداد	29.99998
153	0	0	315	0.003175	1/1/2004	العباس	26	المركز	باب بغداد	26.00001
154	0	0	315	0.003175	1/1/2004	العباس	24	المركز	باب بغداد	24.00001
155	0	0	315	0.003175	1/1/2004	العباس	30	المركز	باب بغداد	30.00004
156	0	0	315	0.003175	1/1/2004	العباس	30	المركز	باب بغداد	30.00004
157	0	0	315	0.003175	1/1/2004	العباس	31	المركز	باب بغداد	31
158	0	0	315	0.003175	1/1/2004	العباس	33	المركز	باب بغداد	33.00005
159	0	0	315	0.003175	1/1/2004	العباس	51	المركز	باب بغداد	51.00003
160	0	0	315	0.003175	1/1/2004	العباس	23	المركز	باب بغداد	23
161	0	0	315	0.003175	1/1/2004	العباس	24	المركز	باب بغداد	23.99999
162	0	0	315	0.003175	1/1/2004	العباس	26	المركز	باب بغداد	25.99999
163	0	0	315	0.003175	1/1/2004	العباس	31	المركز	باب بغداد	31.00007
164	0	0	315	0.003175	1/1/2004	العباس	30	المركز	باب بغداد	29.99987
165	0	0	315	0.003175	1/1/2004	العباس	28	المركز	باب بغداد	27.99994
166	0	0	315	0.003175	1/1/2004	العباس	29	المركز	باب بغداد	29.00008
167	0	0	315	0.003175	1/1/2004	العباس	30	المركز	باب بغداد	29.99997
168	0	0	315	0.003175	1/1/2004	العباس	23	المركز	باب بغداد	22.99996
169	0	0	315	0.003175	1/1/2004	العباس	32	المركز	باب بغداد	32.00001
170	0	0	315	0.003175	1/1/2004	العباس	30	المركز	باب بغداد	30.00004

171	24.966	24.889	400	0.0025	1/1/2007	العباس	67	المركز	باب بغداد	67.01099
172	0	0	315	0.003175	1/1/2007	العباس	33	المركز	باب بغداد	32.99997
173	0	0	315	0.003175	1/1/2004	العباس	30	المركز	باب بغداد	30.00003
174	0	0	315	0.003175	1/1/2004	العباس	30	المركز	باب بغداد	29.99998
175	0	0	315	0.003175	1/1/2004	العباس	32	المركز	باب بغداد	32.00002
176	0	0	315	0.003175	1/1/2004	العباس	30	المركز	باب بغداد	30.00001
177	0	0	315	0.003175	1/1/2004	العباس	31	المركز	باب بغداد	30.99998
178	0	0	315	0.003175	1/1/2004	العباس	20	المركز	باب بغداد	20.00004
179	0	0	315	0.003175	1/1/2004	العباس	20	المركز	باب بغداد	20.00002
180	0	0	315	0.003175	1/1/2007	العباس	25.4	المركز	باب بغداد	25.40811
181	0	0	315	0.003175	1/1/2004	العباس	31	المركز	باب بغداد	31.00006
182	0	0	315	0.003175	1/1/2004	العباس	32	المركز	باب بغداد	32.00001
183	0	0	315	0.003175	1/1/2004	العباس	25	المركز	باب بغداد	24.99999
184	0	0	315	0.003175	1/1/2007	العباس	27	المركز	باب بغداد	27.00001
185	0	0	315	0.003175	1/1/2004	العباس	27	المركز	باب بغداد	26.99999
186	0	0	315	0.003175	1/1/2004	العباس	28	المركز	باب بغداد	28.00002
187	0	0	315	0.003175	1/1/2004	العباس	28	المركز	باب بغداد	27.99997
188	0	0	315	0.003175	1/1/2004	العباس	20	المركز	باب بغداد	20
189	25.759	25.61	315	0.003175	1/1/2007	العباس	67.3	المركز	باب بغداد	67.27319
190	0	0	315	0.003175	1/1/2007	العباس	28	المركز	باب بغداد	28
191	0	0	315	0.003175	1/1/2004	العباس	35	المركز	باب بغداد	35.00002
192	0	0	315	0.003175	1/1/2004	العباس	36	المركز	باب بغداد	36.00004
193	0	0	315	0.003175	1/1/2004	العباس	30	المركز	باب بغداد	30.00003
194	0	0	315	0.003175	1/1/2004	العباس	29	المركز	باب بغداد	28.99997
195	0	0	315	0.003175	1/1/2004	العباس	29	المركز	باب بغداد	29.00003
196	0	0	315	0.003175	1/1/2004	العباس	32.1	المركز	باب بغداد	32.10246
197	0	0	315	0.003175	1/1/2004	العباس	30	المركز	باب بغداد	30
198	0	0	315	0.003175	1/1/2004	العباس	30	المركز	باب بغداد	30.00003
199	0	0	315	0.003175	1/1/2004	العباس	30	المركز	باب بغداد	29.99998
200	0	0	315	0.003175	1/1/2004	العباس	33	المركز	باب بغداد	33
201	0	0	315	0.003175	1/1/2004	العباس	24	المركز	باب بغداد	23.99999
202	0	0	315	0.003175	1/1/2004	العباس	30	المركز	باب بغداد	29.99996
203	0	0	315	0.003175	1/1/2004	العباس	31	المركز	باب بغداد	31.00001
204	0	0	315	0.003175	1/1/2004	العباس	26	المركز	باب بغداد	25.99998
205	0	0	315	0.003175	1/1/2004	العباس	23.5	المركز	باب بغداد	23.49997
206	0	0	315	0.003175	1/1/2007	العباس	22	المركز	باب بغداد	21.99995
207	0	0	315	0.003175	1/1/2004	العباس	30	المركز	باب بغداد	29.99993
208	0	0	315	0.003175	1/1/2004	العباس	31	المركز	باب بغداد	31.00004
209	0	0	315	0.003175	1/1/2004	العباس	41	المركز	باب بغداد	41.00001

210	0	0	315	0.003175	1/1/2004	العباس	40	المركز	باب بغداد	40.00003
211	0	0	315	0.003175	1/1/2004	العباس	58	المركز	باب بغداد	57.99996
212	0	0	315	0.003175	1/1/2004	العباس	21.6	المركز	باب بغداد	21.63831
213	0	0	315	0.003175	1/1/2004	العباس	31	المركز	باب بغداد	30.99995
214	0	0	315	0.003175	1/1/2004	العباس	30	المركز	باب بغداد	29.99999
215	0	0	315	0.003175	1/1/2004	العباس	29	المركز	باب بغداد	28.99997
216	0	0	315	0.003175	1/1/2004	العباس	30	المركز	باب بغداد	29.99998
217	0	0	315	0.003175	1/1/2004	العباس	30	المركز	باب بغداد	30.00001
218	0	0	315	0.003175	1/1/2004	العباس	30	المركز	باب بغداد	29.99998
219	0	0	315	0.003175	1/1/2004	العباس	29	المركز	باب بغداد	29.00001
220	0	0	315	0.003175	1/1/2004	العباس	30	المركز	باب بغداد	30.00001
221	0	0	315	0.003175	1/1/2004	العباس	26	المركز	باب بغداد	25.99998
222	0	0	315	0.003175	1/1/2004	العباس	25	المركز	باب بغداد	24.99999
223	0	0	315	0.003175	1/1/2004	العباس	25	المركز	باب بغداد	25.00004
224	0	0	315	0.003175	1/1/2004	العباس	48	المركز	باب بغداد	48.00002
225	0	0	315	0.003175	1/1/2007	العباس	26	المركز	باب بغداد	26.00008
226	0	0	315	0.003175	1/1/2004	العباس	32	المركز	باب بغداد	31.99987
227	0	0	315	0.003175	1/1/2004	العباس	30	المركز	باب بغداد	30.00003
228	0	0	315	0.003175	1/1/2004	العباس	32	المركز	باب بغداد	31.99992
229	0	0	315	0.003175	1/1/2004	العباس	32	المركز	باب بغداد	32.00004
230	0	0	315	0.003175	1/1/2004	العباس	28	المركز	باب بغداد	27.99996
231	0	0	315	0.003175	1/1/2004	العباس	17	المركز	باب بغداد	16.9672
232	0	0	315	0.003175	1/1/2007	العباس	19	المركز	باب بغداد	19.00004
233	0	0	315	0.003175	1/1/2004	العباس	10	المركز	باب بغداد	10.00002
234	0	0	600	0.001667	1/1/2004	العباس	53	المركز	باب بغداد	52.99997
235	0	0	600	0.001667	1/1/2004	العباس	50	المركز	باب بغداد	50.00003
236	0	0	600	0.001667	1/1/2004	العباس	50	المركز	باب بغداد	49.99996
237	0	0	600	0.001667	1/1/2004	العباس	50	المركز	باب بغداد	50.00002
238	0	0	600	0.001667	1/1/2004	العباس	44	المركز	باب بغداد	44
239	0	0	600	0.001667	1/1/2007	العباس	51.2	المركز	باب بغداد	51.19109
244	0	0	315	0	1/1/2007	العباس	0	المركز	باب بغداد	55.2471

الخلاصة

يحدث فيضان شبكة مياه الأمطار بسبب تغير المناخ وتغير استخدام الأراضي وزيادة التمدن والسكان على نطاق أوسع. تتناول هذه الدراسة تطوير نماذج لتنبئ التغيير المستقبلي في أحداث هطول الأمطار من أجل حماية البنى التحتية لشبكة مياه الأمطار من الفيضانات. تم اختيار حي العباس في مدينة كربلاء ، العراق كدراسة حالة. بالنسبة للتحليل الأول ، فإن تأثير تغير المناخ على كثافة الأمطار المتوقعة للفترة المستقبلية (2017-2070) يعتمد على البيانات التاريخية للفترة 1980 - 2016. وقد تم إجراء هذا باستخدام نموذج الشبكة العصبية الاصطناعية (ANN) تتضمن طبقات الدخول التي تدخل في نموذج ANN عوامل التغير المناخي وتشمل (هطول الأمطار شهرياً ودرجة الحرارة ودرجة الحرارة القصوى وسرعة الرياح والرطوبة وأشعة الشمس). هذه البيانات مقسمة إلى بيانات التدريب تمثل 95 ٪ من البيانات وبيانات الاختبار تمثل 5 ٪ لعملية المعايرة. عوامل الاخراج تشمل كثافة هطول الأمطار. بعد ذلك ، تم بناء نموذج إدارة مياه العواصف (SWMM) من أجل تقييم ظروف الفيضان في منطقة الدراسة لكثافة الأمطار المتوقعة. تشير النتائج إلى أن الحد الأقصى لكثافة الأمطار سيبلغ 46.48 ملم / ساعة. في عام 2067. تمثل هذه القيمة ثلاث مرات من كثافة التصميم. وتزداد نسبة فيضان المنهولات مع تقدم الوقت. تم اختيار خمس مراحل تصميم لكل فترة زمنية محددة خلال فترة تصميم الدراسة والتي كانت 53 عامًا لإظهار التباين في فيضان المنهولات. إنه مثال على ذلك ، فقد انخفض معدل الفيضان خلال المرحلة الأولى بنسبة 39.2 ٪ في عام 2070 بينما في المرحلة الثانية ارتفع المعدل بنسبة 14.2 ٪ ، والمرحلة الثالثة تزداد في 6 مرات ، والمرحلة الرابعة لم تتغير ، والمرحلة الخامسة تزيد مع بمعدل حوالي 6 ٪ مقارنة مع فترة البداية (2017).



جمهورية العراق
وزارة التعليم العالي والبحث العلمي
جامعة كربلاء
كلية الهندسة
قسم الهندسة المدنية

تأثير تغير المناخ على تشغيل شبكات مياه الامطار: دراسة الحالة في مدينة كربلاء

رسالة

مقدمة إلى كلية الهندسة في جامعة كربلاء

وهي جزء من متطلبات نيل درجة ماجستير في الهندسة المدنية

(هندسة البنى التحتية)

من قبل :

غفران عبدالحسين محمدحسن علي

(بكالوريوس في علوم الهندسة المدنية 2015)

بإشراف:

أ.د. باسم خليل نايل

أ.د. واقد حميد حسن